Final Report *June 1975*

DOE/SF/00893--T16

PRESSURE-PULSE PROPAGATION IN PIPING SYSTEMS

By: D J. CAGLIOSTRO, *Project Leader*
S J. WIERSMA
A. L. FLORENCE, *Project Supervisor*

Prepared for:

GENERAL ELECTRIC
NUCLEAR ENERGY DIVISION
BREEDER REACTOR DEPARTMENT
310 DeGUIGNE DRIVE
SUNNYVALE, CALIFORNIA 94086

Purchase Order No. 190-C1H88GX
AN03-76SF00893

STANFORD RESEARCH INSTITUTE
Menlo Park, California 94025 · U.S.A.

8/1/75

DISCLAIMER

STANFORD RESEARCH INSTITUTE
Menlo Park, California 94025 · U.S.A.

Final Report *June 1975*

PRESSURE-PULSE PROPAGATION IN PIPING SYSTEMS

By: D. J. CAGLIOSTRO, *Project Leader*
S. J. WIERSMA
A. L. FLORENCE, *Project Supervisor*

Prepared for:

GENERAL ELECTRIC
NUCLEAR ENERGY DIVISION
BREEDER REACTOR DEPARTMENT
310 DeGUIGNE DRIVE
SUNNYVALE, CALIFORNIA 94086

Purchase Order No. 190-C1H88GX

SRI Project PYD-3840

Approved by:

G. R. ABRAHAMSON, *Director*
Poulter Laboratory

C. J. COOK, *Executive Director*
Physical Sciences Division

FOREWORD

This is the final report to General Electric, Nuclear Energy Division on SRI Project PYD-3840. The results of the experimental program on pressure pulse propagation in piping systems performed by Stanford Research Institute are presented.

ABSTRACT

Experiments were conducted in which well-characterized pulses were generated in water-filled stainless steel piping systems consisting of a straight section of pipe, an open rectangular loop, and a closed rectangular loop. In some of the experiments, the closed loop was fitted with a standoff pipe that was filled with either water or air. The pulse shapes were typical of those expected in the secondary piping system as a result of a sodium-water reaction in a Liquid Metal Fast Breeder Reactor. The pipe thickness and diameter and the elbow radius are those typical of the Clinch River Fast Breeder Reactor reduced to 1/8-scale. Elastic piping response was stimulated (no plastic deformations). Pulse propagation behavior was monitored by pressure transducers installed in the piping wall at key locations.

The overall results show that pulse propagation behavior exhibits (1) reduction of peak pressure and impulse after traversing an elbow, (2) reduction of peak pressure, but not of impulse, after passing a filled standoff pipe, (3) annihilation when meeting an empty standoff pipe, and (4) simple pressure addition when meeting a similar pulse.

ACKNOWLEDGMENTS

This program was performed under the technical direction of Mr. Doyle Knight of the Breeder Reactor Department of the Nuclear Energy Division of General Electric.

Dexter Witherly designed the mechanical apparatus and John Busma coordinated the construction. Frederick Medlong and Mark Nelson conducted the electronic pressure measurements. Curtis Benson assembled the apparatus and constructed the explosive charges. Betty Bain and Muriel Innes carried out the data reduction.

CONTENTS

CONTENTS (Continued)

LIST OF ILLUSTRATIONS

LIST OF ILLUSTRATIONS (Continued)

LIST OF TABLES

I INTRODUCTION AND SUMMARY

A. Introduction and Objectives

In a Liquid Metal Fast Breeder Reactor (LMFBR) plant, a large sodium leak may occur that causes a sodium-water reaction of high energy release in the steam generator. The resulting pulse would propagate along the secondary piping system to the Intermediate Heat Exchanger (IHX), where the piping is coupled with the primary piping system. It is important that the pulse does not breach the primary piping loop at the IHX. As an essential part of a study to assess damage potential of pulses, a basic experimental program has been performed.

The objectives of this experimental program are to provide an understanding of pulse propagation in piping systems, establish confidence in analytical prediction techniques, and assist in interpretation of results from possible future tests with prototypical secondary piping loops.

B. Approach

In the experiments, well-characterized pulses typical of pulses expected from a sodium-water reaction were generated in three simple piping systems consisting of a straight section, an open rectangular loop, and a closed rectangular loop. Some closed loop experiments included a standoff pipe that was either completely filled or almost empty. The pulse magnitudes and piping strength resulted in elastic response (no plastic deformation). Pulse propagation was monitored by pressure transducers mounted in the pipe wall at various stations. In this way, fundamental experimental data were generated for correlation with the theoretical predictions of General Electric.

The pipe thickness and diameter and the elbow radius were those typical of the Clinch River Breeder Reactor Plant secondary system reduced to 1/8 scale. Similarly, the piping material used was 304 stainless steel, but because of the temperature difference between the operating secondary system and the experiments (400°C and 25°C), the modulus of elasticity in the experiments is higher, in the ratio 28:24. Also, water represented the liquid sodium coolant, resulting in a pipe-wave speed that was lower than the prototypical wave speed. To compensate for the difference in wave speeds, the pulse shape predicted in the sodium was scaled and adjusted to provide the same ratio of rise time to the transit time of the pulse through an elbow. This adjustment of pulse shape is based on the assertion that the influence of elbows depends primarily on ratio of pulse rise time to elbow transit time. The prototypical and experimental specifications are listed in Table 1.

In addition to the pulse designated P I, developed to match the specifications of Table 1, Pulse P II was developed having a rise time shorter than the elbow transit time, to see if greater pulse shape changes result. The main pulse characteristics are listed in Table 2. The experimental pulse shapes and scaled, idealized sodium-water reaction pulses are shown in Figure 1.

C. Experiments

Five series of experiments were performed as follows:

- Pulse shaping experiments with a pulse generator attached to a straight pipe (Fig. 2a) to develop pulses P I and P II.
- Open loop experiments (Fig. 2b), to monitor the effect of straight sections and elbows on pulse shape.
- Closed loop experiments (Fig. 2c), to study intersecting pulses.

- Filled standoff pipe experiments (Fig. 2d), to determine effect on pulse shape.
- Empty standoff pipe experiments (Fig. 2d), to determine effect on pulse shape.

From the series of experiments, twelve were selected for presentation and detailed analysis and to form the basis for conclusions. A complete list of the experiments performed is contained in Appendix A.

D. Summary of Results

The main results of the experimental program follow.

- The experimental pulse P I matched the scaled prototypical pulse in peak pressure, rise time, and the first part of the decay (Fig. 1a and Table 2). The shape around the peak pressure was rounded, but this difference is considered unimportant for achieving the program objectives. The experimental pulse P II matched the scaled prototypical pulse (adjusted only by a decrease of rise time) in peak pressure and rise time. Pulse P II had a faster decay rate (Fig. 1b), but again, this difference is considered unimportant for achieving the program objectives.
- On traversing a pipeline section containing elbows (radius of 1.5 pipe diameters), the average peak pressures and impulse* decreases per elbow for pulses P I and P II were:

Pulse	Peak Pressure	Impulse
P I	25%	25%
P II	42%	20%

The average length of section per elbow was 13.2 feet when the section contained three elbows, and 11.3 feet when the section contained two elbows.

* Throughout, impulse implies impulse per unit area.

Results indicate that the sharper the pressure peaks, the greater the reduction.

- Pressure pulses simple add to each other upon intersection.
- On passing a filled standoff pipe, the peak pressures of pulses P I and P II were reduced by 37% and 56%. The impulse change was small, so the pulse was spread over a longer duration.
- On passing an empty standoff pipe, pulses P I and P II were drastically reduced. The empty standoff pipe thus appears to be an excellent safety feature.

E. Recommendations for Future Work

To increase understanding of pulse propagation in piping systems, to assist analytical prediction techniques, and to acquire competence for interpretation of results from possible future tests with more prototypical systems, future work should include:

- Refinement of the pulse generator to reproduce more closely the scaled prototypical pulse and to provide greater versatility in the choice of pulse shape.
- Variation of pulse parameters, such as peak pressure, rise time (emphasizing very short times), and decay rate; also, peak pressure width may be important.
- Different piping anchoring systems.
- Various standoff pipe locations, chambers, and water levels to determine extent of pulse annihilation.
- Study of peak pressure reduction and use of steady-state friction coefficients for a long straight section.
- More highly instrumented elbow tests to provide more definitive data for computer code development.
- Variation of piping parameters, such as radius-to-thickness ratio and pipe diameter-to-elbow ratio.

Table 1

PROTOTYPE AND MODEL SPECIFICATIONS

Parameter	Prototype	Model
Pipe material	304 SS at 400°C	304 SS at 25°C
Young's Modulus of elasticity, E (psi)	24×10^6	28×10^6
Poisson's ratio, μ	0.31	0.31
Density, ρ (g/cm^3)	7.8	7.8
Pipe geometry		
Outside diameter, OD (in.)	24	3
Wall thickness, h (in.)	0.5	0.0625
Elbow radius, R (in.)	36	4.5
Elbow length, $\pi R/2$ (in.)	56.5	7.07
Liquid	Sodium at 400°C	Water at 25°C
Density, ρ_l (g/cm^3)	0.856	1
Bulk modulus, K (psi)	6.94×10^5	3.22×10^5
Kinematic viscosity, ν (cm^2/sec)	2.93×10^{-3}	1.0×10^{-2}
Pressure pulse		
Peak pressure, p (psi)	500	500
Rise time, t_r (msec)	3.5	0.584
Pulse length, t_o (msec)	9	1.50
Particle velocity, u (cm/sec)	246	282
Wave speed in infinite medium, c (m/sec)	2,360	1,498
Impedance in infinite medium, ρc (g/cm^2 sec)	2.02×10^5	1.50×10^5
Wave speed in pipe, a (m/sec)	1,630	1,220
Impedance in pipe, ρa (g/cm^2 sec)	1.40×10^5	1.22×10^5
Transient time through elbow, $\frac{\pi R}{2a} = \tau$ (msec)	0.881	0.147
Transient time across diameter, $D/a = \tau D$ (msec)	0.37	0.062
t_r/t_o	0.389	0.389
t_r/τ	3.97	3.97
Reynolds No. $= \frac{uD}{\nu}$	5.1×10^6	2.1×10^5
R/D	1.5	1.5
t_r/τ_D	9.5	9.

Table 2

MAIN CHARACTERISTICS OF PULSES

Pulse	Peak Pressure p (psi)	Rise Time t_r (msec)	Time Ratio[a] t_r/τ	Impulse[b] I (psi· msec)	Figure Number
1/8-scale prototype	500	0.58	3.97	375	1a
P I	500	0.50	3.40	645	1a
1/8-scale prototype (short rise time)	500	0.10	0.70	375	1b
P II	500	0.10	0.70	402	1b

[a] Transit time through elbow τ = 0.147 msec.

[b] Pressure-time integration over 1.5 msec.

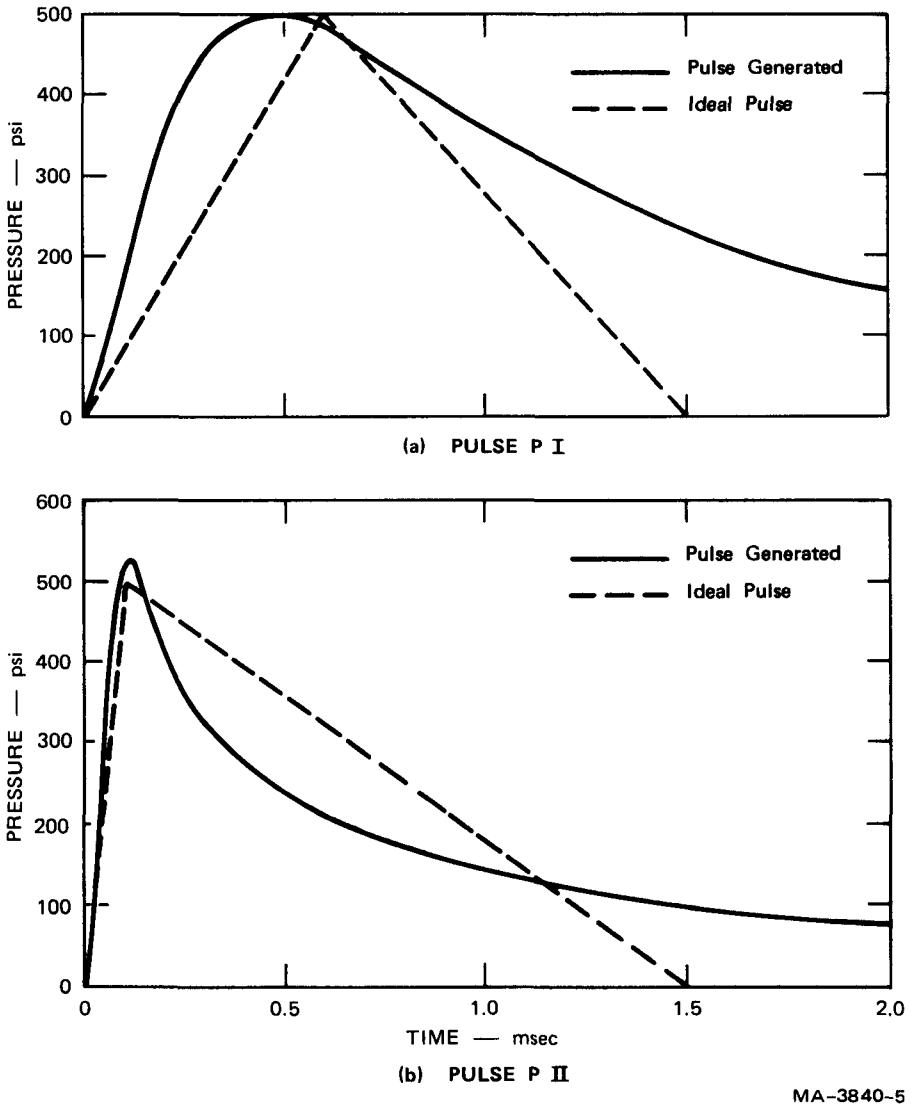

FIGURE 1 EXPERIMENTAL AND IDEAL PROTOTYPICAL PULSE SHAPES (1/8-SCALE)

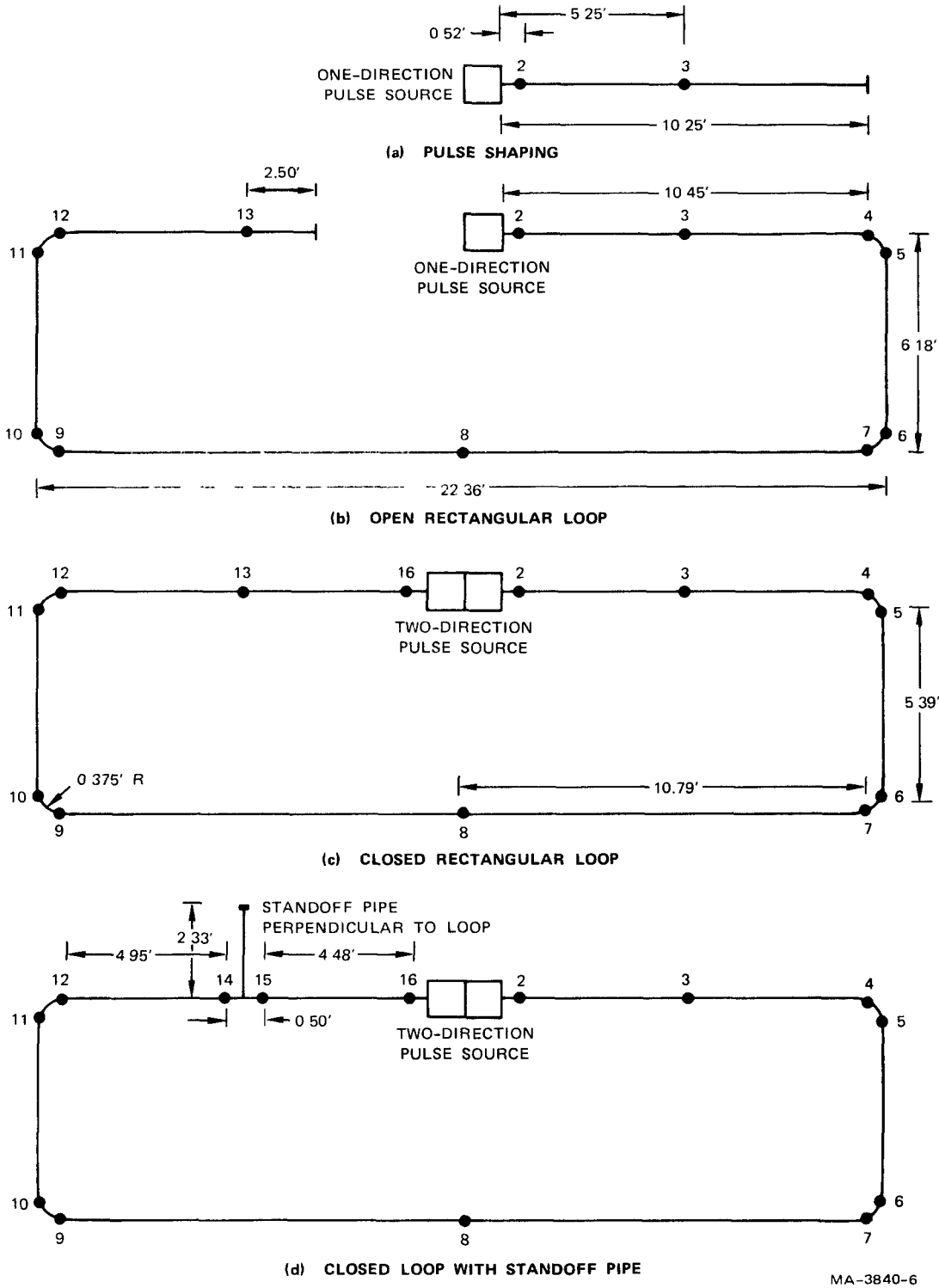

FIGURE 2 SCHEMATIC LAYOUTS OF PIPING SYSTEMS AND PRESSURE TRANSDUCER LOCATIONS (TRANSDUCERS ARRANGED SYMMETRICALLY)

II EXPERIMENTS

Well-characterized pulses were generated by controlled release of low-pressure explosive detonation gases and transmitted along water-filled stainless steel piping systems consisting of a straight section of pipe, an open rectangular loop, and a closed loop with or without a standoff pipe. Pulse behavior was determined by monitoring wall pressure at various stations. Experiments were performed to develop pulse shapes, to study intersecting pulses, and to determine the effect of filled and empty standoff pipes on pulse shapes.

A. Experimental Apparatus

1. Pressure Pulse Source

A diagram of the pressure pulse source is shown in Figure 3. Photographs of the assembled and partially disassembled pulse source are shown in Figure 4. The design parameters were based on the GASLEAK code.[1] When the charge is detonated in the canister, the gaseous detonation products are vented into the charge chamber, V_3, and expand to enter the loading chamber, V_2, through the orifices A_2, and the surroundings through the annular gap, A_3. The pressure in the loading chamber increases and reaches a peak pressure when the rate of flow into V_2 equals the rate of flow out of V_2 to the surroundings through orifice A_1. Pressure in V_2 then decays to atmospheric pressure as the gas exhausts to the surroundings through A_1 and A_3. The pressure pulse is transmitted to the water through a flexible diaphragm. Peak pressure, rise time, and duration of the pulse can be varied by changing the charge mass and the openings A_1, A_2, and A_3. For fixed chambers V_2 and V_3 and fixed openings A_1, A_2, and A_3, the peak pressure varies directly with the charge mass. The rise time of the pulse varies inversely with A_2, and the duration or decay varies inversely with A_1 and A_3.

The charge consists of a mixture of 90% PETN explosive powder and 10% plastic microspheres by weight. The powdered inert material added to the explosive powder greatly reduces the detonation pressure generated by pure explosive and consequently almost entirely eliminates the shock waves that are transmitted to the surrounding medium.[2] The charge and detonator are enclosed in a paper container placed in a canister that consists of stacked and spaced steel rings held between end plates. The canister was used for generating pulse P II but was not used for P I.

The pulse source of Figures 3 and 4 is capabile of transmitting a pulse in one direction. For the loop experiments, in which a pulse is transmitted in two opposite directions, the breech plate was removed and replaced by a mirror image pulse source.

Further details of the pressure pulse source are presented in Appendix B.

2. Piping Systems

Diagrams of the piping systems are shown in Figure 2, Section I. A photograph of the open rectangular loop system is shown in Figure 5. The piping systems comprised 3-inch outside-diameter, 1/16-inch-wall, 304 stainless steel tubing. The horizontal loop is approximately 6 by 22 feet and has 4.5-inch-radius elbows. The 2.33 ft standoff pipe, when used, was oriented vertically. The piping was mounted at each flange to a concrete foundation; a neoprene washer was placed between each flange and support bracket to permit axial strains in the piping and to avoid pipe whip. Further details of the piping system are given in Appendix B.

The water was heated to the boiling point to eliminate air bubbles, because the wave velocity is highly dependent on the percentage of entrained air.[3] The pipeline was evacuated and filled under a pressure head of approximately 8 feet of water. In the empty standoff pipe, the final water level was two inches above the top of the horizontal piping.

The theoretical wave velocity in the pipeline is given by:[3]

$$a = \frac{\sqrt{K/\rho}}{\sqrt{1 + (K/E)\ (D/e)c_1}}$$

where

K = Bulk modulus of water = 3.22×10^5 psi

ρ = Density of water = 1.94 slugs/ft^3 (1 g/cm^3)

E = Young's modulus of stainless steel = 28×10^6 psi

D = Inside pipe diameter = 2.875 inches

e = Pipe wall thickness = 0.0625 inches

c_1 = Constant for Poisson's ratio effects

= $5/4 - \mu$ for a pipe free to move axially

μ = Poisson's ratio of stainless steel = 0.31.

The calculated velocity is 3997 ft/sec (1218 m/sec). A comparison of theoretical and experimental wave velocities is made in Appendix C.

B. Instrumentation

Pressure transducers mounted in the pipe wall at various locations monitored water pressure as a function of time and by comparison of consecutive transducer records, monitored pulse behavior on propagation. Figure 2 shows the locations of the pressure transducers for each type of experiment. All pressure pulses were recorded on magnetic tape. Figure 6 shows printouts from the magnetic tape recordings of five gages in one of the experiments.

In addition to the magnetic tape records, oscilloscope records were obtained from a few selected gages to provide immediate results. Figure 7 shows oscillograms from one of the experiments.

A detailed description of the instrumentation is given in Appendix B.

C. Experimental Program

A total of 60 experiments were conducted, categorized as

- 19--pulse shaping (PS201-PS219)
- 8--open loop (E401-E408)
- 17--closed loop (L301-L317)
- 10--closed loop with a filled standoff pipe (L318-L325, L330, L331)
- 6--closed loop with an empty standoff pipe (L326-L329, L332, L333)

A complete list of experiments is given in Appendix A. From these experiments, the results of 12 were selected for presentation in Section III. Experiments performed to establish the degree of reproducibility and symmetry (for closed loops) are described in Appendix C.

1. Pulse Shaping (PS201-PS219)

In the pulse-shaping experiments, the one-direction pulse source connected to a ten-foot length of pipe was used, as shown in Figure 2a. The first 13 experiments had a pressure transducer at the gage 2 position only. Gage 3 was added for the next 6 experiments. In these experiments pulse shapes P I and P II (Figure 1) were developed by varying charge mass and orifice areas.

2. Open Loop (E401-E408)

In the open rectangular loop experiments, the one-direction pressure pulse source connected to an approximately 53 feet long pipe was used, as shown in Figure 2b. Twelve gages, in positions 2 through 13 monitored the behavior of input pulse shapes P I and P II. Two experiments were carried out to determine the effect of placing a known size air bubble in the system. The results of these experiments are described in Appendix D.

3. Closed Loop (L301-L317)

In the closed rectangular loop experiments, the two-direction pulse source was used to send simultaneous pulses in opposite directions. The piping system was the same as that for the open loop experiments with approximately three feet of pipe added to complete the loop, as shown in Figure 2c. Thirteen gages were located symmetrically about the source, the odd gage (gage 8) being located where the two pulses meet. These experiments allowed investigation of intersecting pulses.

4. Closed Loop With Filled Standoff Pipe (L318-L325, L330, L331)

In these experiments, a vertical standoff pipe was attached by a T-fitting to the closed rectangular loop, as shown in Figure 2d. The standoff pipe material, radius, and thickness were the same as for the loop piping and was 2.33 feet long. The end of the standoff pipe was fitted with a blank flange. Fourteen gages were used to monitor pulse behavior. The interaction of the pulse with the standoff pipe was investigated by comparison with results from loops without a standoff pipe and by comparison of the two pulses propagating in each standoff pipe experiment.

5. Closed Loop With Empty Standoff Pipe (L326-L329, L332, L333)

By use of the same apparatus as that used in the filled standoff pipe experiments (Figure 2d), the water level in the vertical standoff pipe was located two inches above the top of the horizontal piping, leaving a 2.04-feet long column of air in the remaining part of the vertical pipe; the end was again fitted with a blank flange. Fourteen gages were used to monitor pulse behavior. The interaction of the pulse with the standoff pipe was investigated by comparison of the two pulses propagating in each standoff pipe experiment.

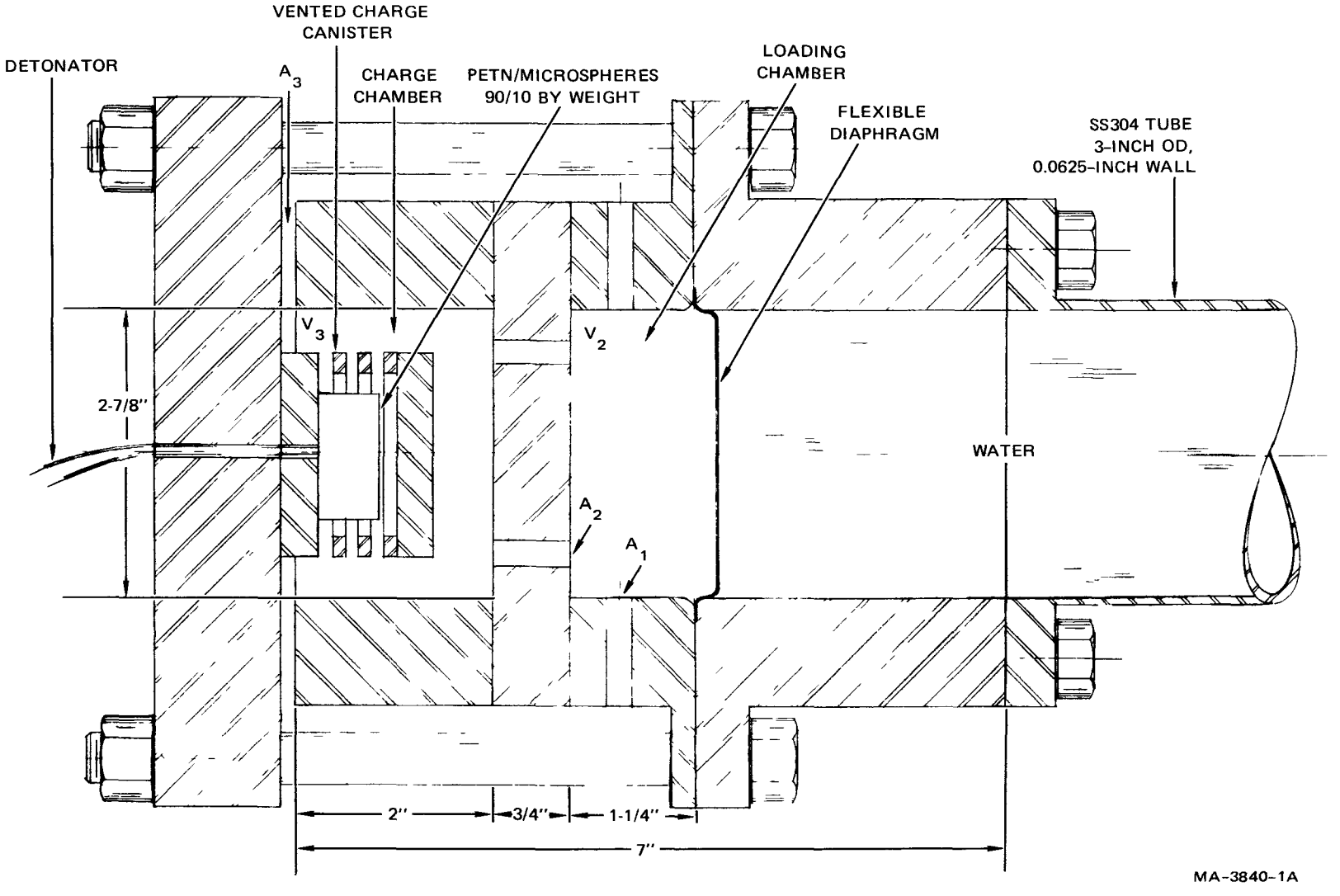

FIGURE 3 ONE-DIRECTION PRESSURE PULSE SOURCE

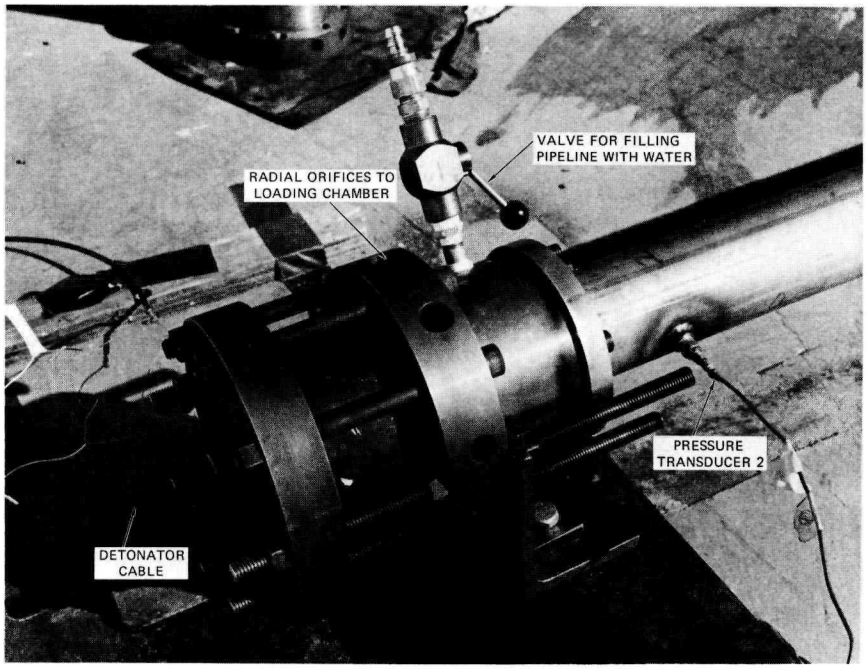

(a) ASSEMBLED PULSE SOURCE

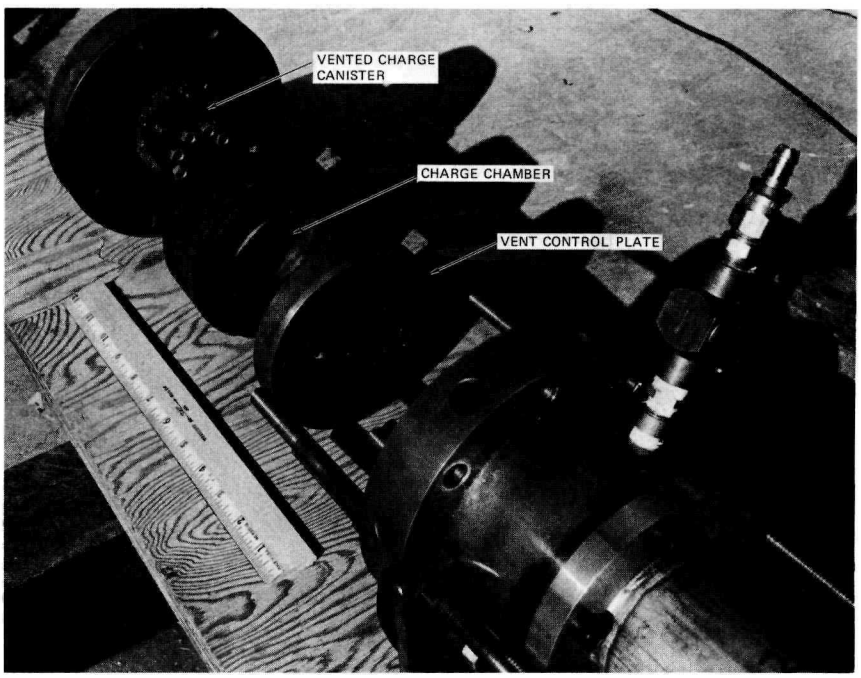

(b) PARTIALLY DISASSEMBLED PULSE SOURCE

MP-3840-7

FIGURE 4 PHOTOGRAPHS OF THE ONE-DIRECTION PULSE SOURCE

MP-3840-8

FIGURE 5 PIPING SYSTEM FOR THE OPEN RECTANGULAR LOOP EXPERIMENTS

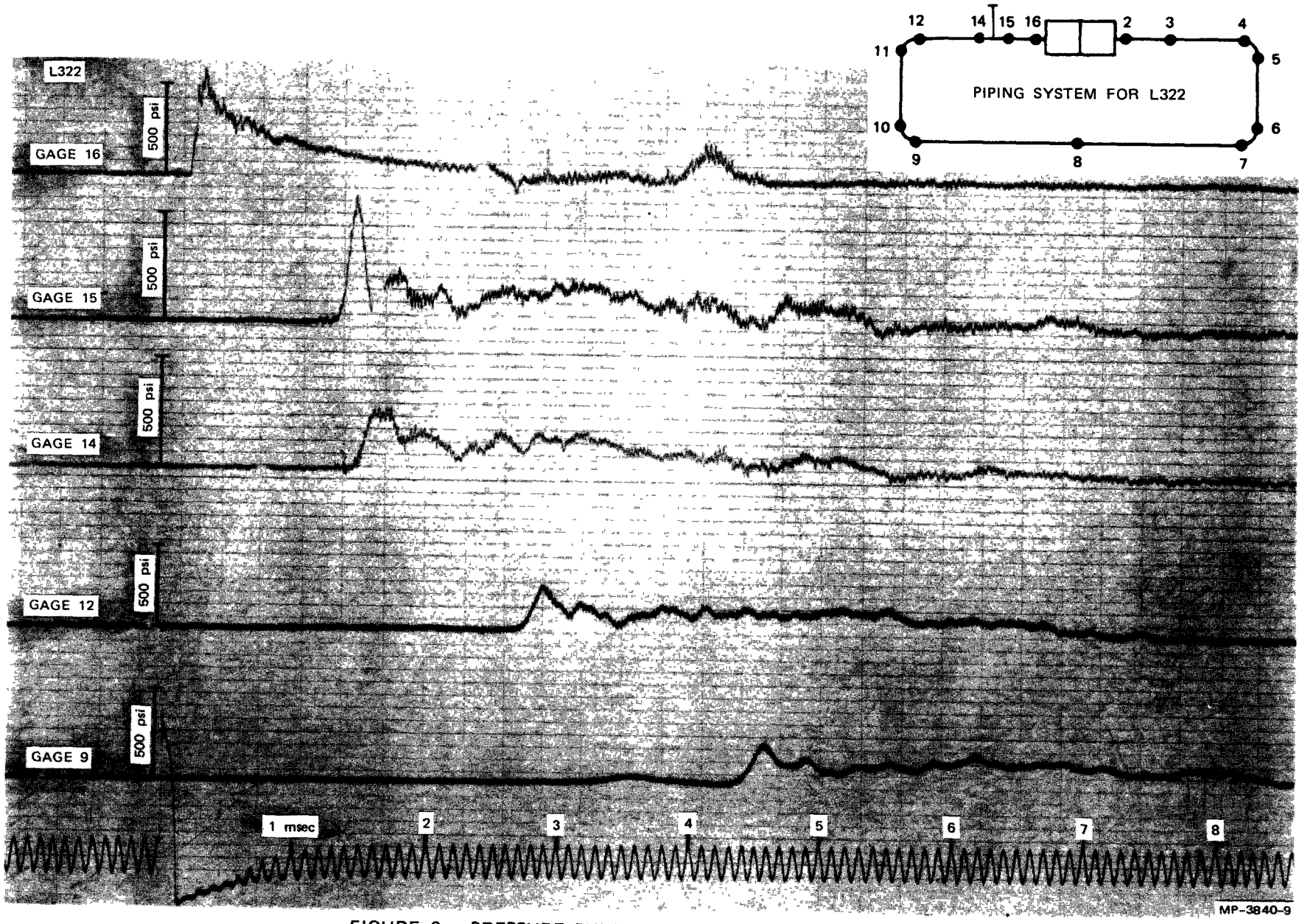

FIGURE 6 PRESSURE PULSE DATA FROM EXPERIMENT L322

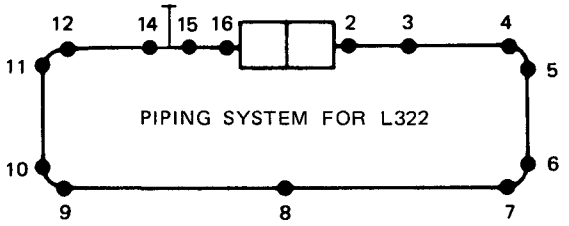

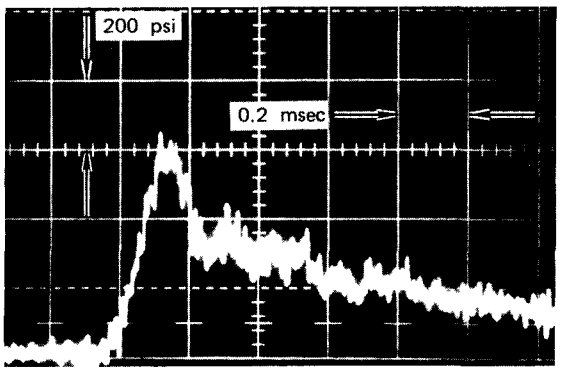

(a) GAGE 3

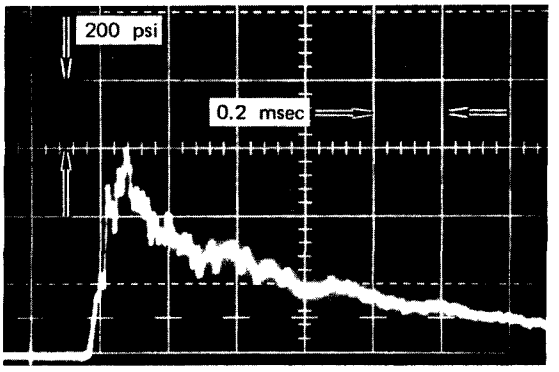

(b) GAGE 16

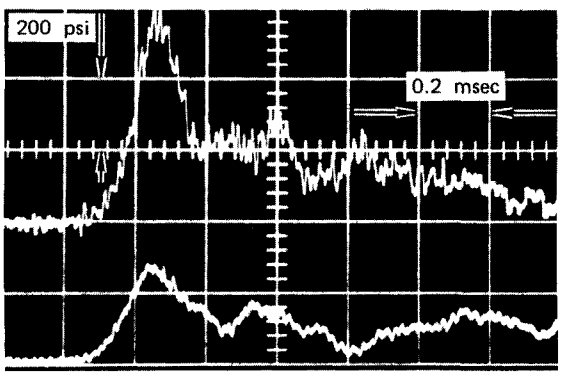

(c) GAGE 4 (UPPER TRACE)
GAGE 12 (LOWER TRACE)

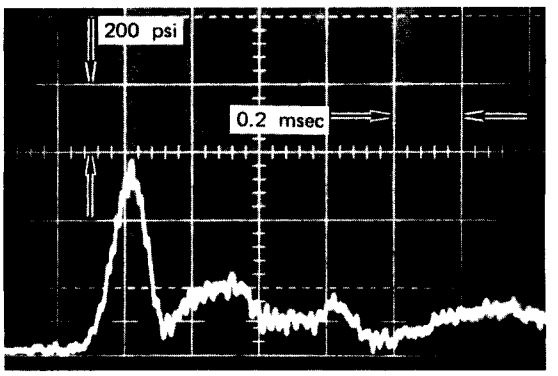

(d) GAGE 15

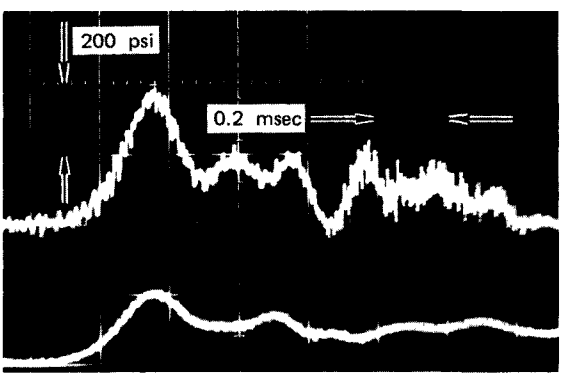

(e) GAGE 7 (UPPER TRACE)
GAGE 9 (LOWER TRACE)

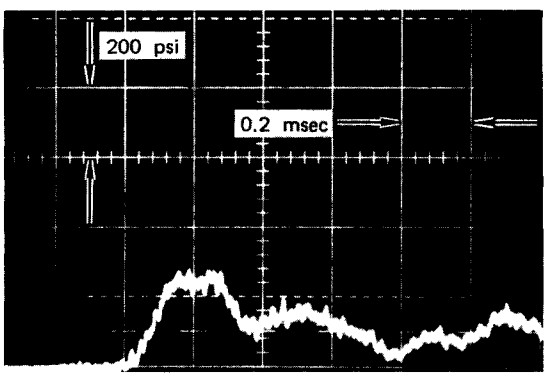

(f) GAGE 14

MP-3840-10

FIGURE 7 OSCILLOGRAM PRESSURE PULSE DATA FROM EXPERIMENT L322

III EXPERIMENTAL RESULTS

In Table 3 are listed the twelve experiments selected for detailed analysis. One experiment with pulse P I and one with pulse P II were selected for each of the four types of piping systems: (1) the open rectangular loop, (2) the closed rectangular loop, (3) the closed loop with filled standoff pipe, and (4) the closed loop with empty standoff pipe. In addition, four repeat experiments were selected to illustrate reproducibility of results. Pressure-time records at each gage location for each of the 12 experiments are given in Appendix E. The results of the experimental program follow.

A. Pulse Shaping

The pulse shapes P I and P II, shown in the oscillograms of Figure 8, were obtained from gage 3, located 5.25 feet from the diaphragm of the pulse generator. A comparison of the pulses with the scaled predicted prototypical pulses is made in Table 2 and Figure 1, Section I. Digitized listings of the pulses suitable for computer code use are given in Appendix F.

Pulse P I was developed to match the peak pressure, the ratio of rise time to transient time through an elbow, and the scaled duration of the prototypical pulse. Figure 1a shows that the peak pressures are the same and that the rise time of pulse P I (and therefore the ratio of rise time to transient time through an elbow) is about 14% lower than the prototype value. The shape around the peak pressure of pulse P I is rounded, but this difference was considered unimportant for achieving the program objectives.

Pulse P II was developed to provide a pulse with a rise time much shorter than the transient time through an elbow to determine if greater pulse shape changes result. In Table 2 and Figure 1b, Section I, pulse P II is compared with the 1/8-scale prototype pulse adjusted to provide the shorter rise time. The peak pressures and the time ratios are the same. Pulse P II decays faster than the prototype pulse, but this difference was considered unimportant for achieving the program objectives.

A third pulse shape, P III, with a higher peak pressure but almost the same rise time as pulse P II, was used in two experiments. A detailed analysis performed on one of these experiments gave results similar to the results from the corresponding experiments with pulse P II. The pulse P III results are presented in Appendix C.

B. Pulse Attenuation in Pipelines

The results of the open and closed rectangular loop experiments are used to measure attenuation of propagating pulses. Attenuation is described by the decrease in peak pressure and by the decrease in impulse* (area under the pressure-time plot). Peak pressure and impulse are important characteristics in assessing damage potential of pulses. Impulse is defined here as the integral of the pulse pressure of the time interval 0 to 2.5 msec, that is,

$$\text{Impulse} = \int_0^{2.5\ \text{msec}} p\ dt$$

The duration of 2.5 msec was chosen as the upper limit of the integral instead of the time when the pressure returns to zero, because reflected

*Throughout, impulse implies impulse per unit area.

pulses returned to some gage locations shortly after 2.5 msec. Also, this duration is comparable with the input pulse duration. In assessing attenuation, impulse deemphasizes the large pressure spikes that occurred in some pulses.

The pressure pulse plots in Figures 9 and 10 illustrate the behavior of pulses P I and P II in the open rectangular loop experiments. The peak pressures decrease and the shapes broaden as the pulses propagate. Pressure pulse plots for all twelve gages for these experiments are contained in Appendix E.

Figures 11 and 12 show the attenuation of the normalized peak pressures and the impulses of pulses P I and P II in an open rectangular loop. Normalization is with respect to values at the gage 3 location. Pressure transducers located immediately after the elbows measured pressures higher than expected. It is suspected that the pressure at these locations was not uniform over the pipe cross-section because of elbow effects and that the gages experienced the highest pressure, because they were located on the outside of the elbows. Consequently, measurements from gages located downstream from the elbows were used to measure attenuation.

The measured attenuation of peak pressure and of impulse for pulses P I and P II are given in Table 4. For the open rectangular loop experiments, E402 and E404, the attenuation was measured between gages 3 and 11, which is a 39.4-foot section of pipe containing three elbows, and between gages 3 and 8, which is a 22.6-foot section of pipe containing two elbows. (See Figure 2b, Section I). For the closed loop experiments, L303, L304, and L305, the attenuation was measured between gages 3 and 8 and between gages 13 and 8, each of which is a 22.6-foot section of pipe containing two elbows. It was assumed that the two similar pulses intersecting at gage 8 simply added; later in this

section, this assumption is shown to be true. Gage 8 malfunctioned in the closed loop experiment L317 with pulse P I, so an attenuation calculation for pulse P I was made only for experiment E402.

Table 4 shows that for pulse P I, the average decreases in peak pressure and impulse per elbow are approximately 25%; the decreases are slightly higher when averaged over three elbows than when averaged over the first two elbows.

For pulse P II, the average decreases in peak pressure and impulse per elbow are approximately 42% and 20%; the decrease of peak pressure is slightly lower when averaged over three elbows than when averaged over the first two elbows.

Definitive measurements of attenuation in linear sections will be made in a following experimental program.

C. Addition of Two Intersecting Pulses

The closed rectangular loop experiments are used to determine the resulting pressure of two intersecting similar pulses. In Figure 13, the combined pressures at the point of intersection are shown for pulse shapes P I and P II, from the closed loop experiments L307 and L305, and the combined pressures are compared to twice the pressure of similar pulses from open loop experiments E402 and E404. Experiment L307 was used in place of experiment L317 in this measurement because gage 8 malfunctioned in L317. For both pulse shapes, the comparison plots are similar with only minor differences in the generated pulses, so it can be concluded that intersecting pulses simply add.

D. Attenuation of Pulses by a Filled Standoff Pipe

In Figures 14 and 15, pulses are compared at symmetrical locations in the piping system. The pulse monitored by gages 16, 14, 11, and 9 passed the filled standoff pipe, and the pulse monitored by gages 2,

3, 5, and 7 did not pass a standoff pipe. The plots of gages 2 and 16 for pulse P I in Figure 14a show that the input pulses propagating in opposite directions were almost the same. The pulse P II measured at gage 16 in experiment L332 shown in Figure 15a did not decay as rapidly as expected. From results of pulse shape measurements in similar experiments it was concluded that gage 16 malfunctioned in L332, and the actual pulse decayed according to the pulse measured by gage 2.

A comparison of the plots for gages 14 and 3 (Figures 14b and 15b) shows that the filled standoff pipe reduced the peak pressures of pulses P I and P II by 37% and 56%. For pulse P I, a second peak was formed with a higher pressure than the first peak. The second peak was displaced from the first peak by 1.16 msec, which is the time taken for a pulse to propagate up the 2.33 foot standoff pipe, reflect from the cap, and return to the piping loop. For pulse P II, the pulse reflected in the standoff pipe did not produce a peak as high as the first peak. The difference in behavior is due to the greater decay rate of P II, so that pulse P I was at a higher pressure than P II when the reflected pulse arrived. The plots from gages 11 and 9 show that the pulses maintained their relative shapes after attenuation by the standoff pipe.

Figures 16 and 17 show the influence of the filled standoff pipe on the peak pressure and impulse attenuation of pulses P I and P II. Although the peak pressure of pulse P I and especially of pulse P II were substantially attenuated, the impulse changes were small.

E. Attenuation of Pulses by an Empty Standoff Pipe

Figures 18 and 19 show the influence on imput pulses P I and P II of the empty standoff pipe with a water level 3.5 inches above the center line of the loop. The gage 14 plot for the P I pulse in Figure 18b shows that the attenuated pulse began like the normal pulse but was chopped off after about 0.5 msec, which was the time taken by the

pulse to traverse the 7 inches to the water surface and back. The low pressure pulse continued to propagate with further attenuation past the empty standoff pipe. The gage 14 plot for the P II pulse in Figure 19b also shows a small pulse after passing the standoff pipe and the plots of gages 11 and 9 show further attenuation. Figures 20 and 21 show the normalized peak pressures and impulses for the normal and attenuated P I and P II pulses and further illustrate the effectiveness of an empty standoff pipe for pulse attenuation.

Table 3

EXPERIMENTS SELECTED FOR DETAILED ANALYSIS

Experiment Number	Pulse Designation	Type of Experiment[a]	Figure Number
E402	P I	Open Rectangular Loop	9, 11, 13, C3, E1
E404	P II	Open Rectangular Loop	10, 12, 13, C3, E2
L317	P I	Closed Rectangular Loop	C3, C4, E6
L305	P II	Closed Rectangular Loop	13, C2, C3, C4, E5, F2
L330	P I	Closed Loop with Filled Standoff Pipe	14, 16, C1, E10
L322	P II	Closed Loop with Filled Standoff Pipe	15, 17, E7
L332	P I	Closed Loop with Empty Standoff Pipe	18, 20, E12, F1
L328	P II	Closed Loop with Empty Standoff Pipe	19, 21, E9
L325	P I	Repeat of L332	C1
L331	P I	Repeat of L330	C1, E11
L303	P II	Repeat of L305	C2, E3
L304	P II	Repeat of L305	C2, E4

[a] Experiments L325, L331, L303, and L304 were performed to demonstrate reproducibility.

Table 4

ATTENUATION OF PULSES IN PIPELINE SECTIONS[a]

Pulse[b]	Experiment No.	Average Attenuation per Elbow (%)		Number of Elbows	Average Length of Section per Elbow (ft)
		Peak Pressure	Impulse		
P I	E402	26	28	3	13.2
P I	E402	24	22	2	11.3
P II	E404	37	23	3	13.2
P II	E404	43	17	2	11.3
P II	L303	44	21	2[c]	11.3
P II	L304	44	22	2	11.3
P II	L305	40	16	2	11.3

[a]Characteristics of the pipe material and geometry are given in Table 1, Section I.

[b]Pulse characteristics are given in Table 2 and illustrated in Figure 1, Section I.

[c]For each closed loop experiment, both pulses are used.

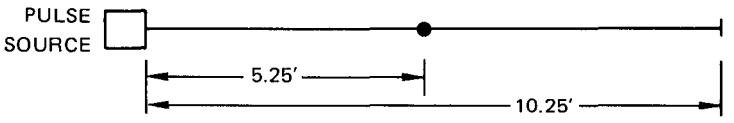

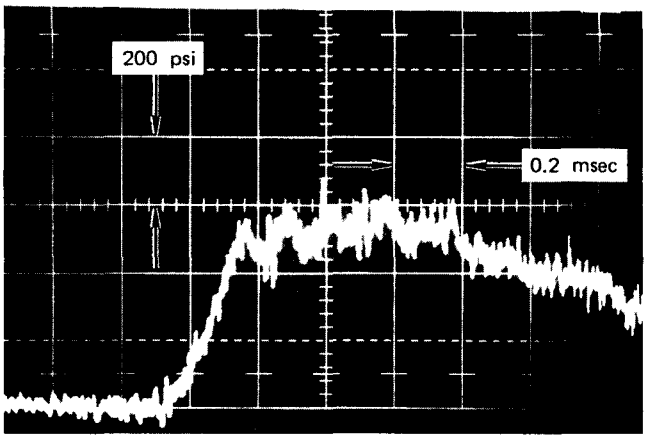

(a) P I

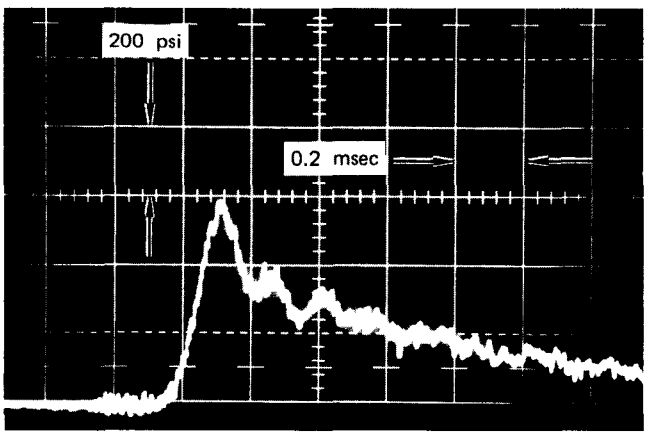

(b) P II

MP-3840-11

FIGURE 8 PULSE SHAPES P I AND P II AT THE GAGE 3 LOCATION

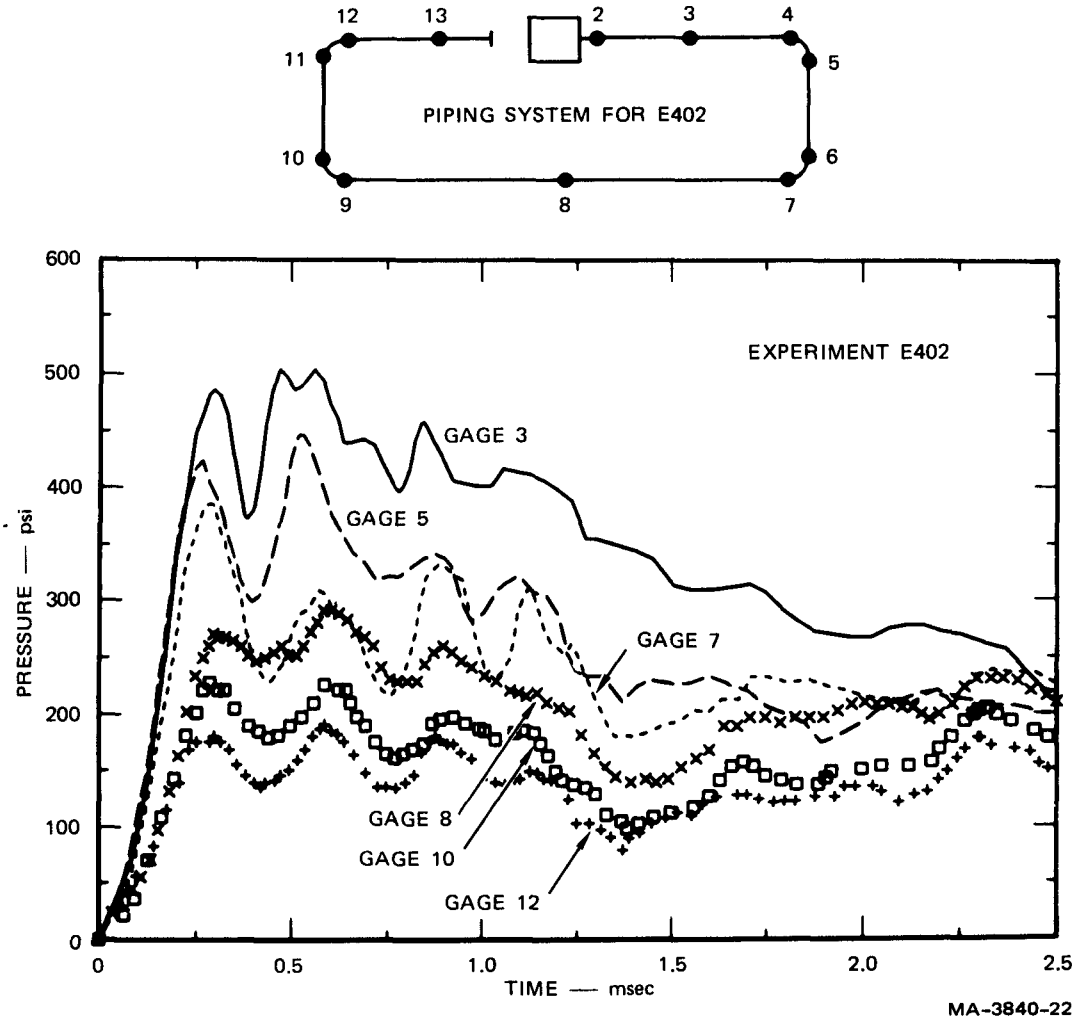

FIGURE 9 ATTENUATION OF PULSE P I IN AN OPEN LOOP

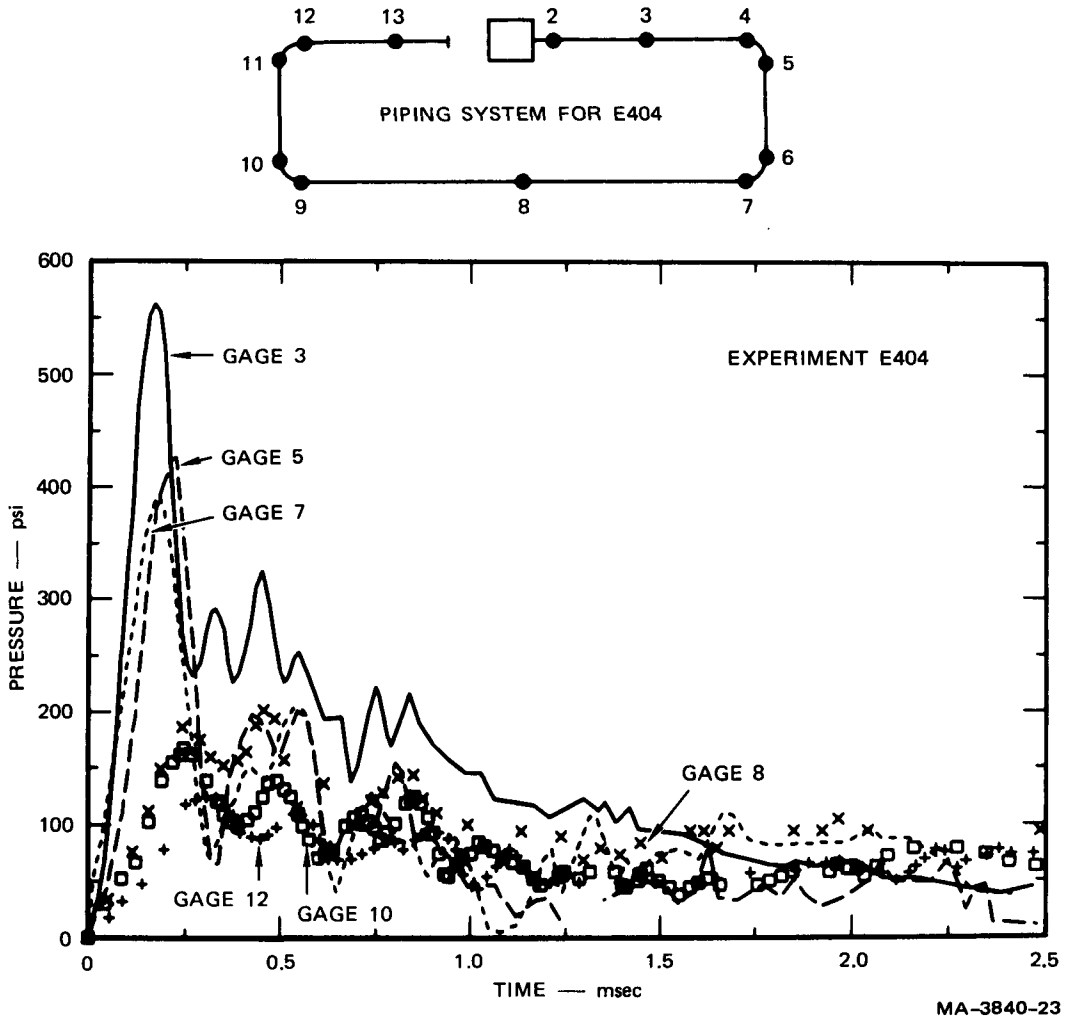

FIGURE 10 ATTENUATION OF PULSE P II IN AN OPEN LOOP

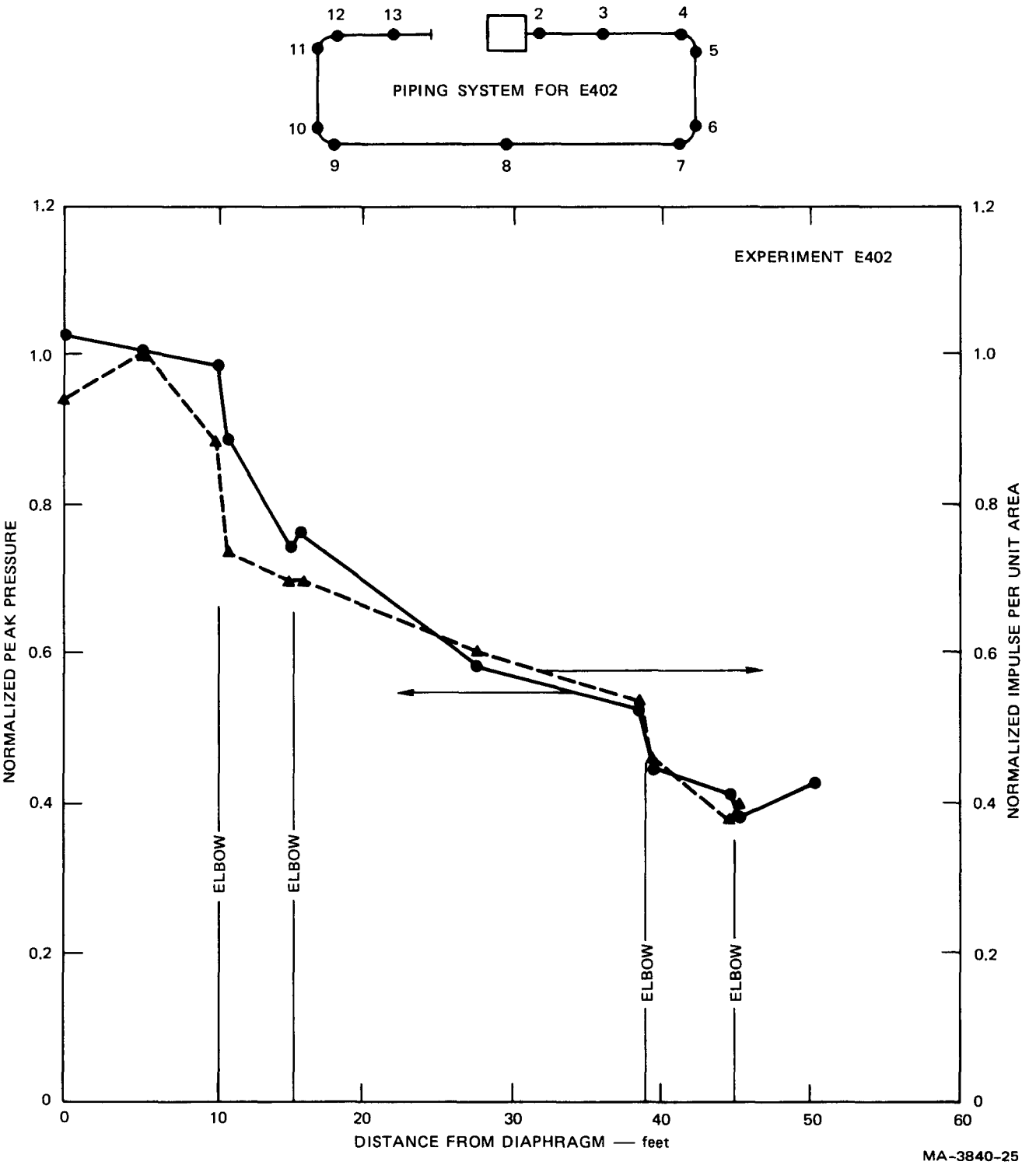

FIGURE 11 MEASUREMENTS OF THE ATTENUATION OF PULSE P I IN AN OPEN LOOP

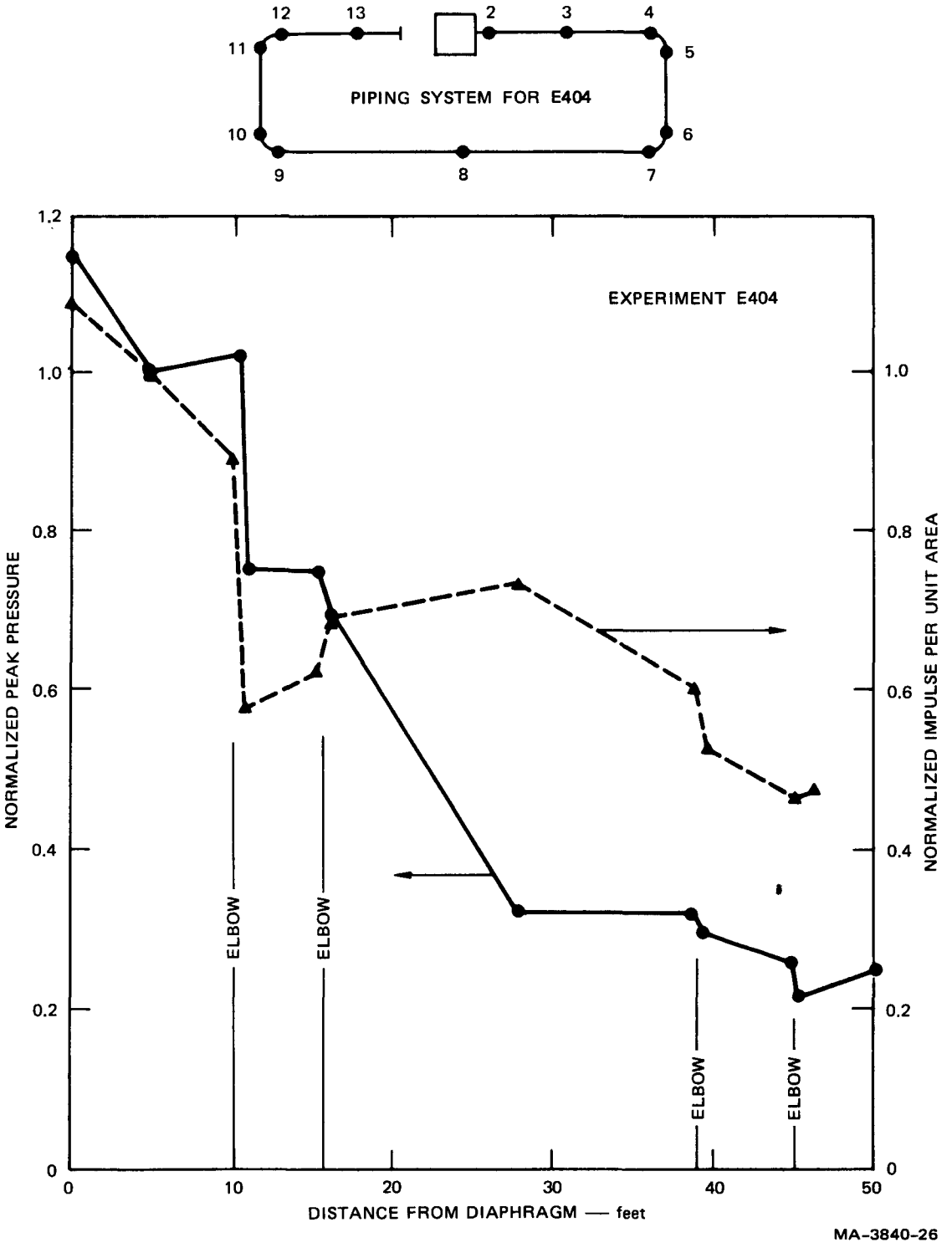

FIGURE 12 MEASUREMENTS OF THE ATTENUATION OF PULSE P II IN AN OPEN LOOP

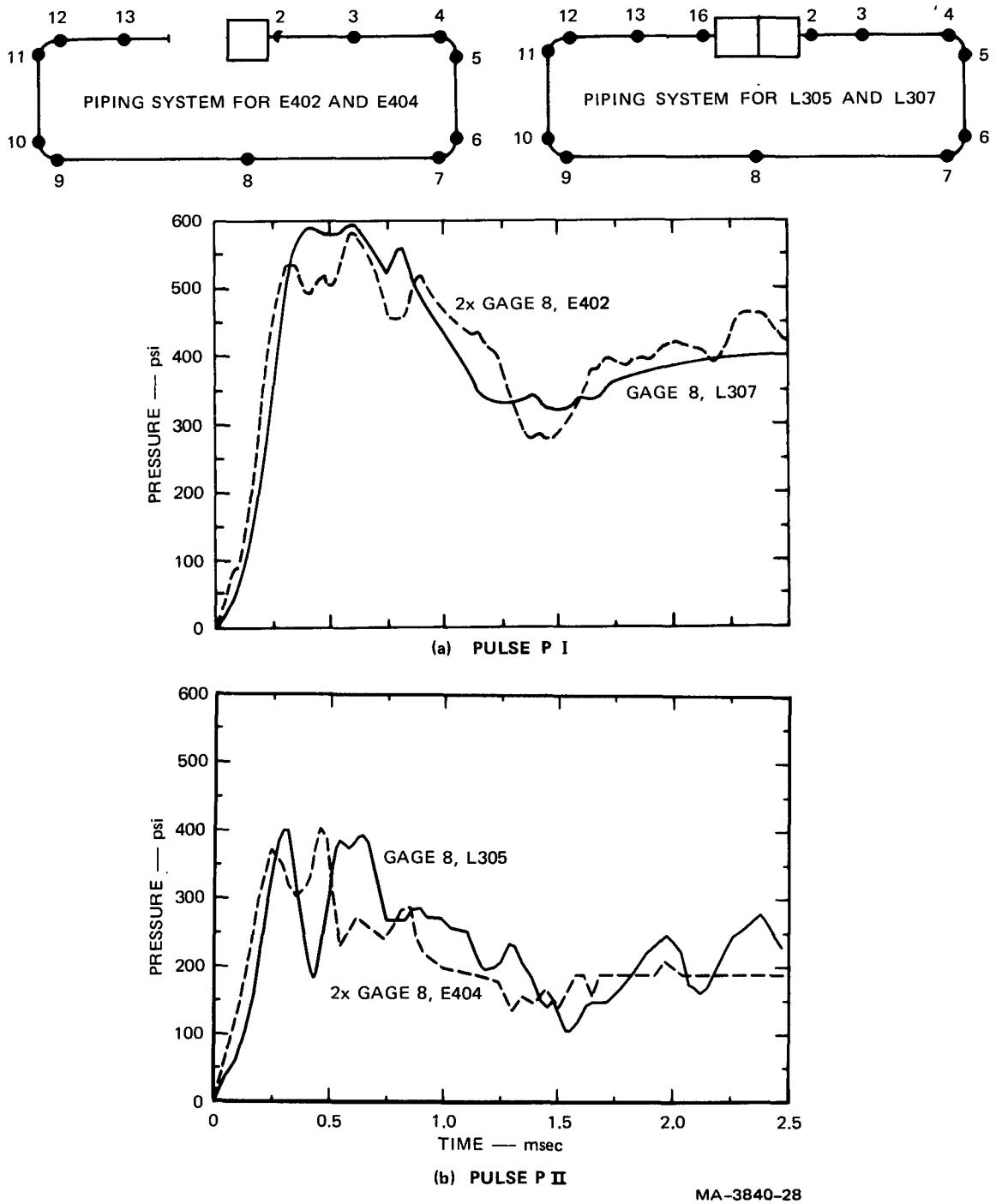

FIGURE 13 ADDITION OF TWO INTERSECTING PULSES

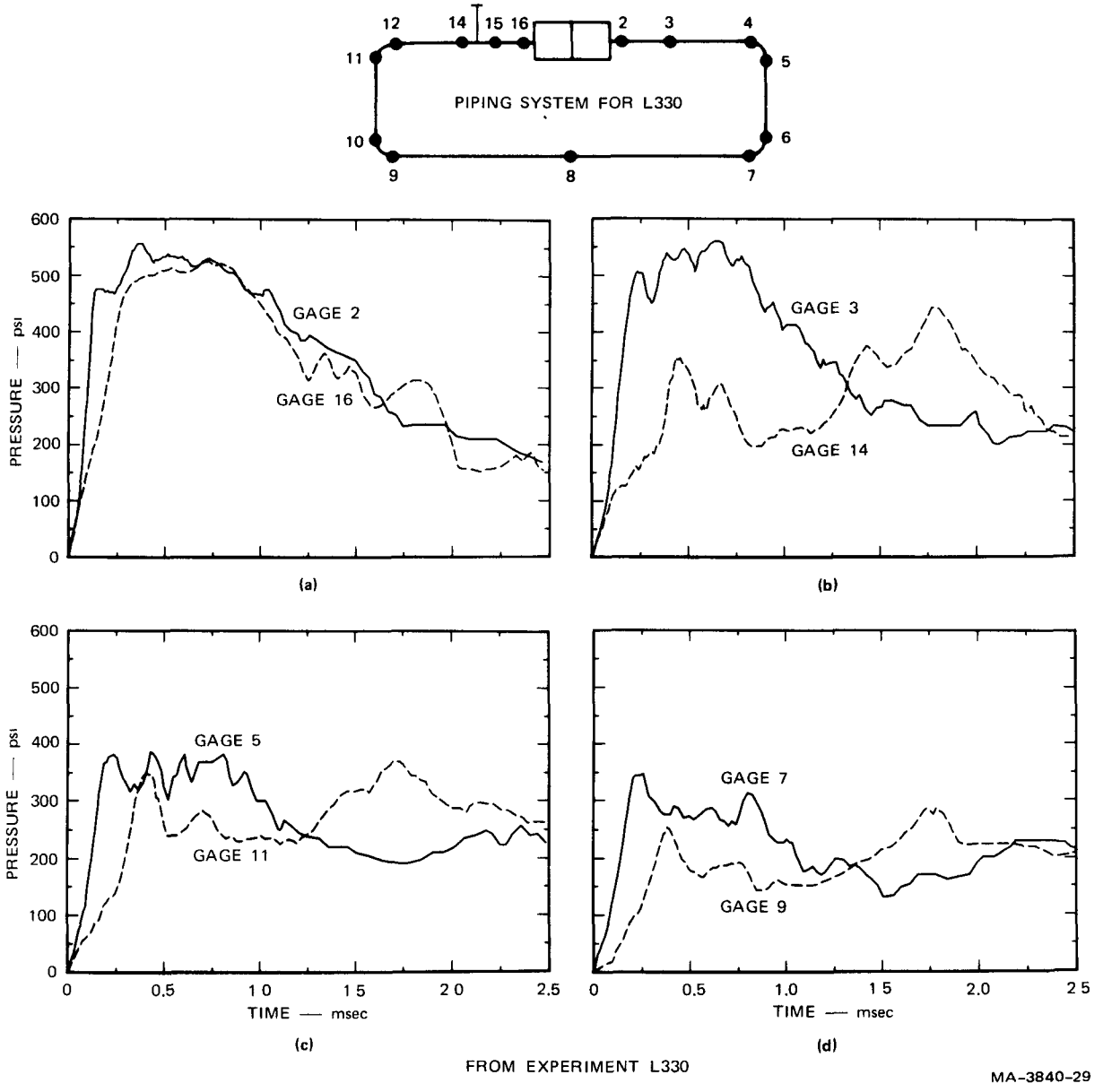

FIGURE 14 ATTENUATION OF PULSE P I PASSING A FILLED STANDOFF PIPE

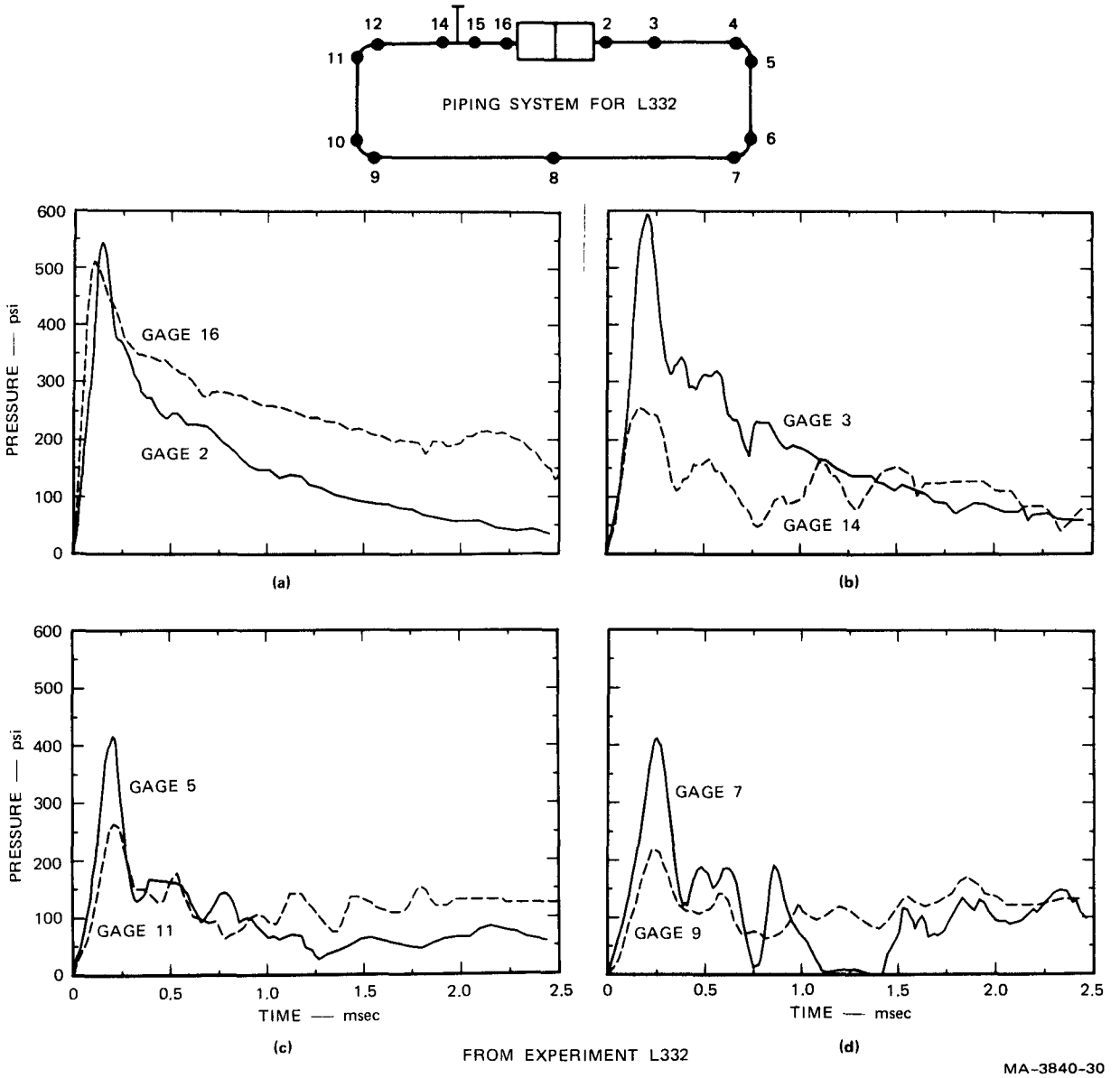

FIGURE 15 ATTENUATION OF PULSE P II PASSING A FILLED STANDOFF PIPE

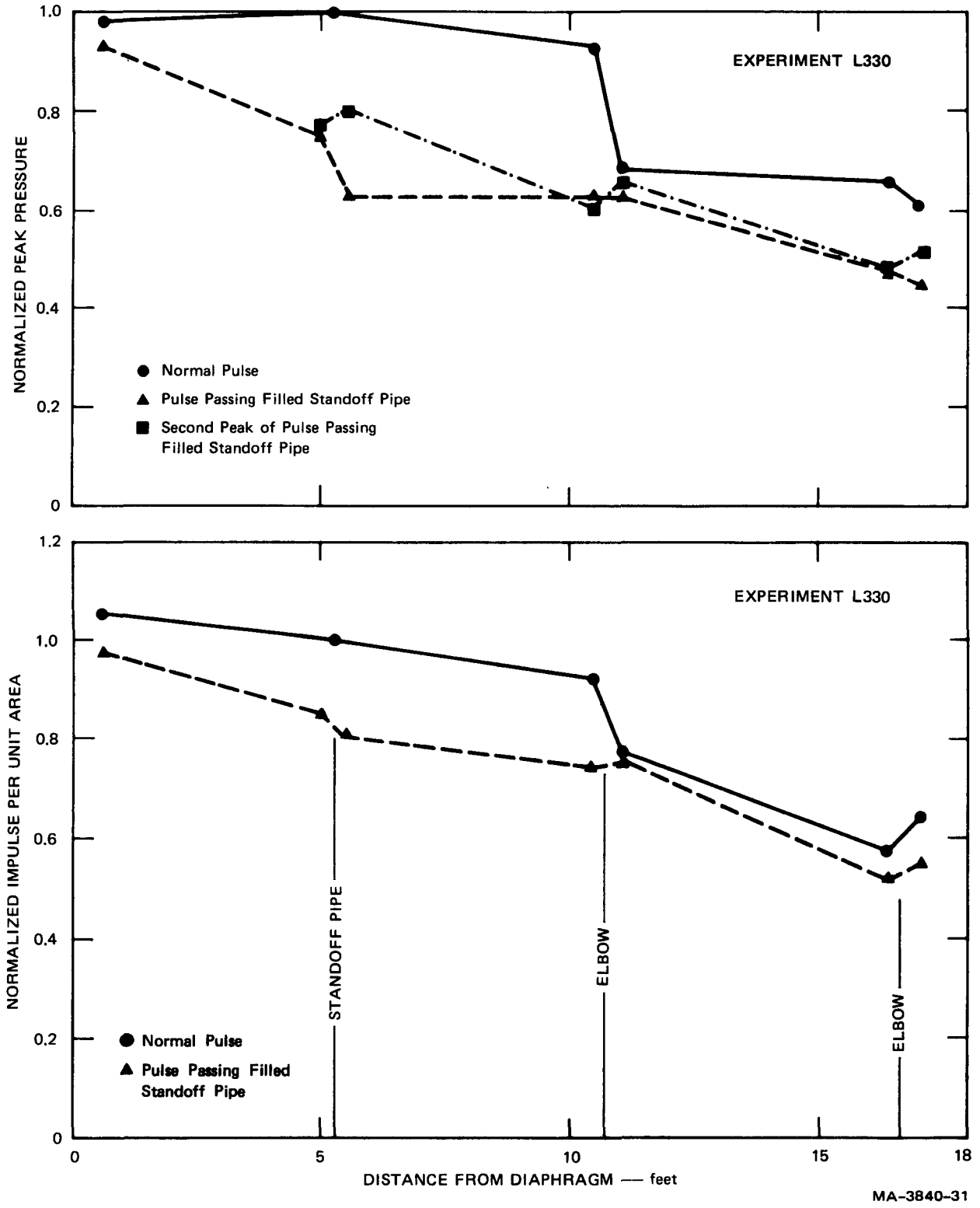

FIGURE 16 MEASUREMENTS OF THE ATTENUATION OF PULSE P I PASSING A FILLED STANDOFF PIPE

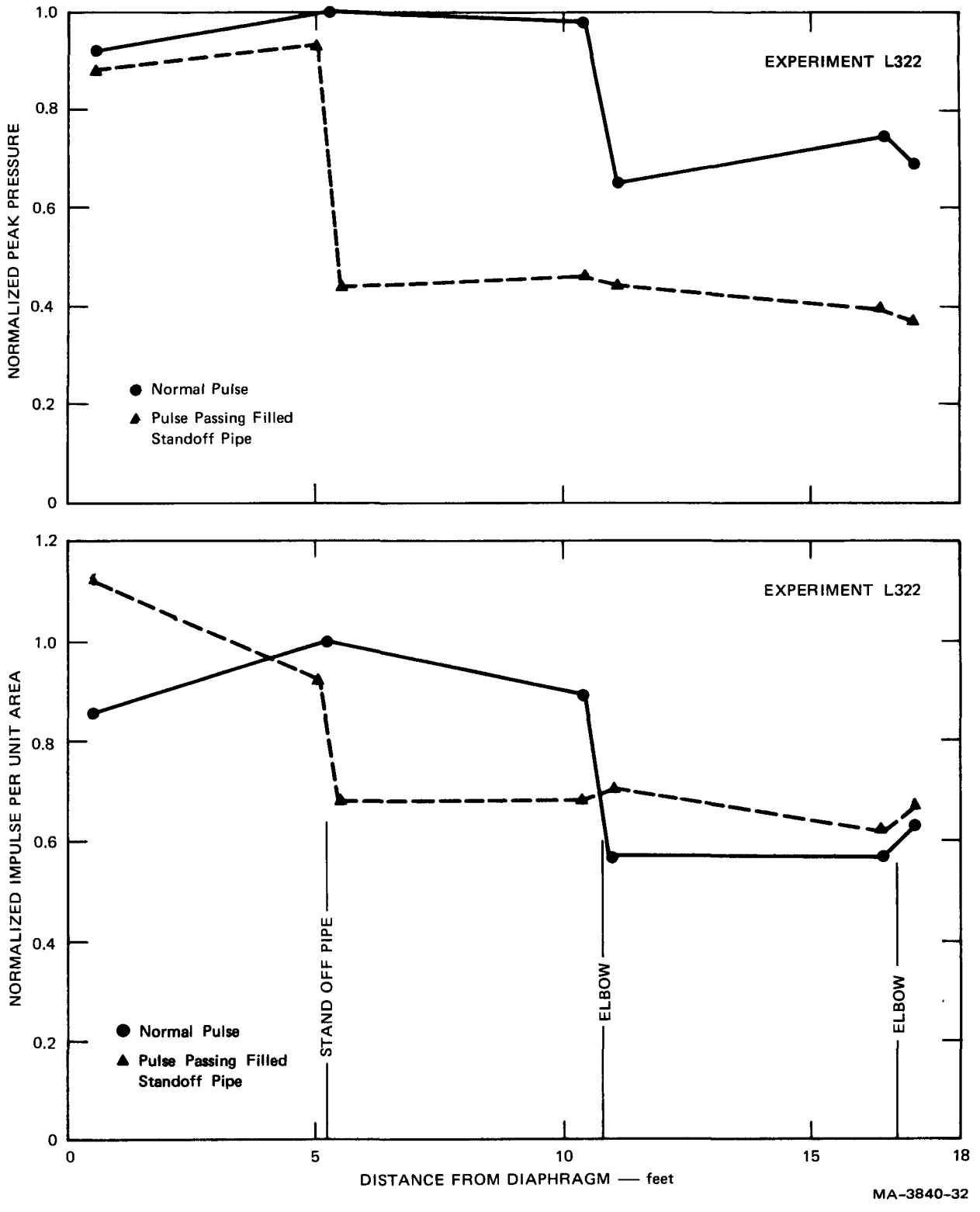

FIGURE 17 MEASUREMENTS OF THE ATTENUATION OF PULSE P II PASSING A FILLED STANDOFF PIPE

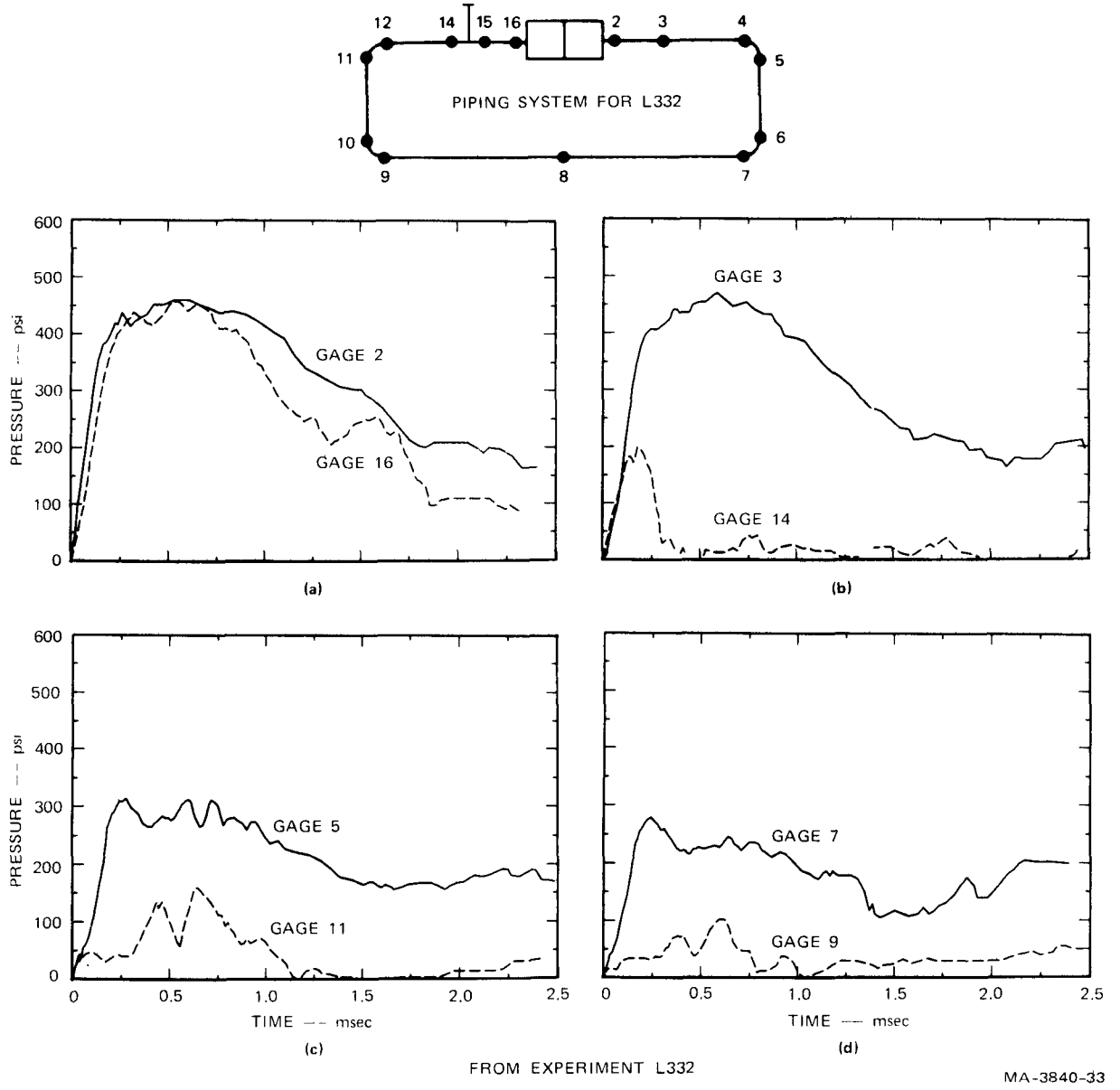

FIGURE 18 ATTENUATION OF PULSE P I PASSING AN EMPTY STANDOFF PIPE

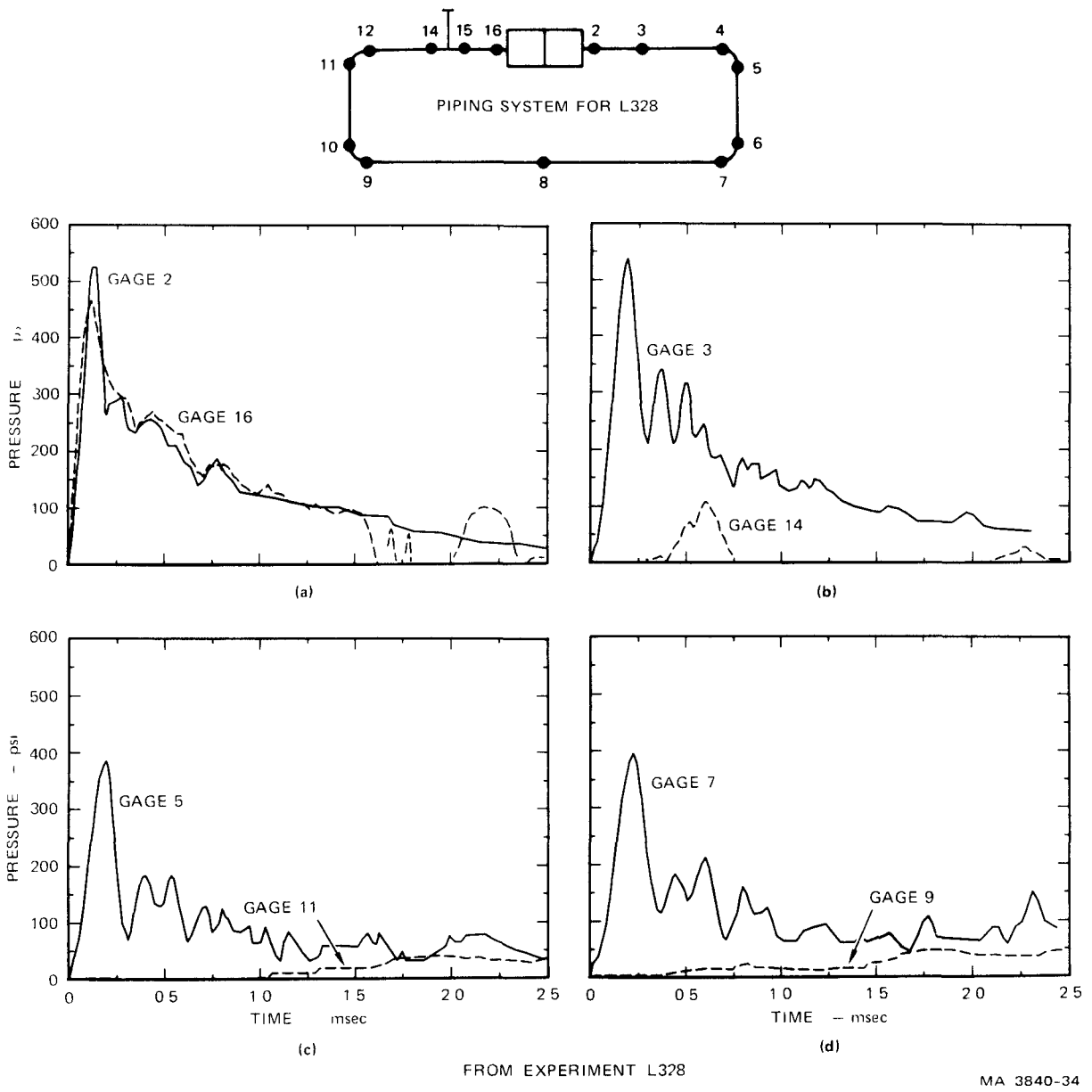

FIGURE 19 ATTENUATION OF PULSE P II PASSING AN EMPTY STANDOFF PIPE

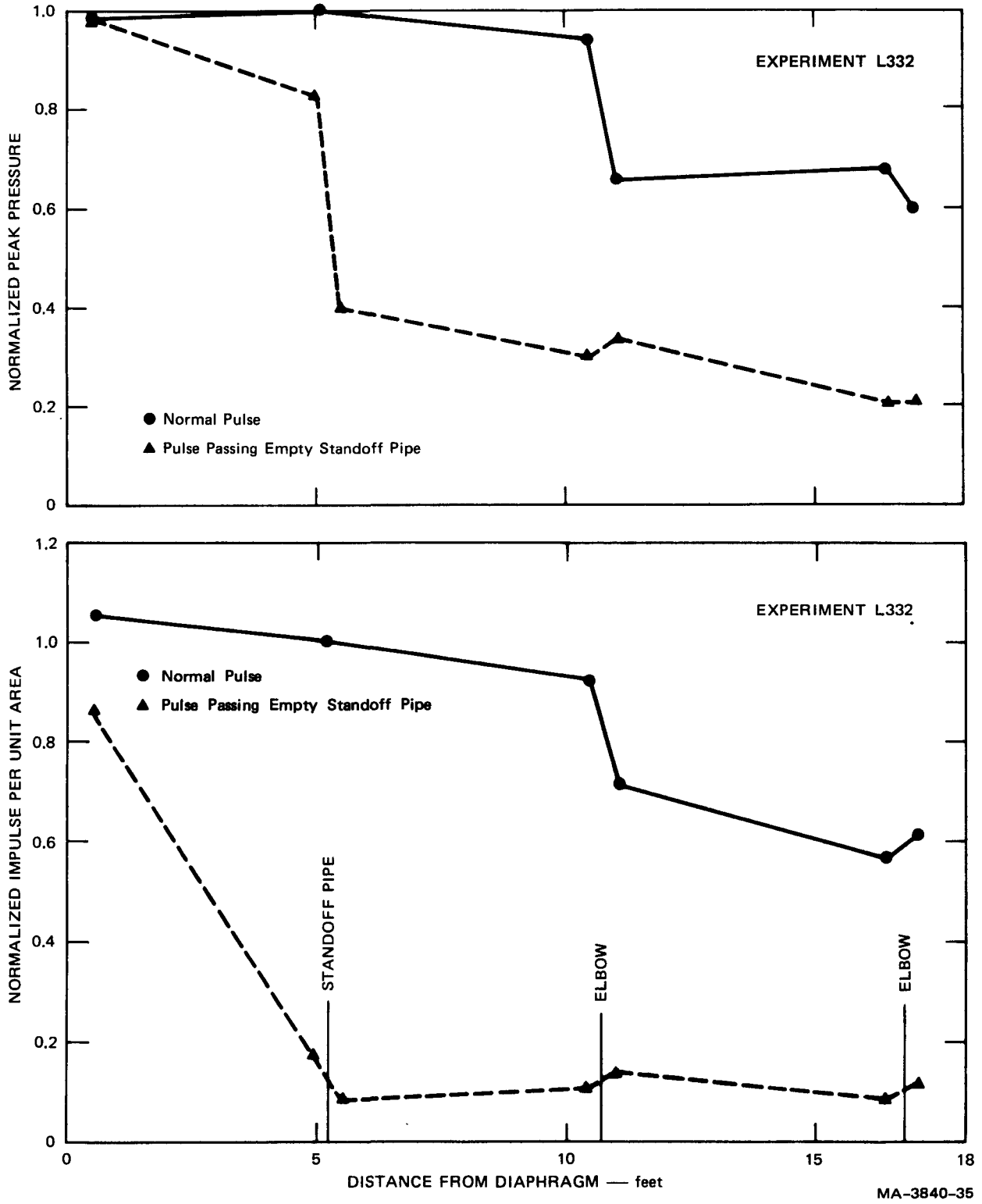

FIGURE 20 MEASUREMENTS OF THE ATTENUATION OF PULSE P I PASSING AN EMPTY STANDOFF PIPE

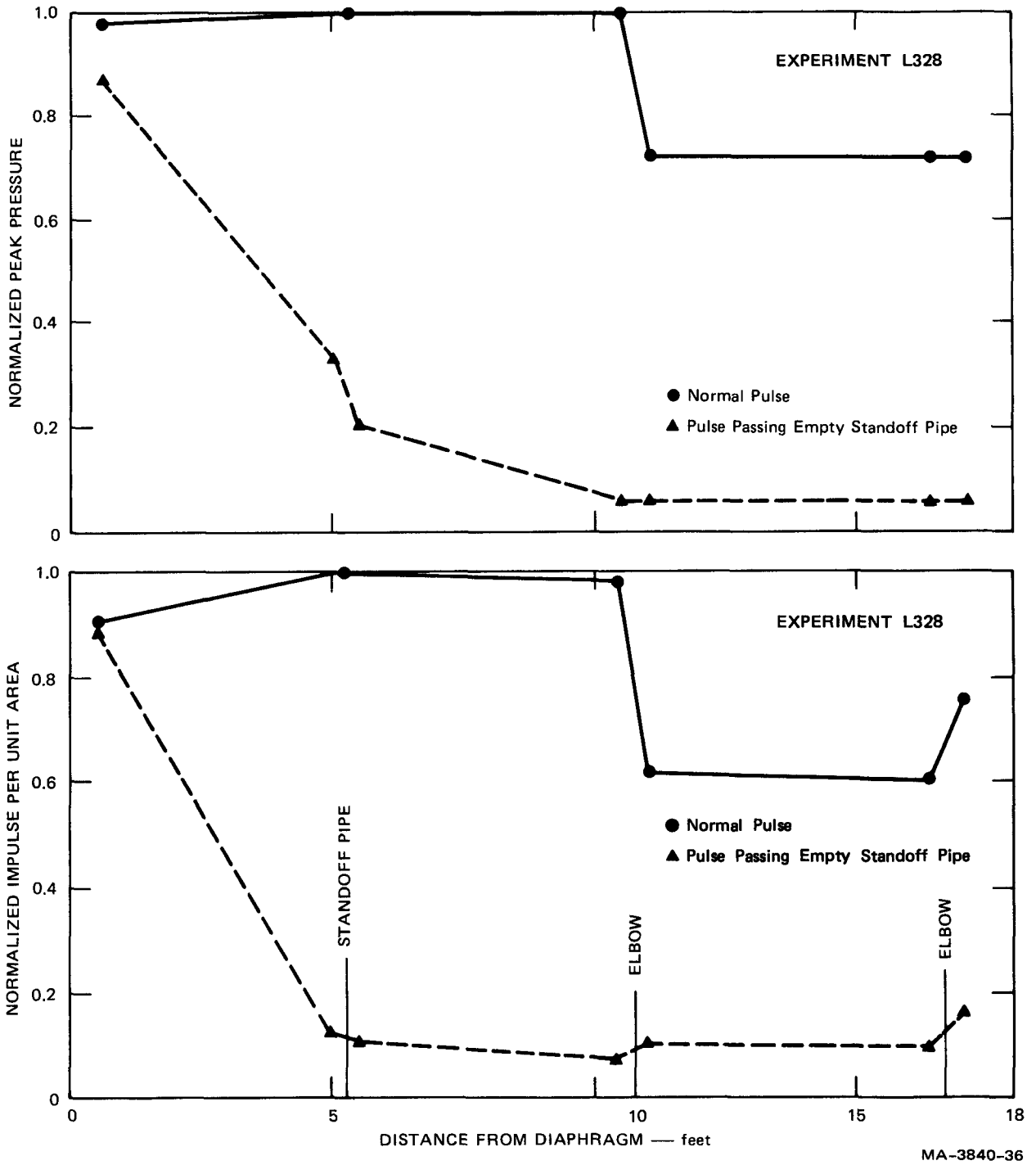

FIGURE 21 MEASUREMENTS OF THE ATTENUATION OF PULSE P II PASSING AN EMPTY STANDOFF PIPE

REFERENCES

1. Cagliostro, D. J. and T. J. Marciniak, "A Pressure Source for Loading Subassembly Ducts," to be presented at the Third SMIRT Conference, London, September 1-5, 1975.

2. Cagliostro, D. J., A. L. Florence, and G. R. Abrahamson, "Characterization of an Energy Source for Modeling Hypothetical Core-Disruptive Accidents in Nuclear Reactors," Nuclear Engineering and Design, Vol. 27, p. 94 (March 1974).

3. Streeter, V. L. and E. B. Wylie, "Hydraulic Transients," McGraw-Hill Book Company, New York (1967).

Appendix A

LIST OF EXPERIMENTS

Table A-1 lists and briefly describes each of the sixty experiments performed. The experiments are categorized as

- Pulse shaping (PS201-PS219)
- Open rectangular loop (E401-E408)
- Closed rectangular loop (L301=L317)
- Closed loop with filled standoff pipe (L318-L325, L330, L331)
- Closed loop with empty standoff pipe (L326-L329, L332, L333)

Table A-1

LIST OF EXPERIMENTS

Experiment Number	Purpose of Experiment	90/10 Charge Mass (g)	Charge Mass in Detonator (g)	A_1[a] (cm^2)	A_2 (cm^2)	A_3 (cm^2)	Canister Used	Peak[b] Pressure (psi)	Rise Time (msec)	Remarks
PS201	Pulse shaping for Pulse I	1.2	~ 0.3	2.33	2.27	6.64	No	~ 400	~ 0.3	Signal noisy
PS202	Repeat of PS201	1.2	~ 0.3	2.33	2.27	6.64	No	~ 400	~ 0.3	Signal noisy
PS203	Use insulated gage in place of uninsulated gage	1.2	~ 0.3	2.33	2.27	6.64	No	300	0.3	Signal much improved
PS204	Use lower energy electrical detonating unit	1.2	~ 0.3	2.33	2.27	6.64	No	350	0.3	Signal slightly improved from PS203
PS205	Repeat of PS204	1.2	~ 0.3	2.33	2.27	6.64	No	400	0.4	
PS206	Effect of 65/35 explosive in place of 90/10	1.8[c]	~ 0.3	2.33	2.27	6.64	No	450	0.4	Results similar to PS205
PS207	Pulse shaping for Pulse II	3.5	~ 0.3	1.43	18.10	4.19	No	~ 1600	?	Too much charge
PS208	Pulse shaping for Pulse I	3.2	~ 0.3	2.33	2.27	6.64	No	650	0.3	Increased charge mass from PS205 to increase peak pressure
PS209	Repeat of PS208	3.2	~ 0.3	2.33	2.27	6.64	No	650	0.3	
PS210	Repeat of PS209	3.2	~ 0.3	2.33	2.27	6.64	No	650	0.4	Pulse very flat at peak
PS211	Pulse shaping for Pulse II	0.9	~ 0.3	1.43	18.10	4.19	No	700	0.1	
PS212	Repeat of PS211	0.9	~ 0.3	1.43	18.10	4.19	No	700	0.1	
PS213	Repeat of PS212	0.9	~ 0.3	1.43	18.10	4.19	No	700	0.1	Good reproducibility of results
PS214	Pulse shaping for Pulse I	6.1	~ 0.3	2.33	1.14	6.64	No	650	0.35	Halved A_2 from PS210 to increase rise time
PS215	Repeat of PS214	6.1	~ 0.3	2.33	1.14	6.64	No	650	0.3	
PS216	Determine effect of canister around charge for Pulse II	0.8	~ 0.3	1.43	18.10	4.19	Yes	600	0.1	Canister greatly reduced signal noise for Pulse II
PS217	Pulse shaping for Pulse II	0.8	0.15	1.43	18.10	4.19	Yes	600	0.1	Reduced and standardized charge in detonator
PS218	Pulse shaping for Pulse I	2.0	0.15	0	2.28	6.64	No	550	0.4	Closed A_1 from PS215 to increase rise time
PS219	Determine effect of canister around charge for Pulse I	2.0	0.15	0	2.28	6.64	Yes	550	0.4	Canister did not affect Pulse I signal
L301	Closed loop test for Pulse I	2.0	0.15	0	1.52	6.64	No	420	0.4	Two pulses not uniform. Suspect bubble in line
L302	To improve Pulse I shape	2.0	0.15	0	1.52	4.19	No	450	0.4	Reduced A_3 to increase rise time
L303	Closed loop test for Pulse II	0.7	0.15	1.43	18.10	4.19	Yes	580	0.15	Good test for Pulse II behavior in simple loop
L304	Repeat of L303	0.7	0.15	1.43	18.10	4.19	Yes	540	0.15	
L305	Repeat of L304	0.7	0.15	1.43	18.10	4.19	Yes	580	0.15	Good reproducibility
L306	Pulse shaping for Pulse I	2.0	0.15	0	2.28	3.32	No	600	0.5	Increased A_2 and decreased A_3 from L302
L307	Pulse shaping for Pulse I	1.7	0.15	0	2.28	3.32	No	550	0.5	Decreased charge mass to reduce peak pressure
L308	Repeat of L307	1.7	0.15	0	2.28	3.32	No	650	0.45	Unsatisfactory reproducibility
L309	To improve Pulse I shape	2.0	0.15	0	1.14	2.10	No	450	0.4	Two pulses not uniform. Suspect bubble in line
L310	To improve Pulse I shape	2.0	0.15	0	1.14	3.32	No	400	0.5	Suspect bubble in line
L311	Repeat of L309	2.0	0.15	0	1.14	2.10	No	450	0.5	Pulse flat at peak. Suspect bubble in line
L312	To improve Pulse I shape	3.5	0.15	0.72	1.14	2.10	No	700	0.3	Decreased rise time instead of desired increase

Table A-1 (concluded)

Experiment Number	Purpose of Experiment	90/10 Charge Mass (g)	Charge Mass in Detonator (g)	A_1 (cm^2)	A_2 (cm^2)	A_3 (cm^3)	Canister Used	Peak Pressure (psi)	Rise Time (msec)	Remarks
L313	To improve Pulse I shape	3.0	0.15	0	1.14	6.64	No	500	0.5	Suspect bubble in line
L314	To improve Pulse I shape	4.0	0.15	0	0.57	4.19	No	450	0.4	Air bubble out of line but pulse unsatisfactory
L315	To improve Pulse I shape	3.0	0.15	0	1.20	6.64	No	500	0.5	2 larger holes for A_2 replaced 6 small holes in L313
L316	To improve Pulse I shape	2.0	0.15	0	1.80	6.64	No	500	0.3	Not as good as L315 pulse
L317	Repeat of L315	3.0	0.15	0	1.20	6.64	No	560	0.5	This pulse is Pulse I in remaining experiments
L318	Closed loop with filled standoff pipe, Pulse I	3.0	0.15	0	1.20	6.64	No	500	0.4	Suspect air bubble in line
L319	Repeat of L318	3.0	0.15	0	1.20	6.64	No	500	0.4	Suspect air bubble in line
L320	Repeat of L319	3.0	0.15	0	1.20	6.64	No	450	0.4	Suspect air bubble in line
L321	Closed loop with filled standoff pipe, Pulse II	0.7	0.15	1.43	18.10	4.19	Yes	550	0.1	Suspect air bubble in line
L322	Repeat of L321	0.7	0.15	1.43	18.10	4.19	Yes	590	0.15	Good test
L323	Repeat of L322	0.7	0.15	1.43	18.10	4.19	Yes	550	0.1	Good reproducibility
L324	Closed loop with filled standoff pipe, Pulse I	3.0	0.15	0	1.80	6.64	No	500	0.3	Left 3 holes open for A_2 instead of 2
L325	Repeat of L320	3.0	0.15	0	1.20	6.64	No	500	0.45	
L326	Closed loop with empty standoff pipe, Pulse I	3.0	0.15	0	1.20	6.64	No	600	0.4	
L327	Repeat of L326	3.0	0.15	0	1.20	6.64	No	450	0.4	Unsatisfactory reproducibility
L328	Closed loop with empty standoff pipe, Pulse II	0.7	0.15	1.43	18.10	4.19	Yes	530	0.15	
L329	Repeat of L328	0.7	0.15	1.43	18.10	4.19	Yes	550	0.1	Good reproducibility
L330	Repeat of L325	3.0	0.15	0	1.20	6.64	No	530	0.5	
L331	Repeat of L330	3.0	0.15	0	1.20	6.64	No	550	0.55	Fairly good reproducibility
L332	Repeat of L327	3.0	0.15	0	1.20	6.64	No	470	0.5	
L333	Repeat of L332	3.0	0.15	0	1.20	6.64	No	500	0.4	Fair reproducibility of L326, L327, L332, and L333
E401	Open loop, Pulse I	3.0	0.15	0	1.20	6.64	No	500	0.35	
E402	Repeat of E401	3.0	0.15	0	1.20	6.64	No	500	0.45	Fairly good reproducibility
E403	Open loop, Pulse II	0.7	0.15	1.43	18.10	4.19	Yes	550	0.1	
E404	Repeat of E403	0.7	0.15	1.43	18.10	4.19	Yes	560	0.15	Good reproducibility
E405	Open loop, Pulse III	0.7	0.15	1.43	--	4.19	Yes	850	0.1	Rise time greater than desired
E406	Repeat of E405	0.7	0.15	1.43	--	4.19	Yes	850	0.15	Good reproducibility
E407	Determine effect of air bubble next to diaphragm	0.7	0.15	1.43	18.10	4.19	Yes	550	0.1	2.5 cm^3 air bubble injected next to diaphragm
E408	Determine effect of air bubble at gage 3	0.7	0.15	1.43	18.10	4.19	Yes	550	0.1	Confirm speculation that air bubbles were affecting pulses in some of the previous tests

[a] The orifice areas given are for a one direction pulse source. When the two direction pulse source is used (experiments with "L" prefix), A_1 is the area of each loading chamber exhaust orifice, A_2 is the area of each vent orifice between the charge chamber and the loading chambers, and A_3 is one-half of the area of the charge chamber exhaust orifice.

[b] Peak pressure and rise time were measured at gage 3 (or gage 2 for PS201-PS210) see Fig. 2 in Section I.

[c] The explosive in this test was a mixture of 65% PETN and 35% glass microballoons by weight.

Appendix B

PRESSURE PULSE SOURCE, PIPING SYSTEM, AND INSTRUMENTATION

B.1 Pressure Pulse Source

The one-direction pulse generator assembly used for tests with the straight pipe and open rectangular loop is shown in Figure B-1. A diagram of the generator is shown in Figure 3, Section II.

The basic components, from left to right in Figure B-1, are:

- Rigid end plate to withstand the reaction forces
- Vented charge canister attached to the end plate by a bolt through which the detonator leads pass
- Explosive or charge chamber
- Vent control plate (also shown in Figure B-2)
- Loading or expansion chamber (also shown in Figure B-3)
- Diaphragm backup plate
- Bellofram rolling diaphragm seal at the gas/water interface
- Water filled transition chamber extending from the diaphragm to the piping system (also shown in Figure B-4)

Photographs of the one-direction pulse source are shown in Figure 4, Section II.

The pulse shape (peak pressure, rise time, and pulse duration) is controlled by the charge mass and by the relative magnitudes of explosive chamber volume (V_3), the loading chamber volume (V_2), and the three venting areas (A_3, A_2, and A_1). For the pulse generator shown in Figure B-1, the following dimensions apply:

V_3 - The explosive chamber volume with the vent gap A_3 closed is 213 cm^3 minus the solid volume of the canister, 65 cm^3 (when a canister is used). The volume V_3 is increased 10.6 cm^3 for each 0.1-inch increase in the gap A_3.

V_2 - The loading chamber volume is 119 cm^3 when there is no displacement of the diaphragm.

A_3 - The explosive chamber exhaust area can be varied by placing shims between the end plate and the walls of the explosion chamber; the area increases by 0.058 cm^2 for each 0.001-inch increase of shim thickness.

A_2 - The venting area between V_3 and V_2 can be adjusted by blocking off the appropriate combination of holes of various diameters with removable plugs (see Figure B-2). The area A_2 can be varied in 12 increments of 0.189 cm^2 for a total of 2.277 cm^2, in 7 increments of 0.5989 cm^2 for an additional 4.192 cm^2, and finally, in 12 increments of 0.9699 cm^2 for another 11.639 cm^2, providing a total available vent area of 18.108 cm^2.

A_1 - The loading chamber exhaust area can be adjusted by blocking off the appropriate combination of radial ports. It can be varied in 4 increments of 0.3585 cm^2 for 1.434 cm^2 and 4 increments of 0.5824 cm^2 for an additional 2.329 cm^2, providing a total area of 3.763 cm^2.

The two-direction pulse generator assembly used for the loop experiments is shown in Figure B-5 and the photographs are shown in Figure B-6. Basically, the generator consists of two of the one-direction pulse sources mounted back to back. The reaction plate, no longer needed, is removed. A 1/16-inch-thick and 1-inch-wide steel bar, spanning the explosive chamber and positioned by two of the 1/2-inch-diameter tie rods, is used to support the canisters, as shown in Figure B-5 and B-6c. Figure B-6 c also shows the paper container for the charge and detonator.

The potential for pulse shaping is the same as that for the one-direction pulse generator.

B.2 Piping System

The piping systems consist of straight sections, elbows, and a tee section, all of 3-inch outside diameter, 1/16-inch wall, stainless steel (type 304 SS) tubing. Drawings of the loop with standoff pipe and an elbow section are shown in Figures B-7 and B-8. Figure B-9 shows photographs of the loop with standoff pipe, an elbow section, and the tee section. Sections of pipe can be added or removed as desired. A blank flange is used at the end of the open loop and standoff pipe.

The piping system is cushion-mounted at each flange to permit axial strains but to prevent pipe whip, as shown in Figure B-9d. Washers of 1/4-inch thick neoprene between the flanges and the mounting brackets provide the cushion.

B.3 Instrumentation

Figures B-9b and B-9c show pressure transducers mounted in the pipe wall in a horizontal position for monitoring pressure changes as a function of time at various locations. Figure B-9c also shows a port with the gage removed. The gages near the elbows (numbers 4-7 and 9-12) are located on the outside of the loop; the other gages are located on the inside of the loop. Table B-1 lists the locations and serial numbers of the gages for each test; the distances are measured along the center line of the pipe. The 3000 series are Kistler Model 603H transducers, the 800 series are PCB Model 113A transducers, and the 700 series are PCB Model 112A transducers. All gages have a 1 μsec rise-time response. The gages are recessed 50 mils in the pipe wall and are covered with a 50-mil layer of RTV resin for protection. Charge amplifiers (Kistler, Model 504E) amplify the transducer output, and two magnetic tape recorders (Bell & Howell, Model 3700) and several oscilloscopes (Tektronix, Models 543B, 546, 555, and 535A) record the gage signals.

Table B-1

PRESSURE GAGE LOCATION AND IDENTIFICATION

Gage Number	Distance from Previous Gage (ft)	Distance from First Diaphragm (ft)	Distance from Second Diaphragm (ft)	Gage Serial Numbers						
				PS201-PS202 and PS208-PS213	PS203-PS207	PS214-PS219	L301-L308	L309-L317	L318-L333	E401-E408
2		0.52	55.18	3855	3578	3858	854	854	854	854
3	4.73	5.25	50.45			852	855	855	855	855
4	5.20	10.45	45.25				768	768	768	768
5	0.61	11.06	44.64				3578	3578	3578	3578
6	5.39	16.45	39.25				834	834	834	834
7	0.61	17.06	38.54				835	835	835	835
8	10.79	27.85	27.85				853	853	853	853
9	10.79	38.54	17.06				856	857	857	857
10	0.61	39.25	15.45				852	852	852	852
11	5.39	44.64	11.06				766	766	766	766
12[a]	0.61	45.25	10.45				3855	3855	3855	3855
13[a]	5.20	50.45	5.25				3548	3548		3548
16[a]	4.73	55.18	0.52				857	856		
14[a]	4.95	50.20	5.50						3548	
15	0.50	50.70	5.00						3868	
16	4.48	55.18	0.52						856	

[a] These gages used in closed loops with standoff pipe.

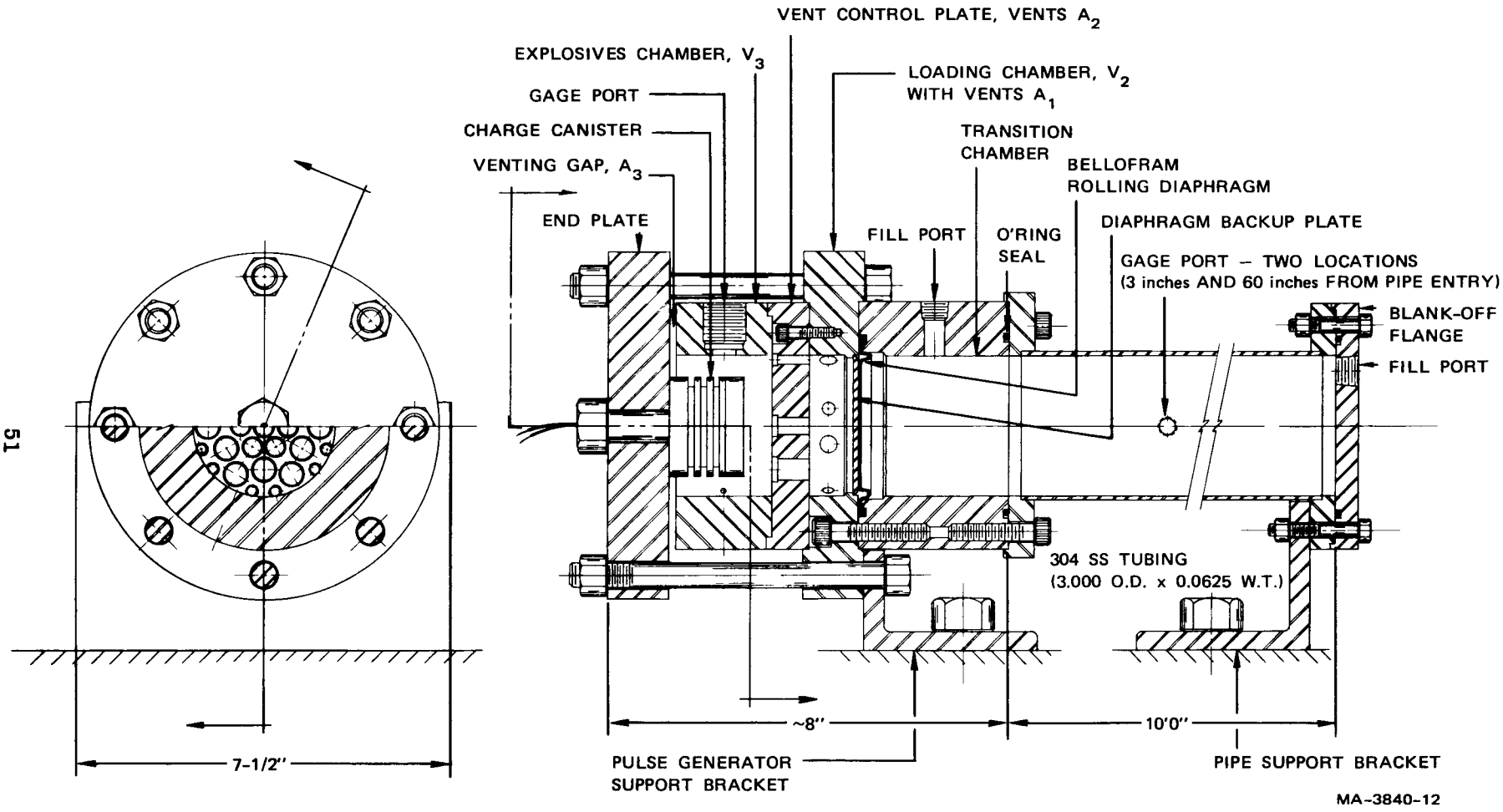

FIGURE B-1 ONE-DIRECTION PULSE SOURCE ASSEMBLY

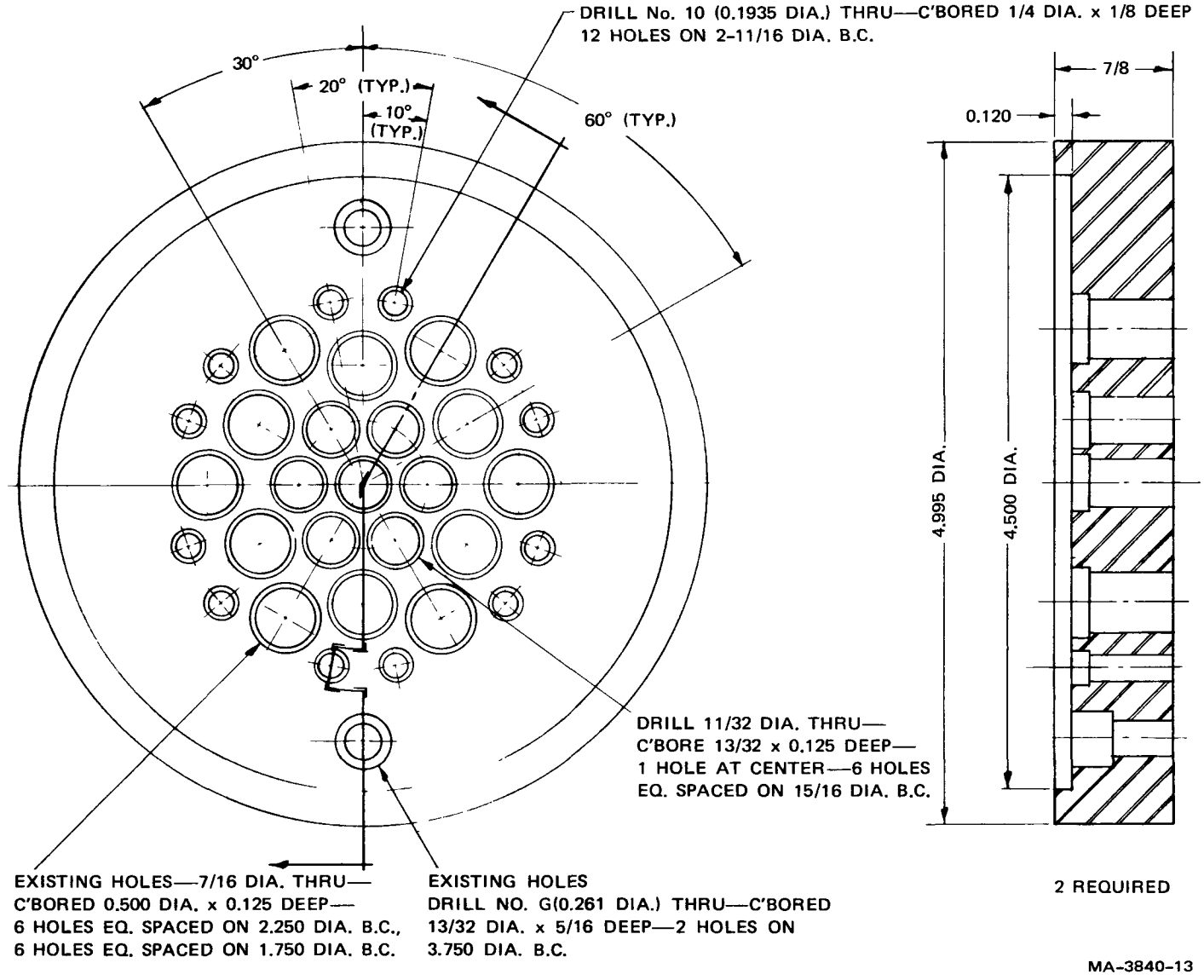

FIGURE B-2 VENT CONTROL PLATE

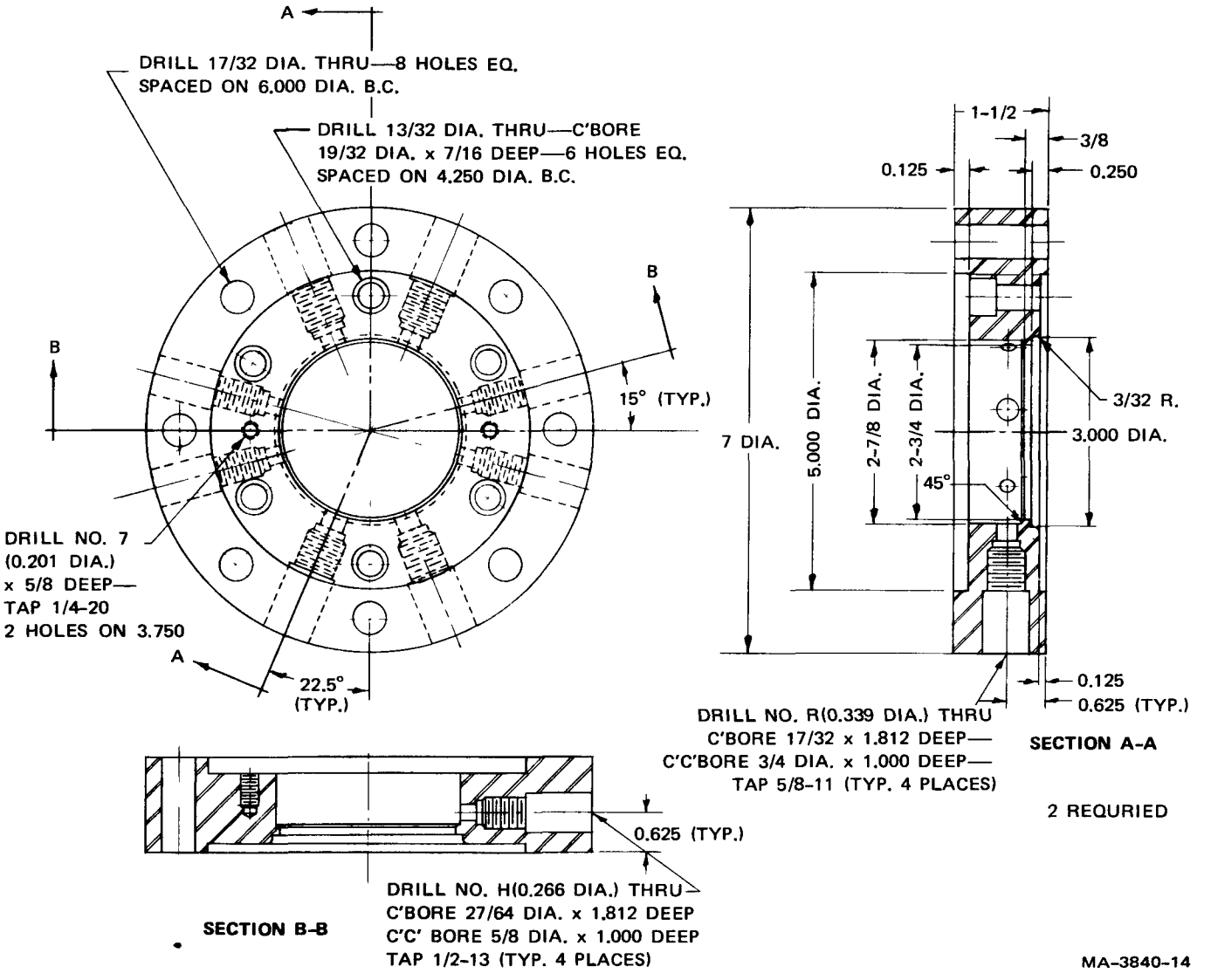

FIGURE B-3 LOADING OR EXPANSION CHAMBER

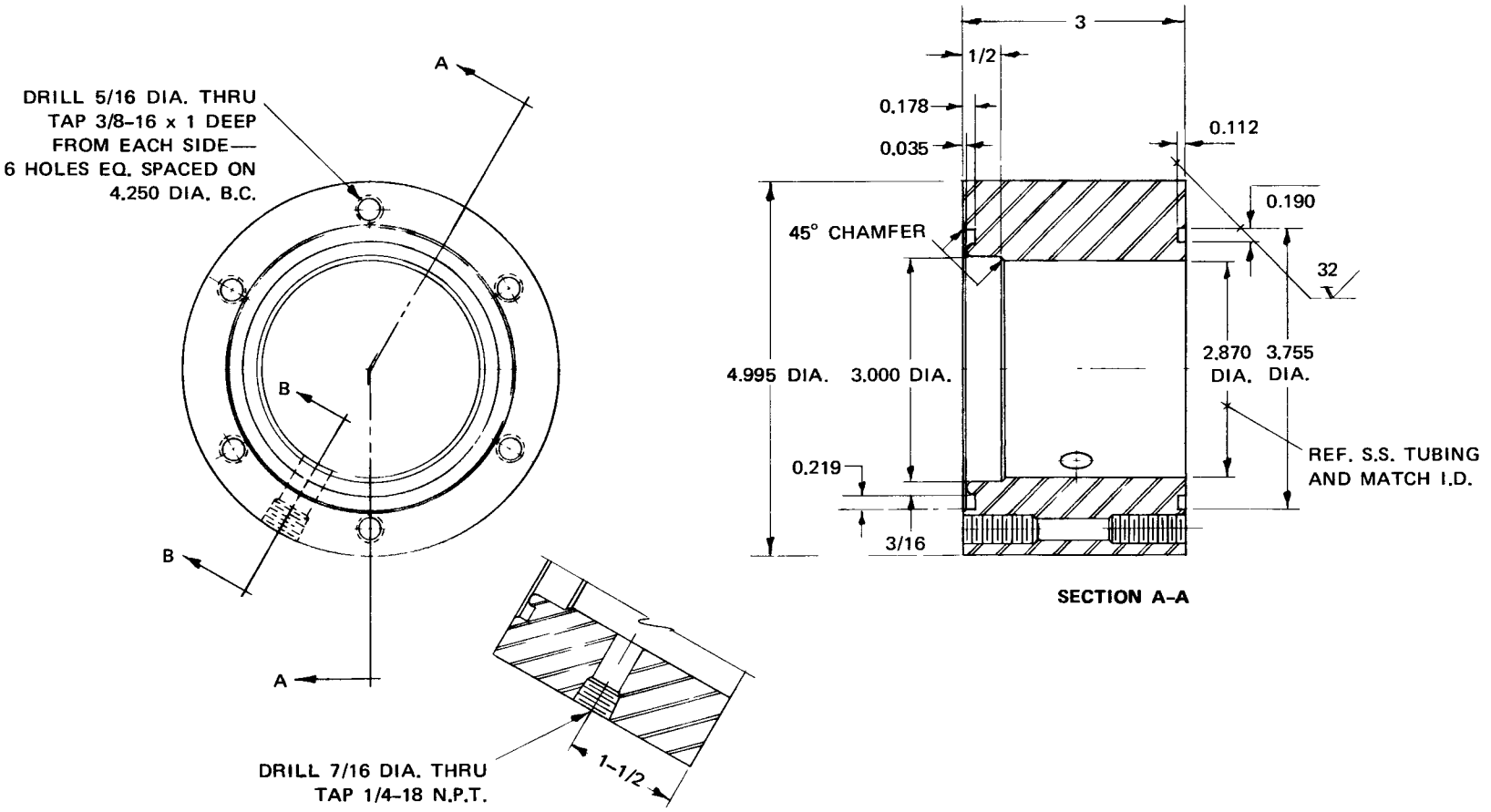

FIGURE B-4 TRANSITION CHAMBER

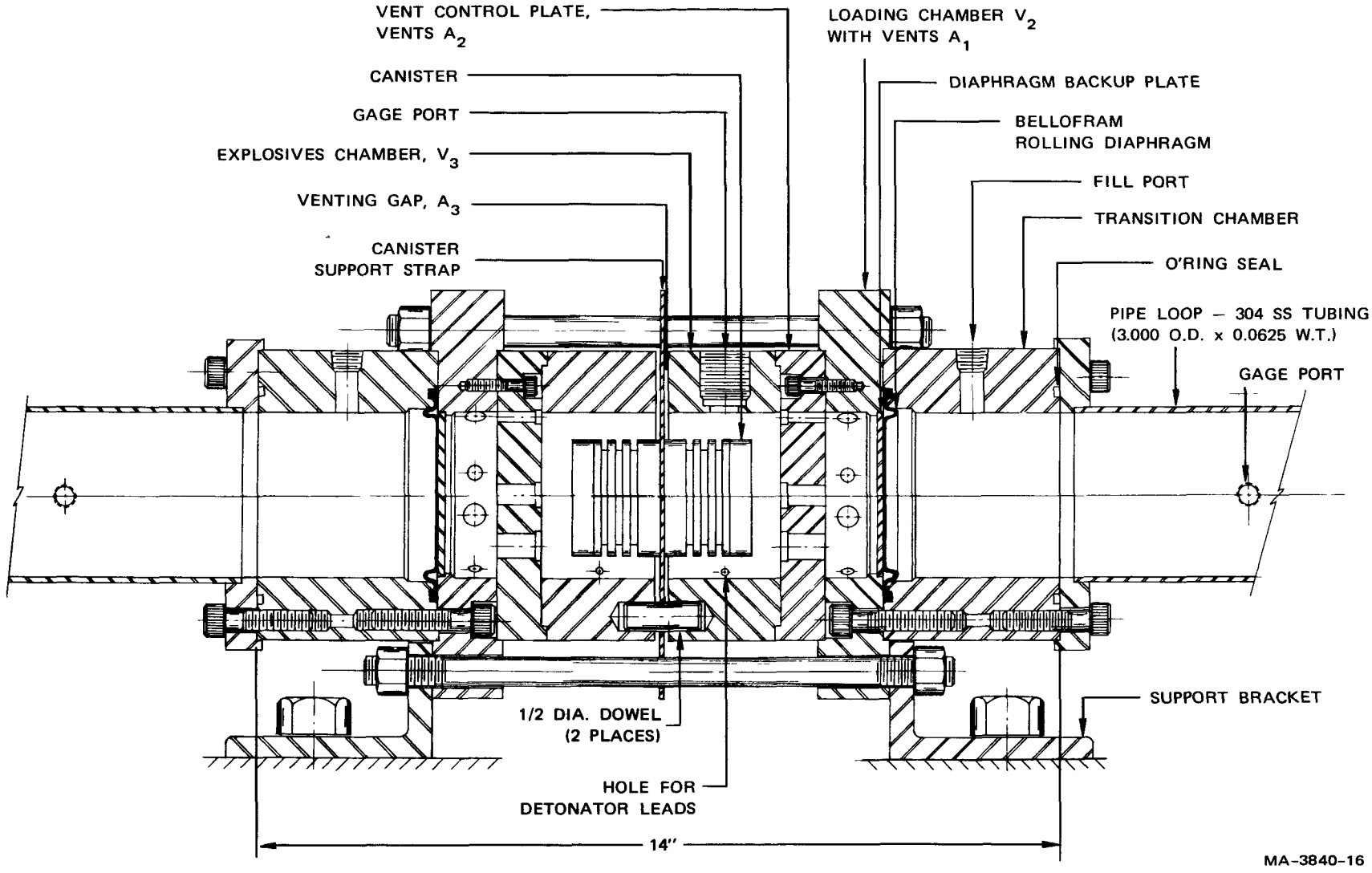

FIGURE B-5 TWO-DIRECTION PULSE SOURCE ASSEMBLY

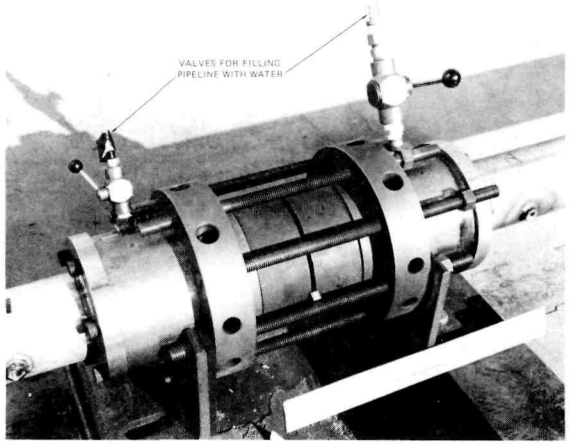

(a) ASSEMBLED PULSE SOURCE

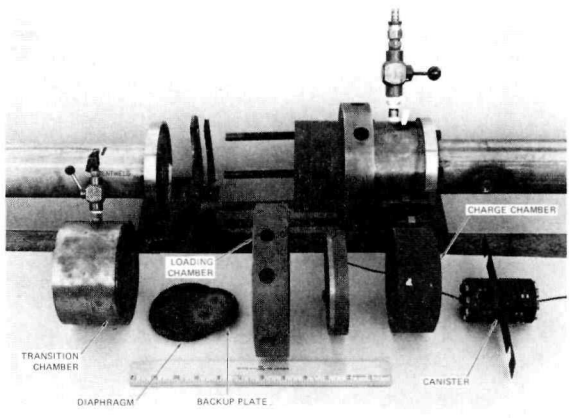

(b) PARTIALLY DISASSEMBLED PULSE SOURCE

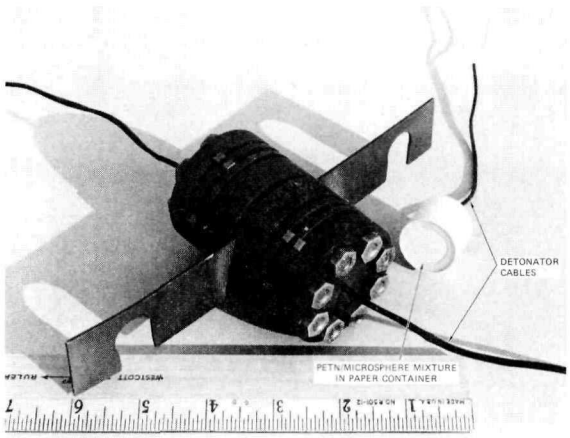

(c) VENTED CHARGE CANISTER

MP-3840-17

FIGURE B-6 PHOTOGRAPHS OF THE TWO-DIRECTION PULSE

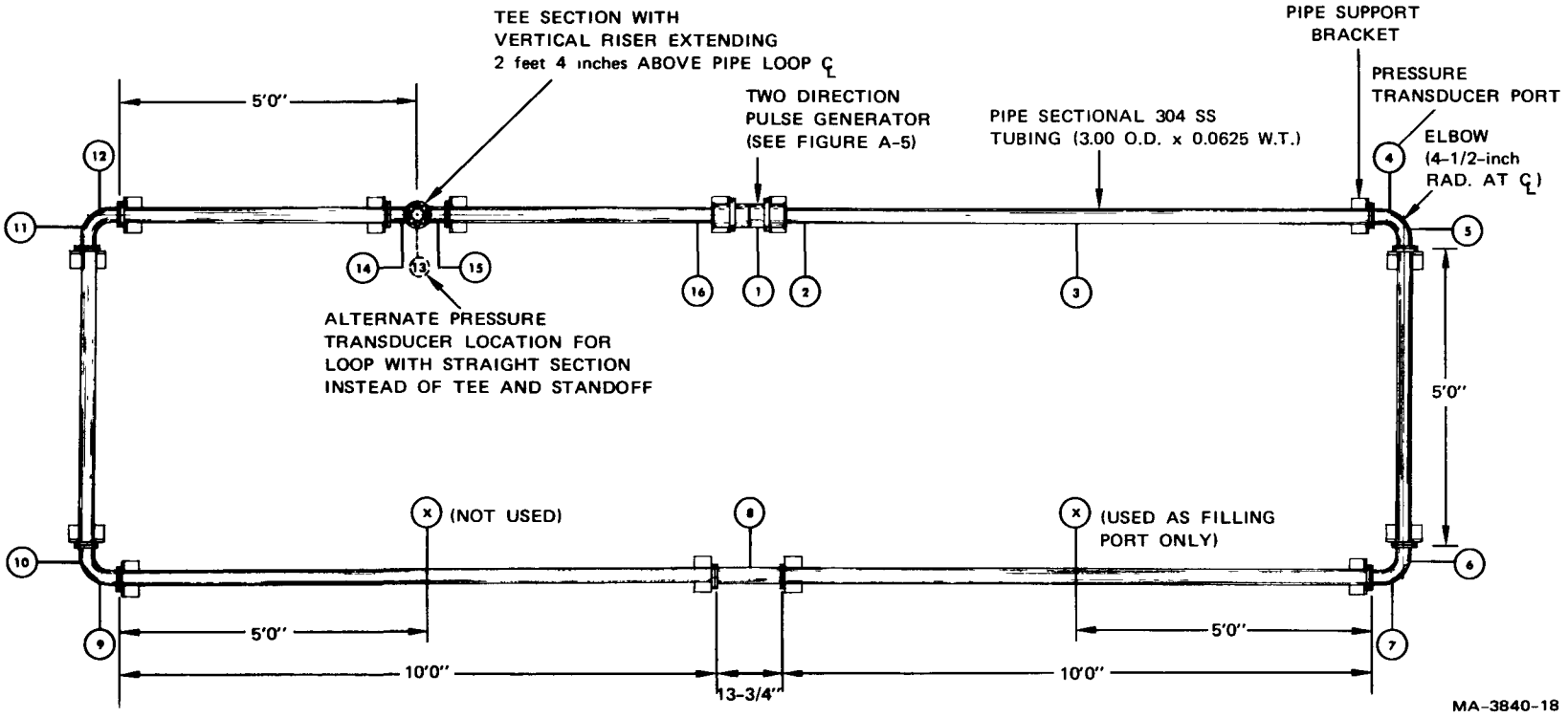

FIGURE B-7 PIPING SYSTEM FOR THE CLOSED LOOP WITH STANDOFF PIPE EXPERIMENTS

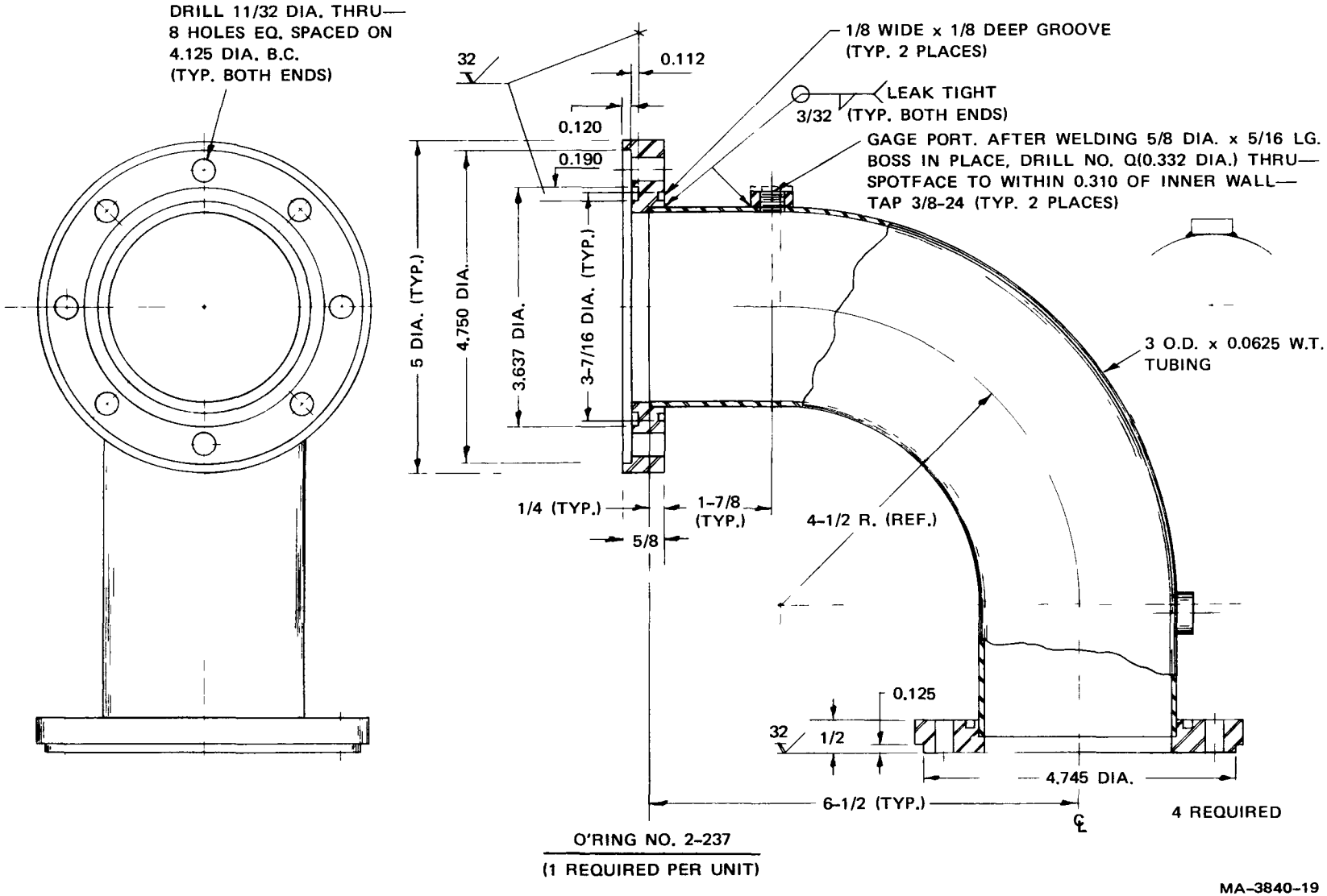

FIGURE B-8 ELBOW SECTION

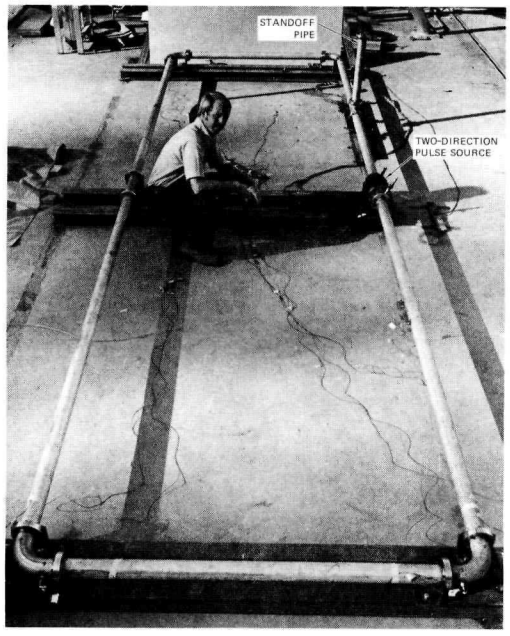

(a) PIPE SYSTEM USED FOR THE CLOSED LOOP WITH STANDOFF PIPE EXPERIMENTS

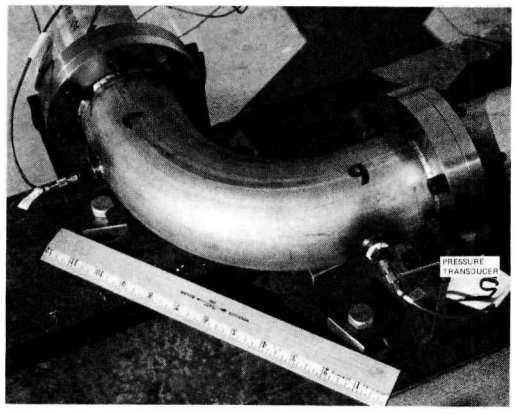

(b) ELBOW SECTION

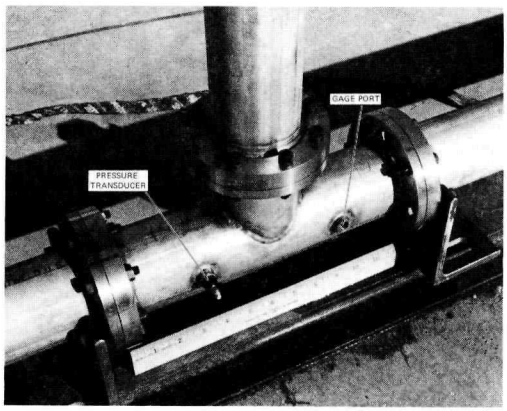

(c) TEE SECTION

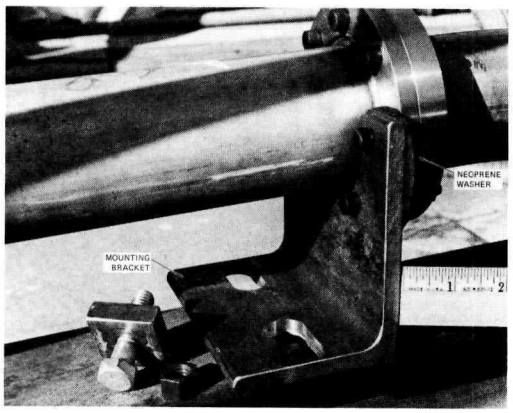

(d) FLANGE AND MOUNTING BRACKET

MP-3840-20

FIGURE B-9 PHOTOGRAPHS OF THE PIPING SYSTEM

Appendix C

REPRODUCIBILITY AND WAVE VELOCITY

C.1 Reproducibility Between Experiments

Experiments were repeated to determine if pulse behavior was reproducible. Three experiments with identical initial conditions for pulse P I (Experiments L325, L330, and L331) and for pulse P II (Experiments L303, L304, and L305) were selected for detailed analysis and are used to illustrate the reproducibility of pulses.

Figure C-1 shows the pressure pulses at gage 16 and gage 9 locations of experiments L325, L330, and L331 with P I in a closed loop with a filled standoff pipe. Gage 16 measures the pressure pulse before it is affected by the standoff pipe, and gage 9 measures the pressure pulse after it has passed the standoff pipe and traversed two elbows.

Figure C-2 shows the pressure pulses at the gage 3 and gage 7 locations of experiments L303, L304, and L305 with P II in a closed loop. Gage 3 measures the input pulse, and gage 7 measures the pressure pulse after it has traversed two elbows. Complete pressure transducer records of all six experiments used in this analysis are given in Appendix E.

As shown in Figures C-1 and C-2, the peak pressures of the pulses generated vary by about $\pm$ 17% at the gage 16 location for the three experiments with pulse P I and about $\pm$ 4% at the gage 3 location for experiments with pulse P II. The shapes of the pulses were similar from experiment to experiment aside from the differences in peak pressure. As the pulses propagated to their gage locations--gage 9 for P I, and gage 7 for P II--the relative differences in peak pressure were maintained.

Some variation in peak pressure of repeated experiments can be attributed to variation in explosive charges and to errors in data processing. The charge mass may vary by ± 5%. Also, different batches of explosive mixtures may have slightly different characteristics. Data processing has an estimated error of less than ± 5%. The ± 4% difference in peak pressures of the three replications of P II pulses is accountable by these sources of error. The ± 17% difference in peak pressures of the three replications of P I pulses is larger than expected from the above sources of error and is currently unexplained. Throughout the experiments, pulse P II was more reproducible than pulse P I.

C.2 Comparison of Pulses from the One- and Two-Direction Pulse Sources

Figure C-3 shows a comparison of the pressure pulses P I generated by the one- and two-direction pulse sources. Pulses at gages 3 and 7 of experiment L317 are generated by the two-direction pulse source. Similar traces from experiments E404 and L305 compare the P II pulses. The difference in these comparative pulses is less than the difference experienced in the reproducibility experiments discussed above. The results indicate that the one- and two-direction pulse sources produce similar pulses, especially for P II.

C.3 Similarity of Pulses in Two Directions

It is important that identical pulses be generated in opposite directions by the two-direction pulse source so that the attenuation of the pulse passing a standoff pipe can be related to the attenuation of a pulse not passing a standoff pipe. The closed rectangular loop experiments provided a symmetrical geometry to compare pulse behavior in the two directions.

Figure C-4 shows two experiments comparing pulse P I and pulse P II at two pairs of symmetrical locations, gages 3 and 13, and gages 7 and 9. The initial pulses, at gages 3 and 13, are similar. The pulses at

gages 7 and 9, which record the pulses after they have traversed two elbows, are similar in the P II case. In the P I case, the pulses at gages 7 and 9 differ by about ± 10% in peak pressures, but late time differences become substantial and may be caused by the differences in stiffness of the support system.

C.4 Pulse Propagation Velocity Measurements

The pulse propagation velocity was calculated in Section II to be 3997 ft/sec. The velocity was measured by noting the time of arrival of the pressure pulse at each of the gages in the open rectangular loop experiments. The distances were measured along the center line of the pipeline. Table C1 shows the arrival times in three experiments and the calculated arrival times for a pulse propagating at 3997 ft/sec. Figure C-5 plots the measured and calculated arrival times against the distance propagated. The average measured pulse propagation rate is 3938 ft/sec and is only 1.5% less than the calculated rate.

Table C-1

PULSE PROPAGATION VELOCITY MEASUREMENTS

Gage No.	Distance from Gage 2 (feet)	Pulse Arrival Time (msec) E402	E404	E406	Calculated Time for a=3997 ft/sec (msec)
2	0	0	0	0	
3	4.73	1.22	1.21	1.19	1.18
4	9.93	2.50	2.53	2.48	2.48
5	10.54	2.69	2.65	2.64	2.64
6	15.93	4.08	4.02	4.00	3.99
7	16.54	4.29	4.21	4.15	4.14
8	27.33	7.95	6.93	6.95	6.84
9	38.12	9.74	9.73	9.65	9.54
10	38.73	9.88	9.84	9.81	9.69
11	44.12	11.22	11.16	11.19	11.04
12	44.73	11.41	11.32	11.23	11.19
13	49.93	12.74	12.71	12.63	12.49

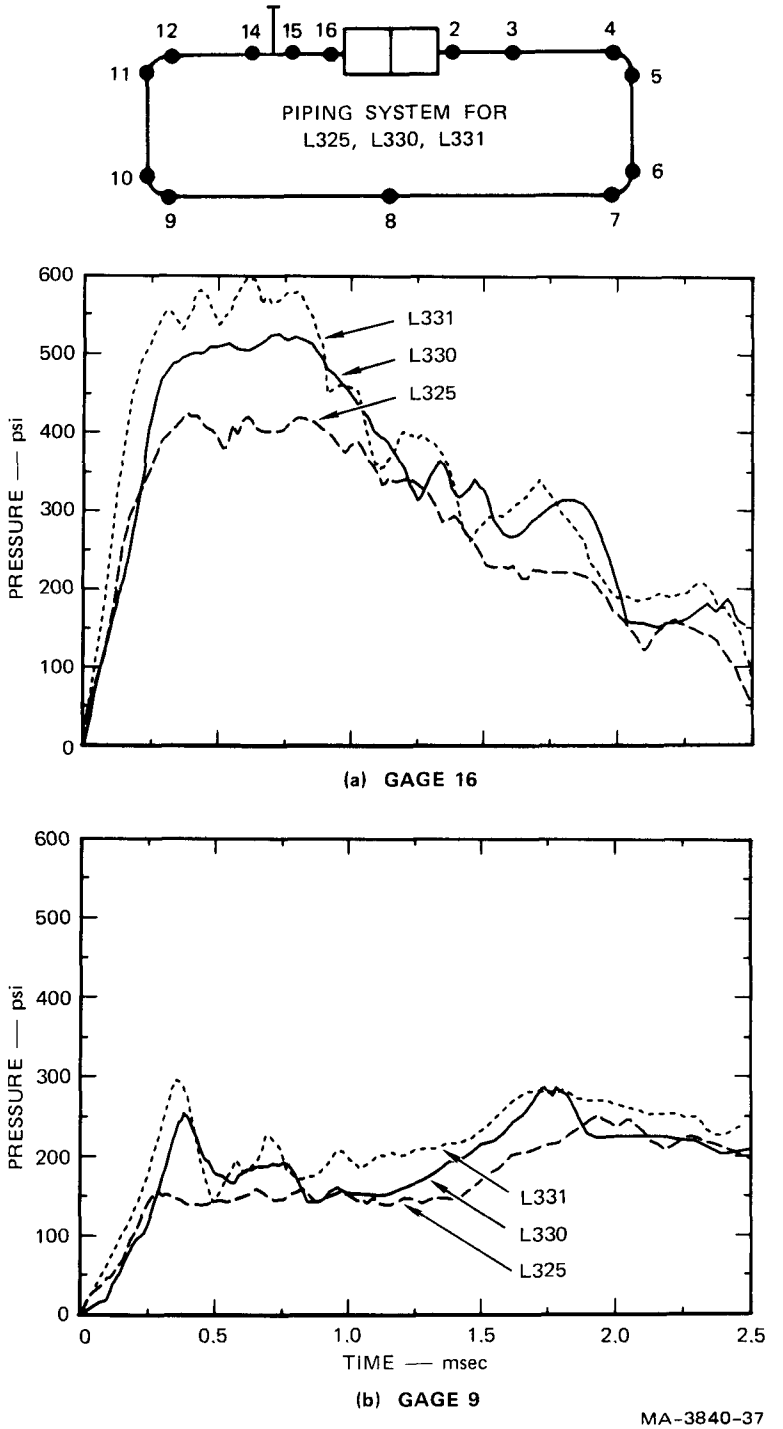

FIGURE C-1 EXPERIMENTAL REPRODUCIBILITY: PULSE P I

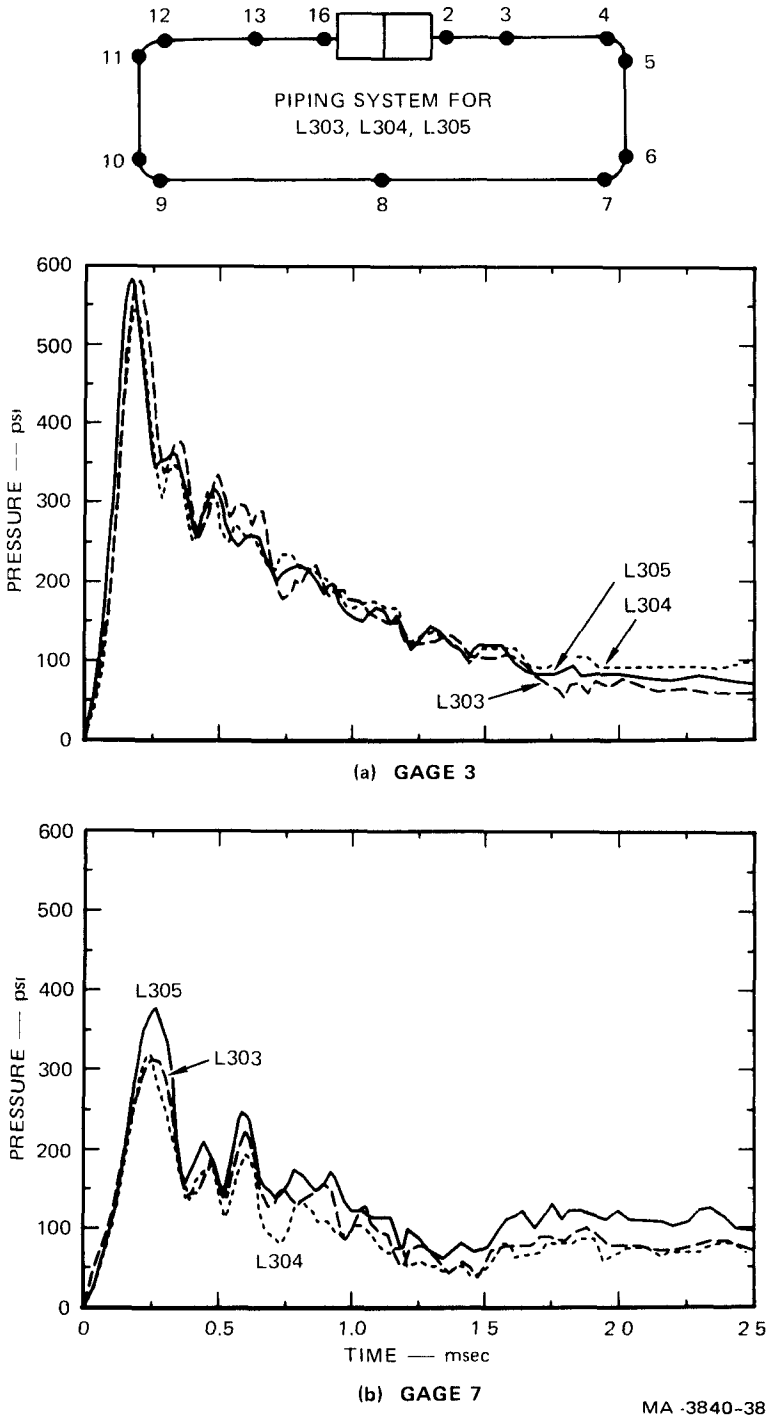

FIGURE C-2 EXPERIMENTAL REPRODUCIBILITY: PULSE P II

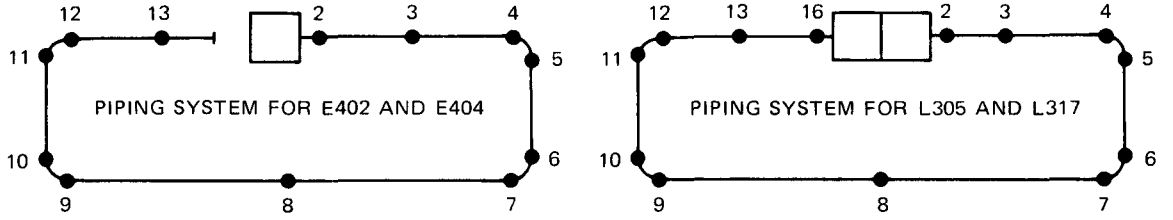

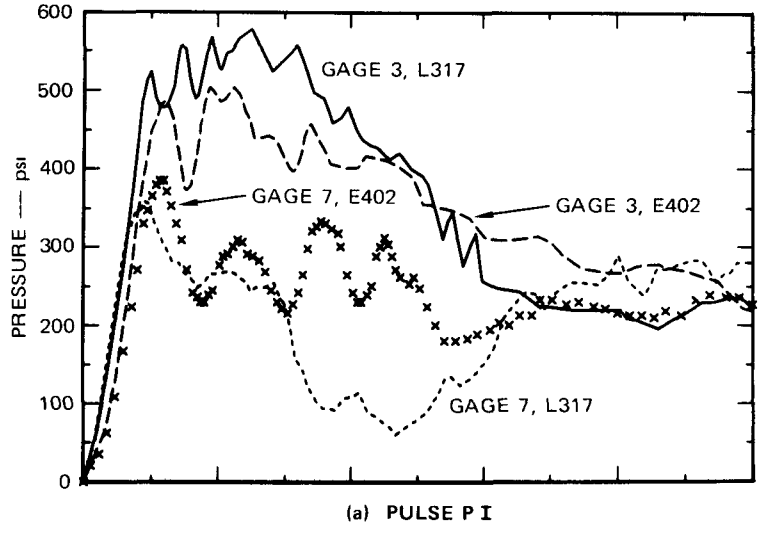

(a) PULSE P I

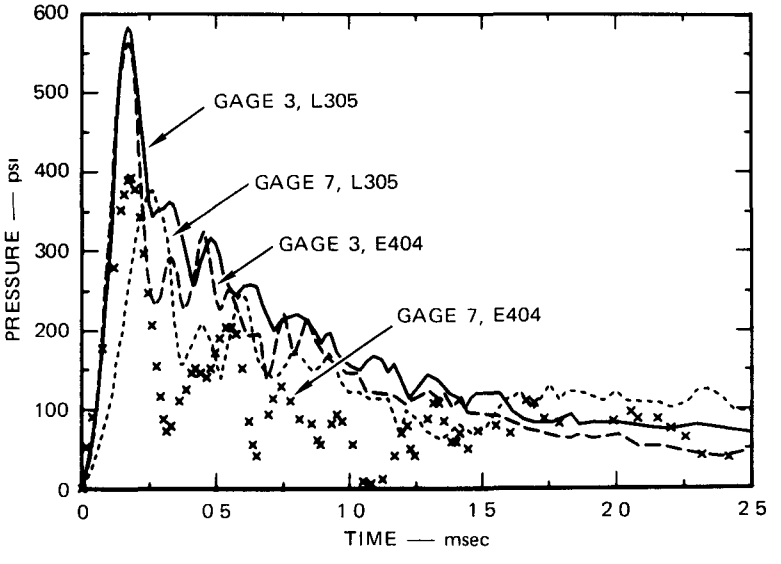

(b) PULSE P II

MA-3840-39

FIGURE C-3 PULSES FROM ONE- AND TWO-DIRECTION PULSE SOURCES

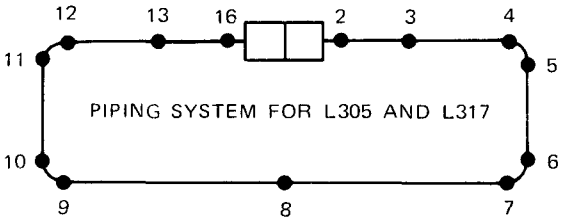

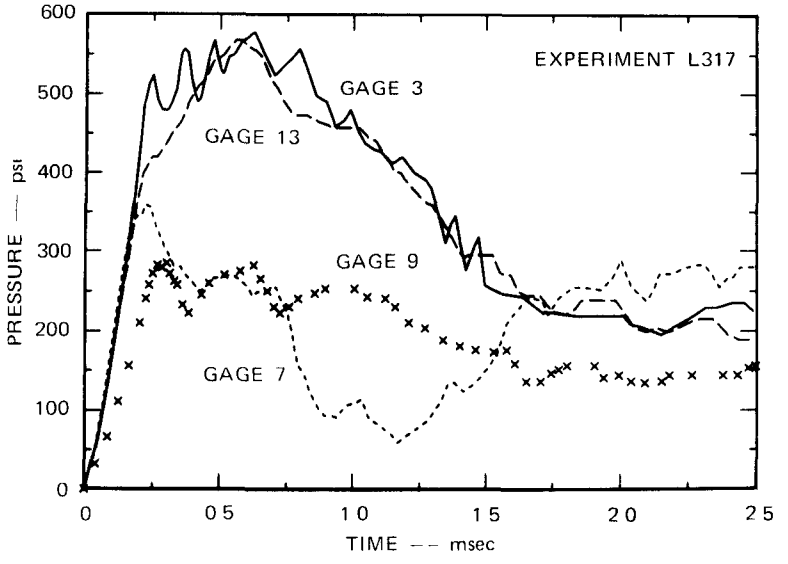

(a) **PULSE P I**

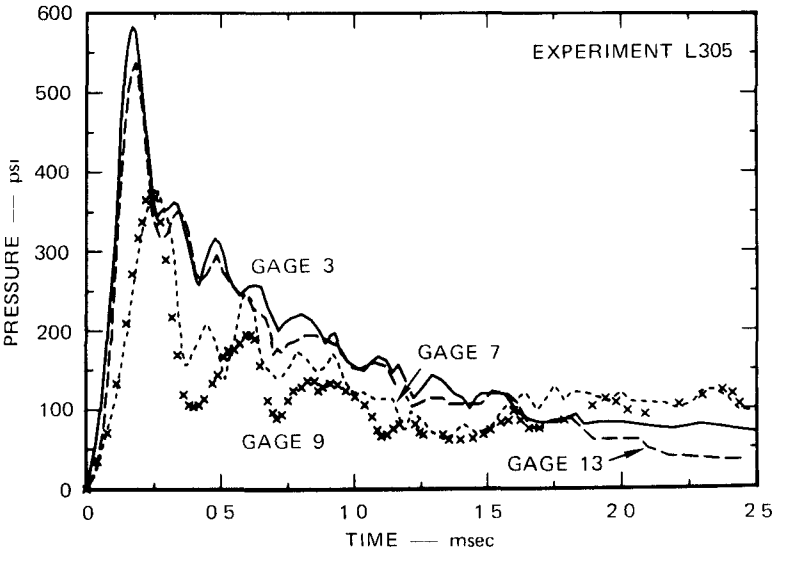

(b) **PULSE P II**

MA 3840-40

FIGURE C-4 PULSES FROM THE TWO-DIRECTION PULSE SOURCE

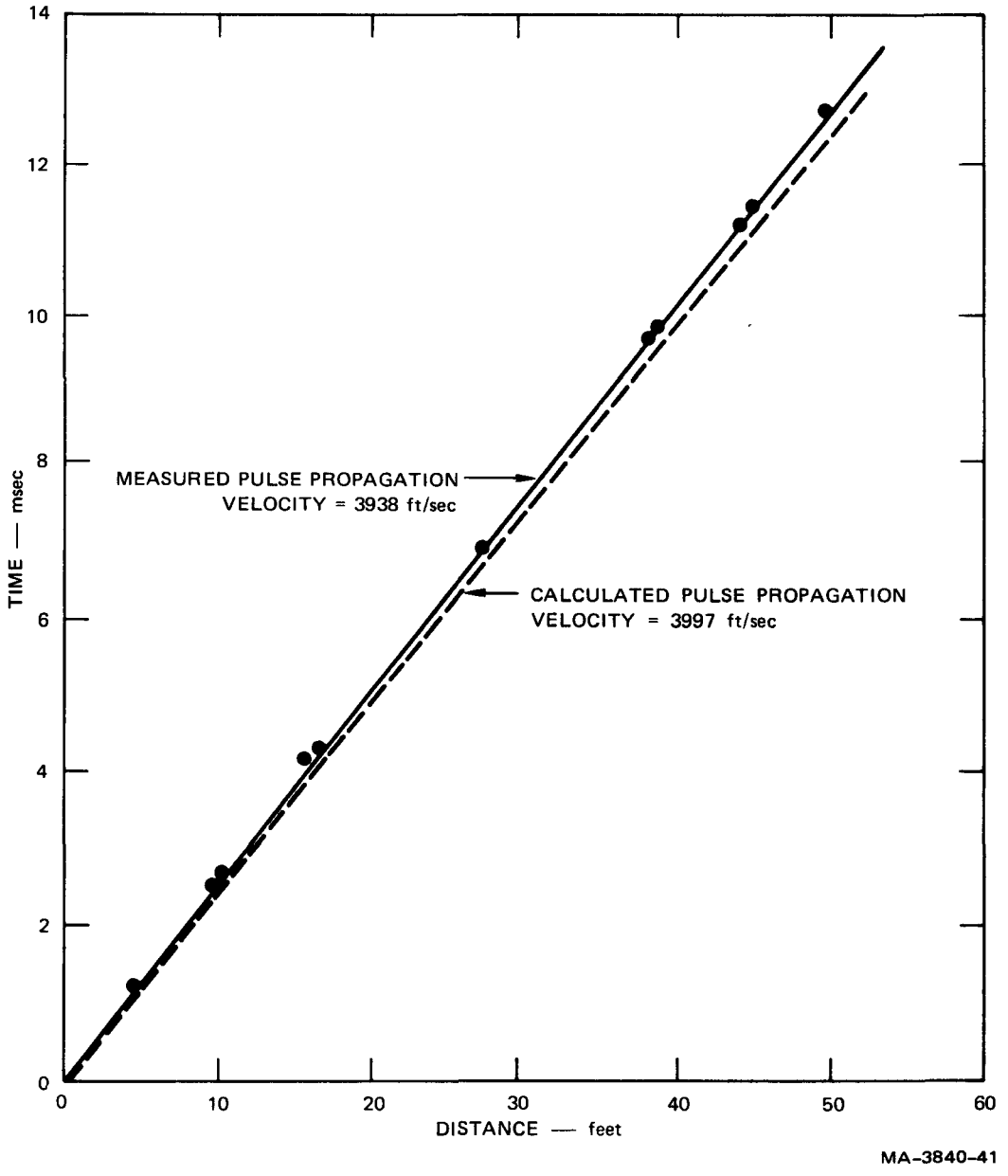

FIGURE C-5 TIME-DISTANCE DIAGRAM OF PULSE IN PIPELINE: THEORY AND EXPERIMENT

Appendix D

EFFECT OF AN AIR BUBBLE ON PULSE SHAPE

In some of the closed rectangular loop experiments, the two pulses in opposite directions differed. Because the differences always occurred just after the piping system had been filled with water, it was suspected that an air bubble trapped in the pipeline was causing one of the pulses to be altered. Two experiments, E407 and E408, were conducted with the open rectangular loop in which an air bubble was injected at a known location, to evaluate the effect of an air bubble on a pulse.

In experiment E407, a 2.5 cm^3 air bubble was injected into the water next to the diaphragm separating the gas and water in the pulse source. In experiment E408, a small air bubble (between 1 and 3 cm^3) was injected into the water at the gage 3 location.

Figure D-1 shows the records from gages 3 and 10 in experiments E403, E407, and E408. The initial conditions, except for the air bubble in E407 and E408, were identical in the three experiments. The air bubbles thus caused a substantial change in the pulse shape at the gage 3 location and a moderate change at the gage 10 location.

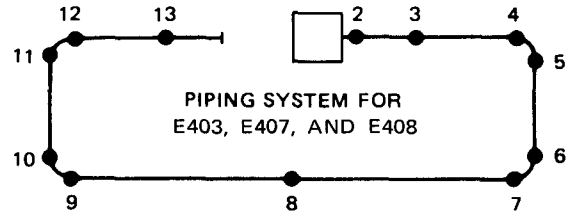

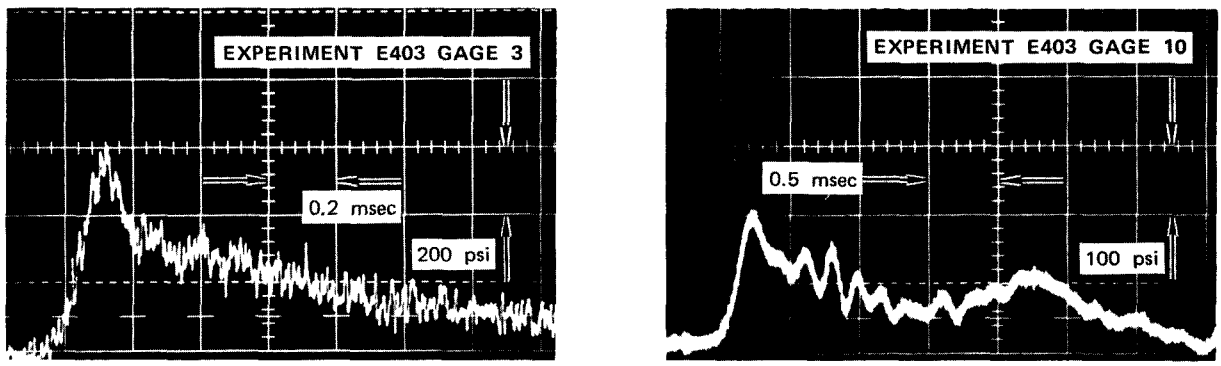

(a) NORMAL PULSE

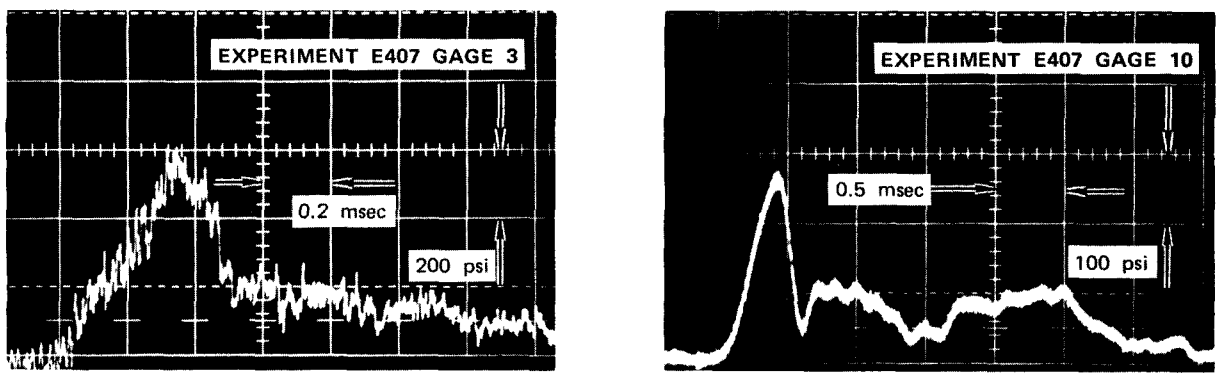

(b) AIR BUBBLE NEXT TO DIAPHRAGM

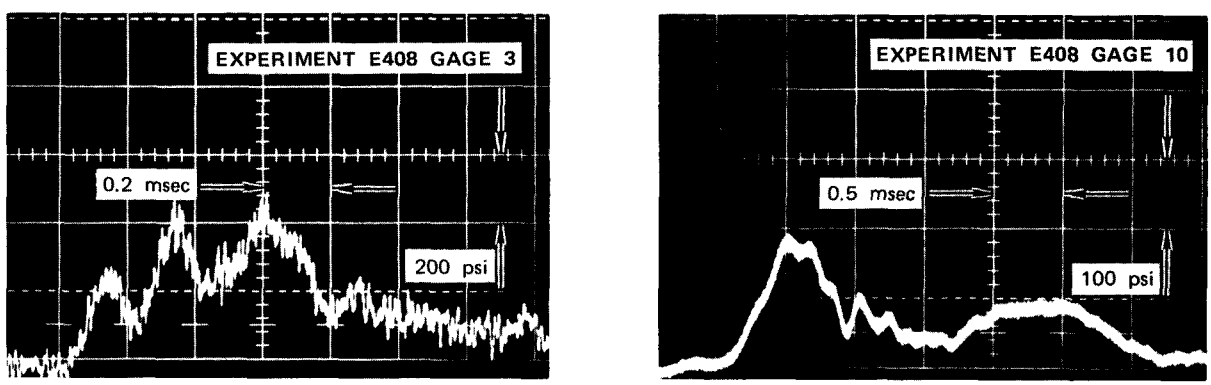

(c) AIR BUBBLE NEXT TO GAGE 3

MP-3840-21

FIGURE D-1 THE EFFECT OF AN AIR BUBBLE IN THE PIPELINE ON THE PULSE SHAPE

Appendix E

PRESSURE-TIME RECORDS FOR SELECTED EXPERIMENTS

Pressure-versus-time plots from each gage used in the twelve experiments selected for detailed analysis are shown in Figures E-1 through E-12. The twelve experiments are:

Figure	Experiment	Pulse Designation	Type of Experiment
E-1	E402	P I	Open Rectangular Loop
E-2	E404	P II	Open Rectangular Loop
E-3	L303	P II	Closed Rectangular Loop
E-4	L304	P II	Closed Rectangular Loop
E-5	L305	P II	Closed Rectangular Loop
E-6	L317	P I	Closed Rectangular Loop
E-7	L322	P II	Closed Loop with Filled Standoff Pipe
E-8	L325	P I	Closed Loop with Filled Standoff Pipe
E-9	L328	P II	Closed Loop with Empty Standoff Pipe
E-10	L330	P I	Closed Loop with Filled Standoff Pipe
E-11	L331	P I	Closed Loop with Empty Standoff Pipe
E-12	L332	P I	Closed Loop with Empty Standoff Pipe

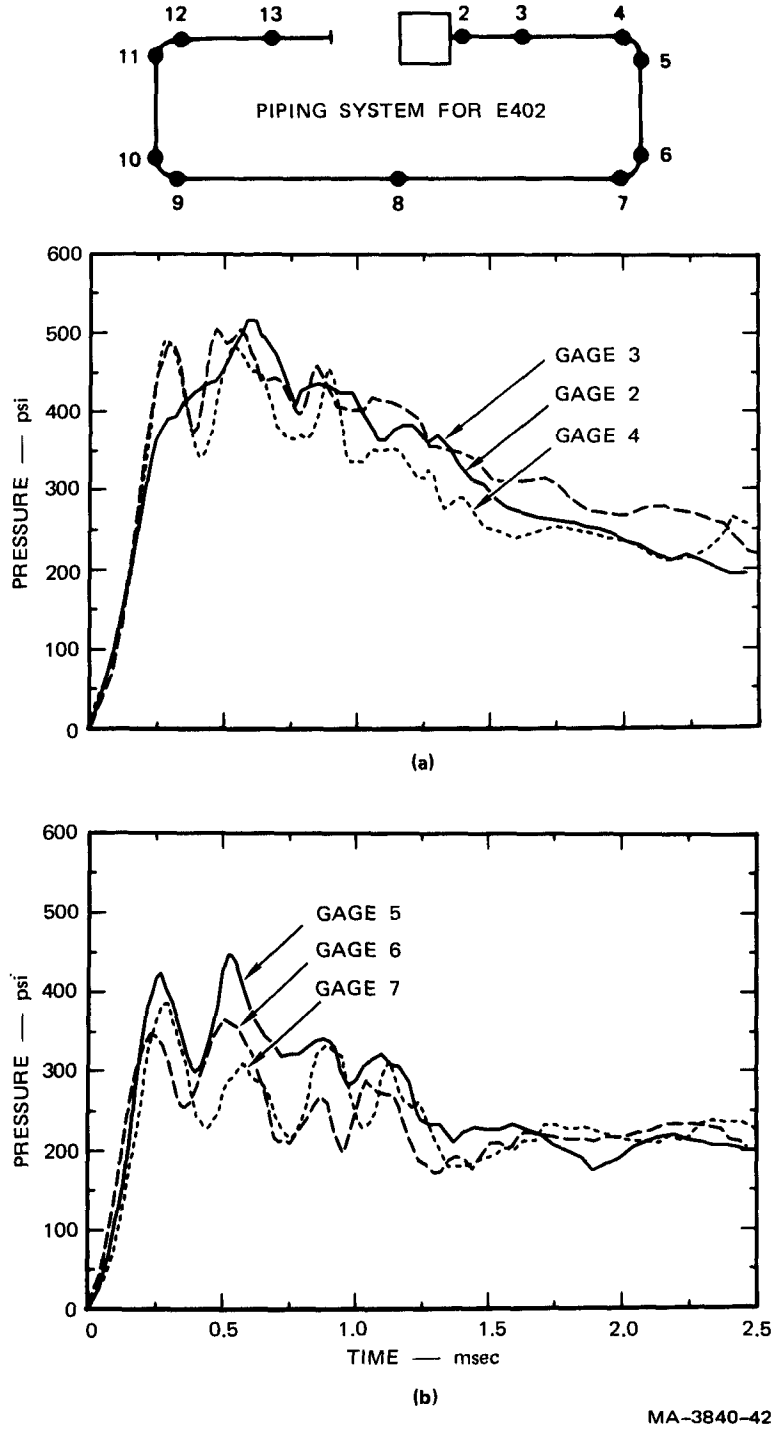

FIGURE E-1 PRESSURE-TIME RECORDS FOR EXPERIMENT E402

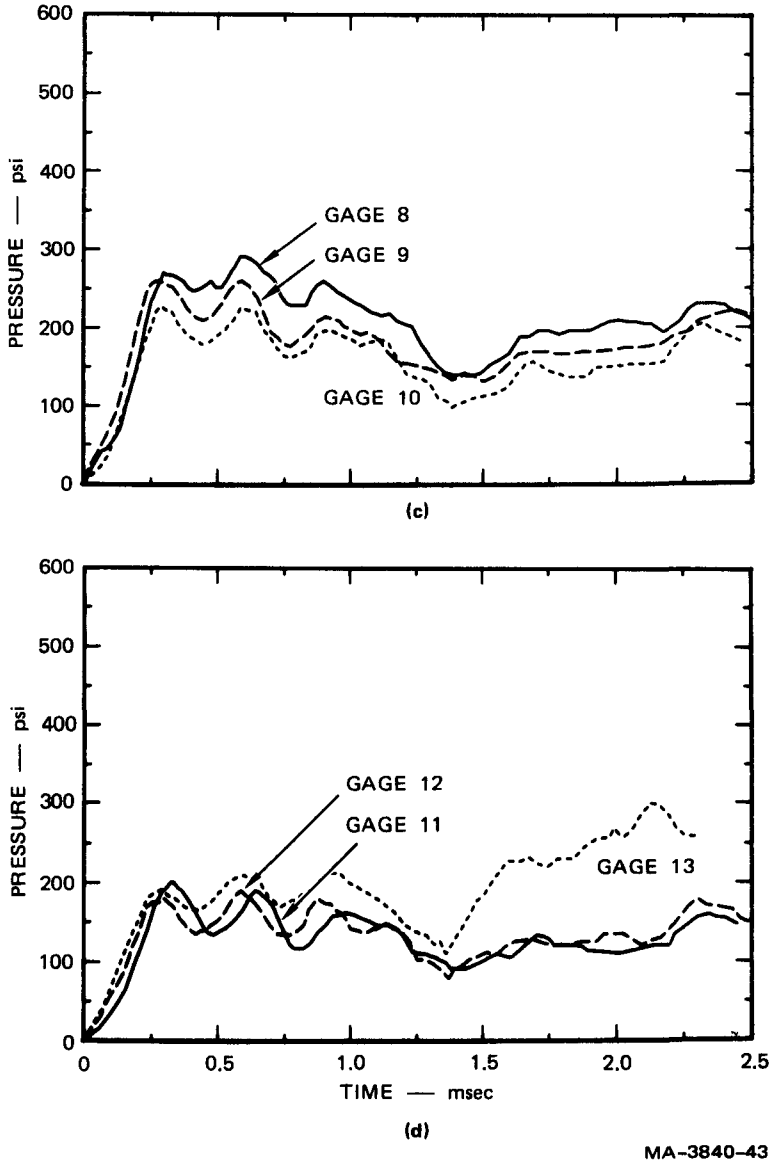

FIGURE E-1 PRESSURE-TIME RECORDS FOR EXPERIMENT E402 (Concluded)

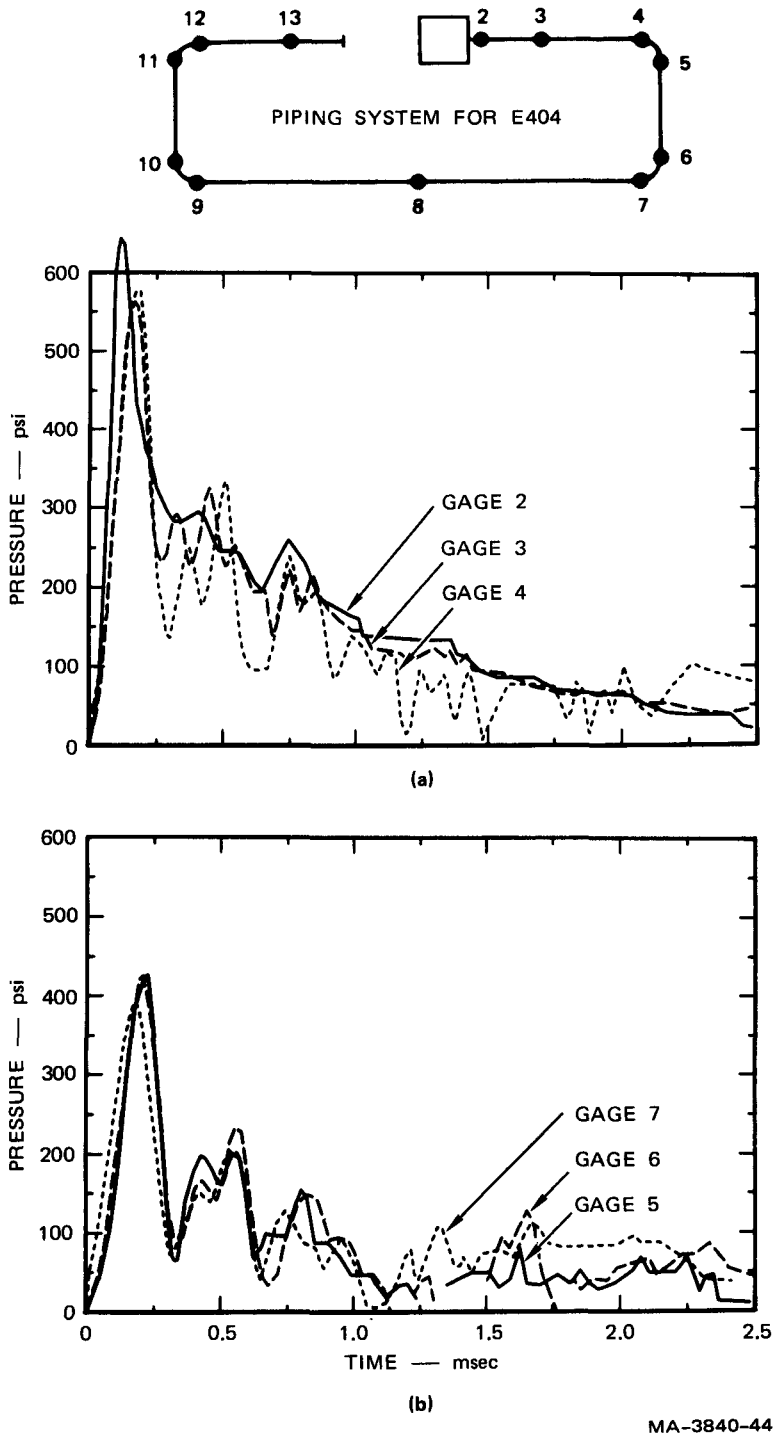

FIGURE E-2 PRESSURE-TIME RECORDS FOR EXPERIMENT E404

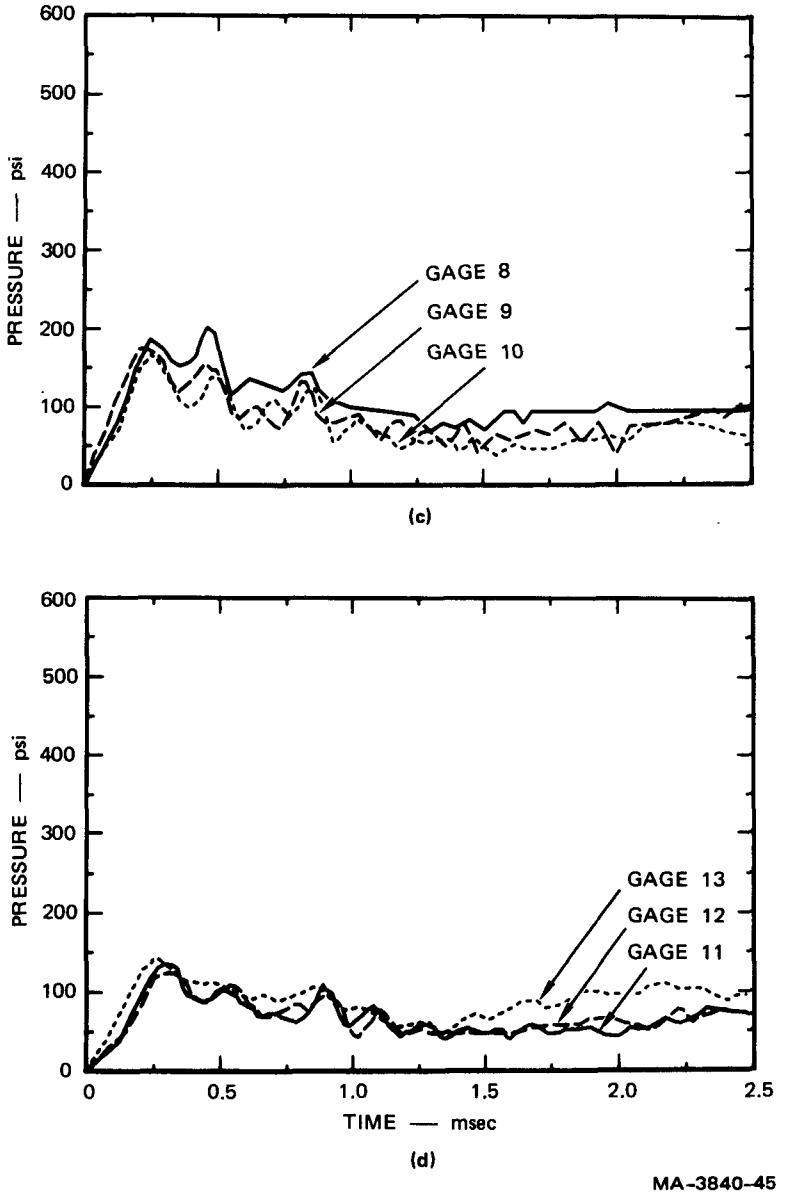

FIGURE E-2 PRESSURE-TIME RECORDS FOR EXPERIMENT E404 (Concluded)

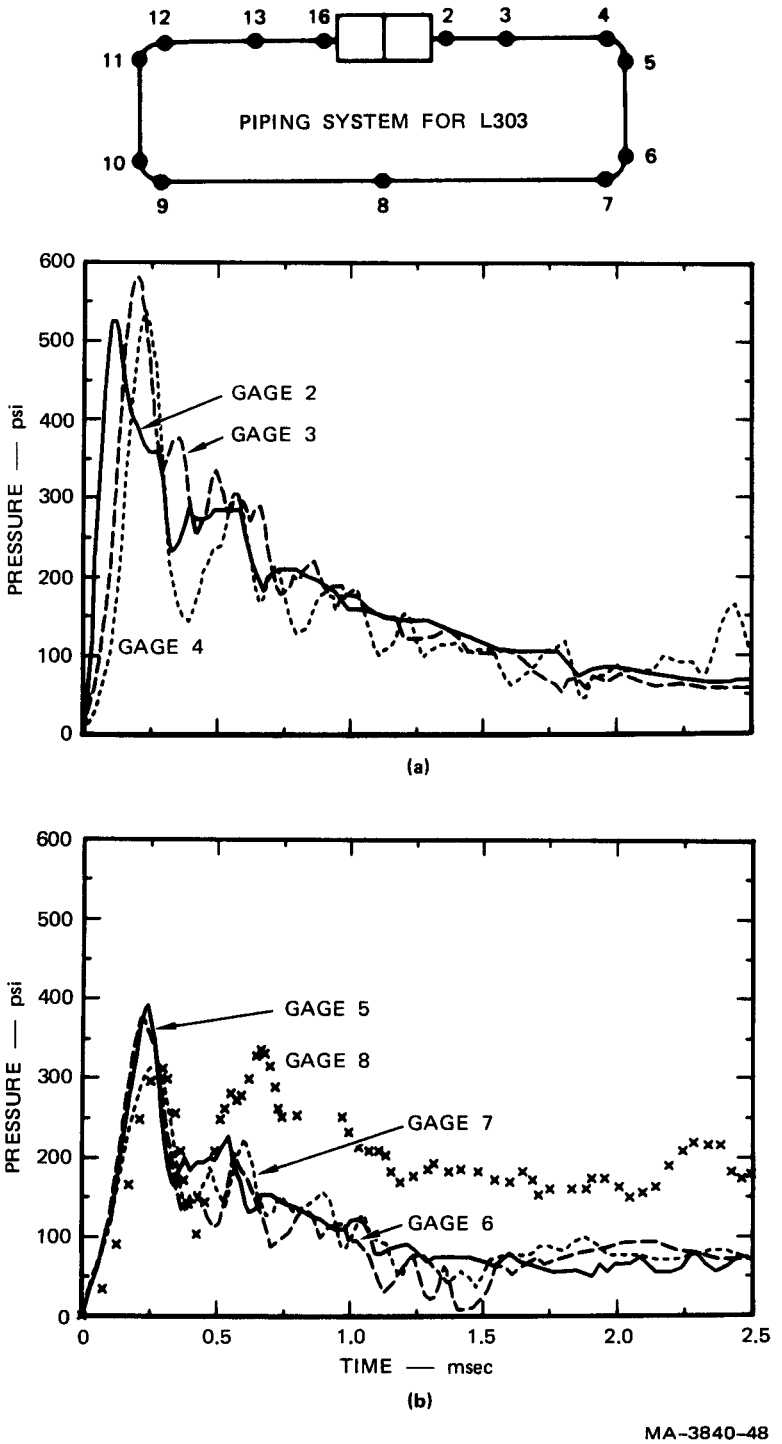

FIGURE E-3 PRESSURE-TIME RECORDS FOR EXPERIMENT L303

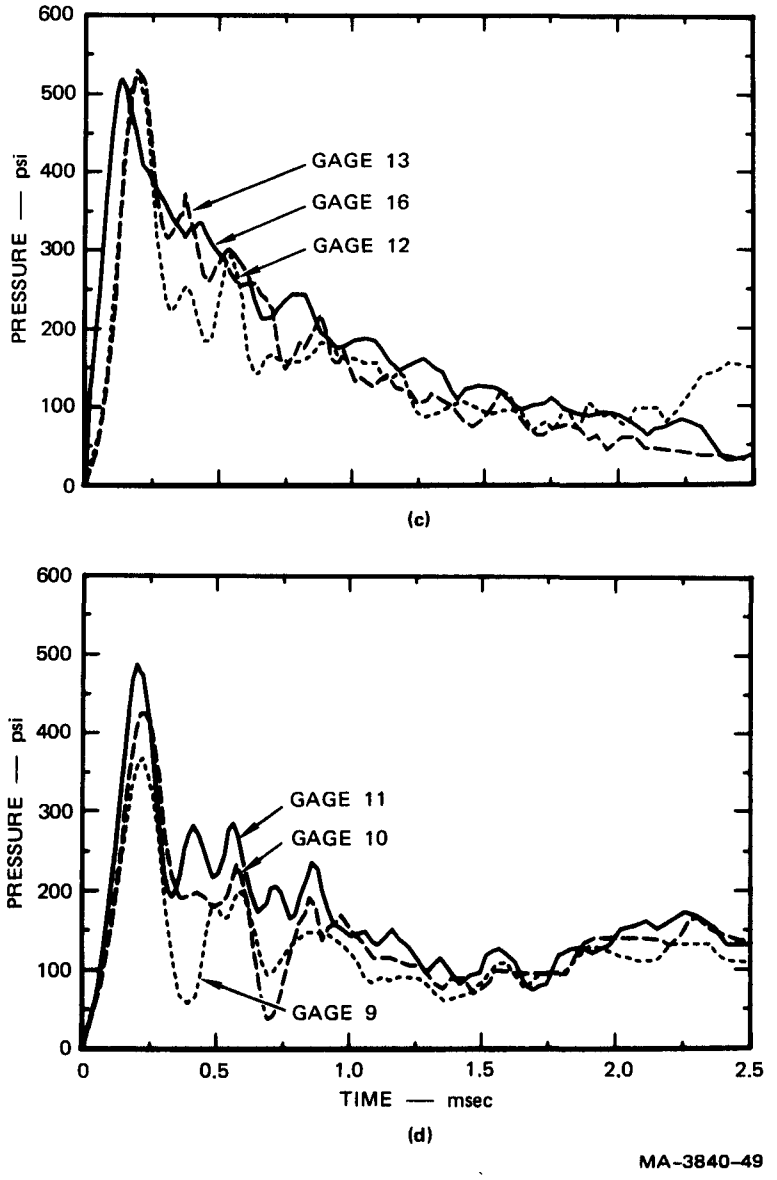

FIGURE E-3 PRESSURE-TIME RECORDS FOR EXPERIMENT L303 (Concluded)

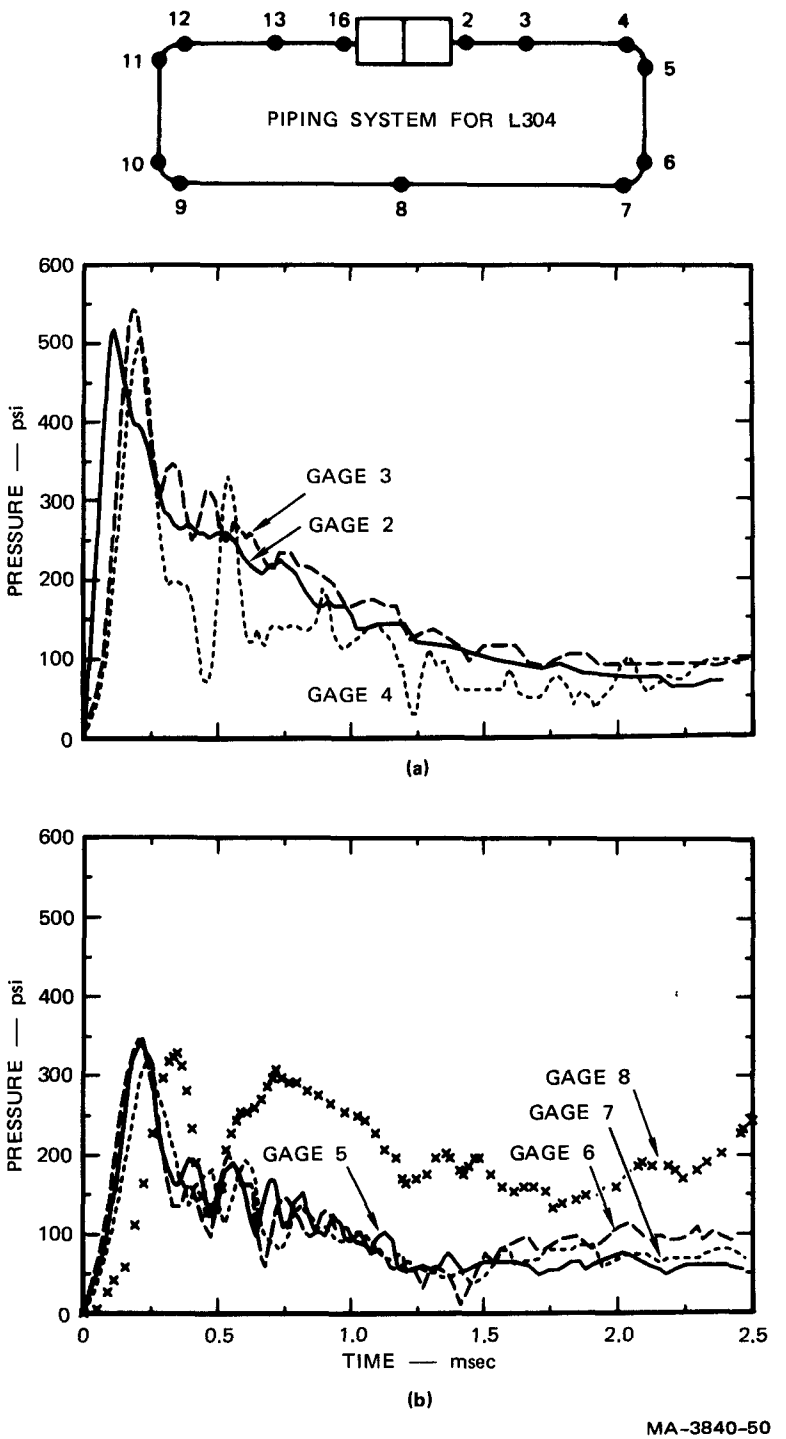

FIGURE E-4 PRESSURE-TIME RECORDS FOR EXPERIMENT L304

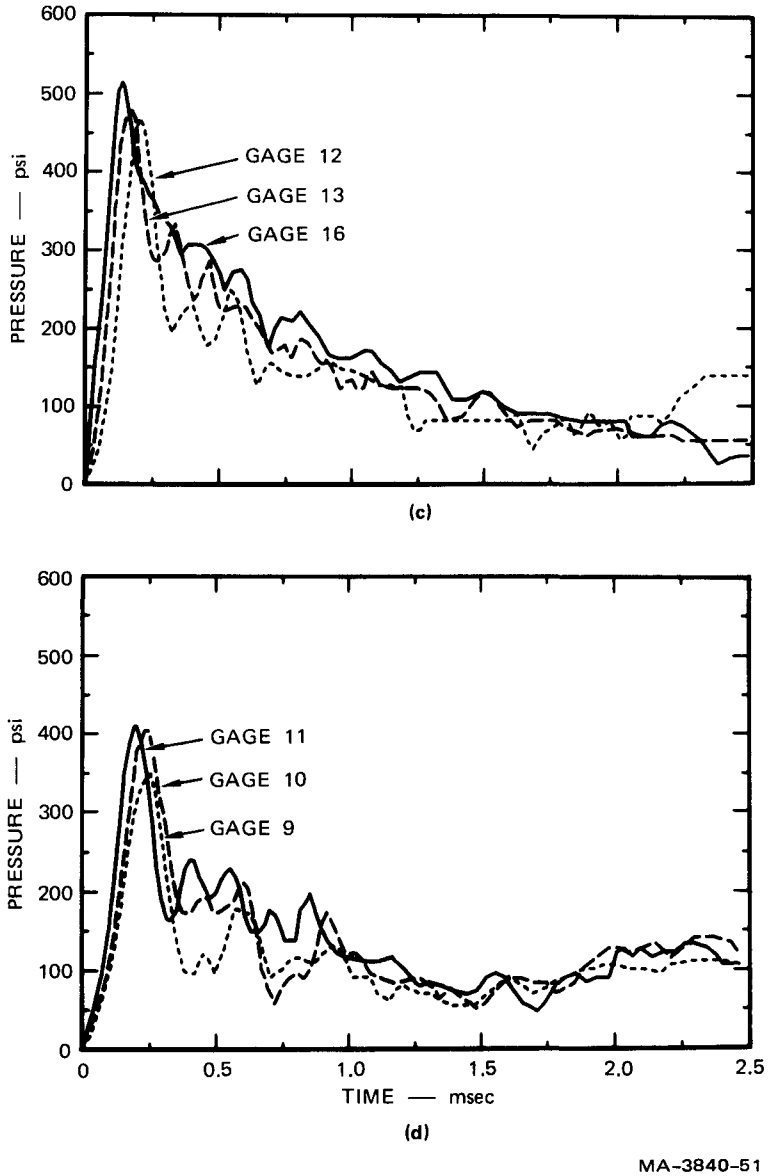

FIGURE E-4 PRESSURE-TIME RECORDS FOR EXPERIMENT L304 (Concluded)

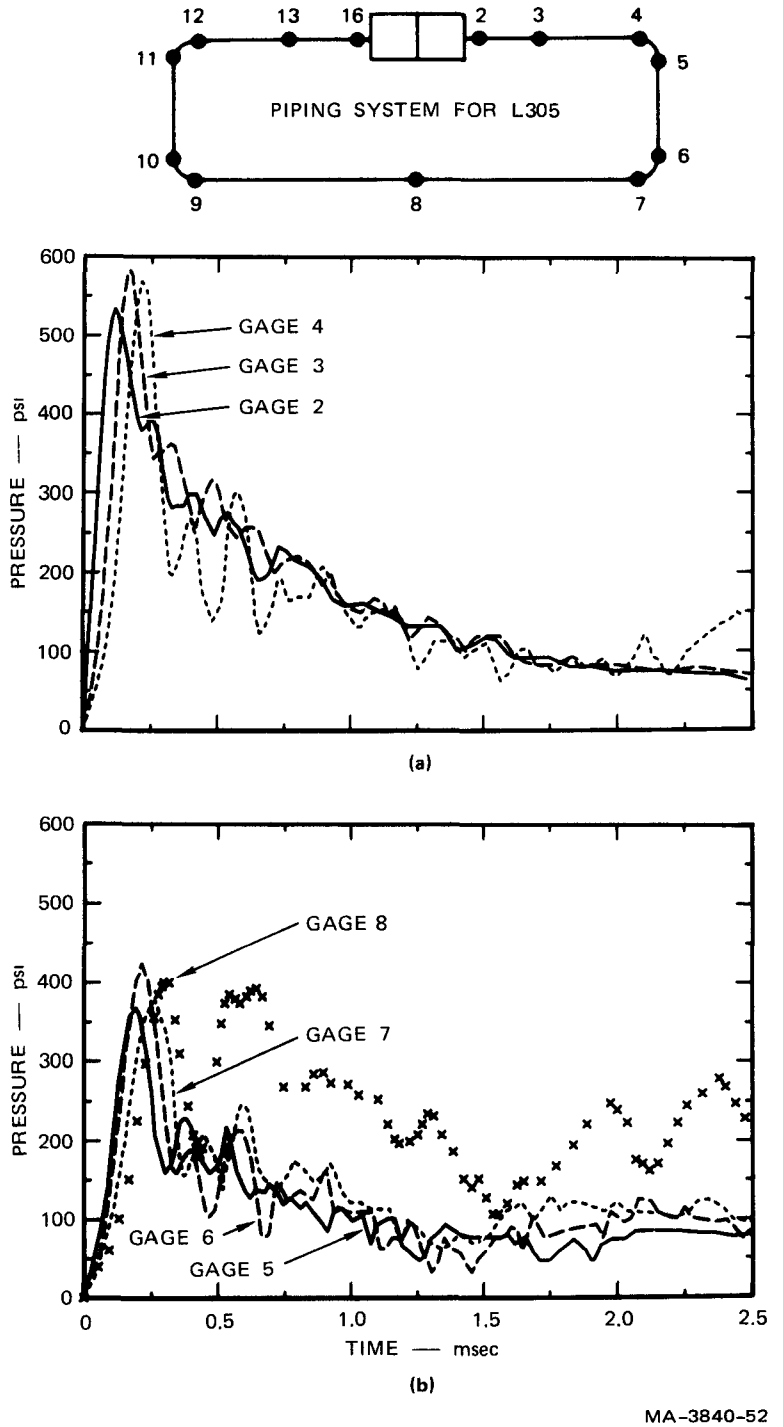

FIGURE E-5 PRESSURE-TIME RECORDS FOR EXPERIMENT L305

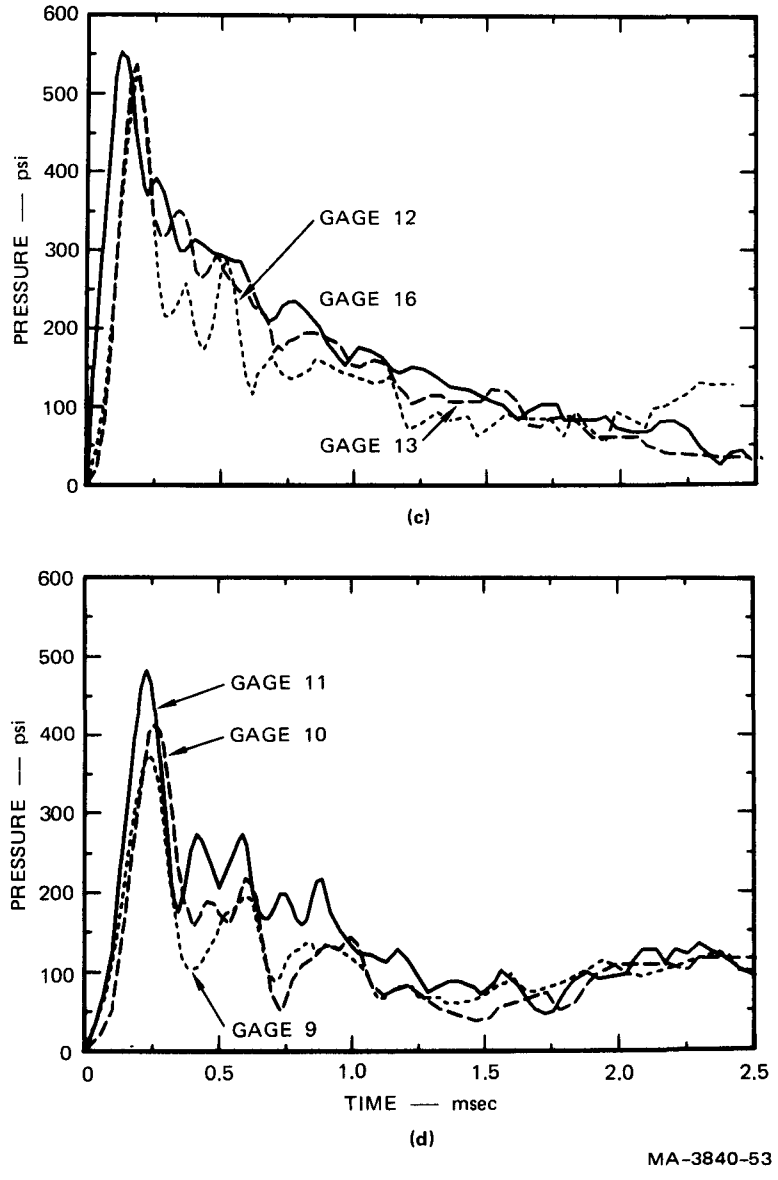

FIGURE E-5 PRESSURE-TIME RECORDS FOR EXPERIMENT L305 (Concluded)

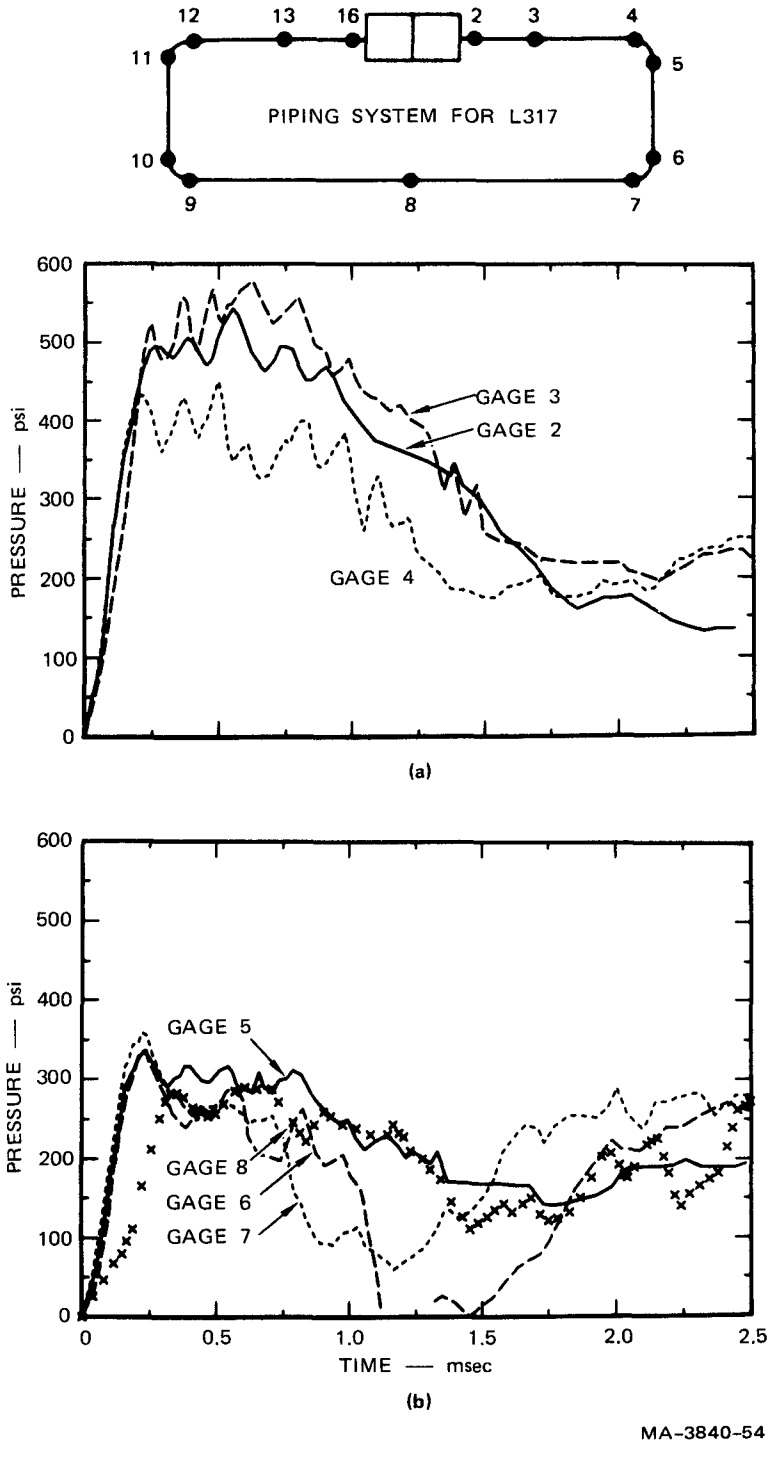

FIGURE E-6 PRESSURE-TIME RECORDS FOR EXPERIMENT L317

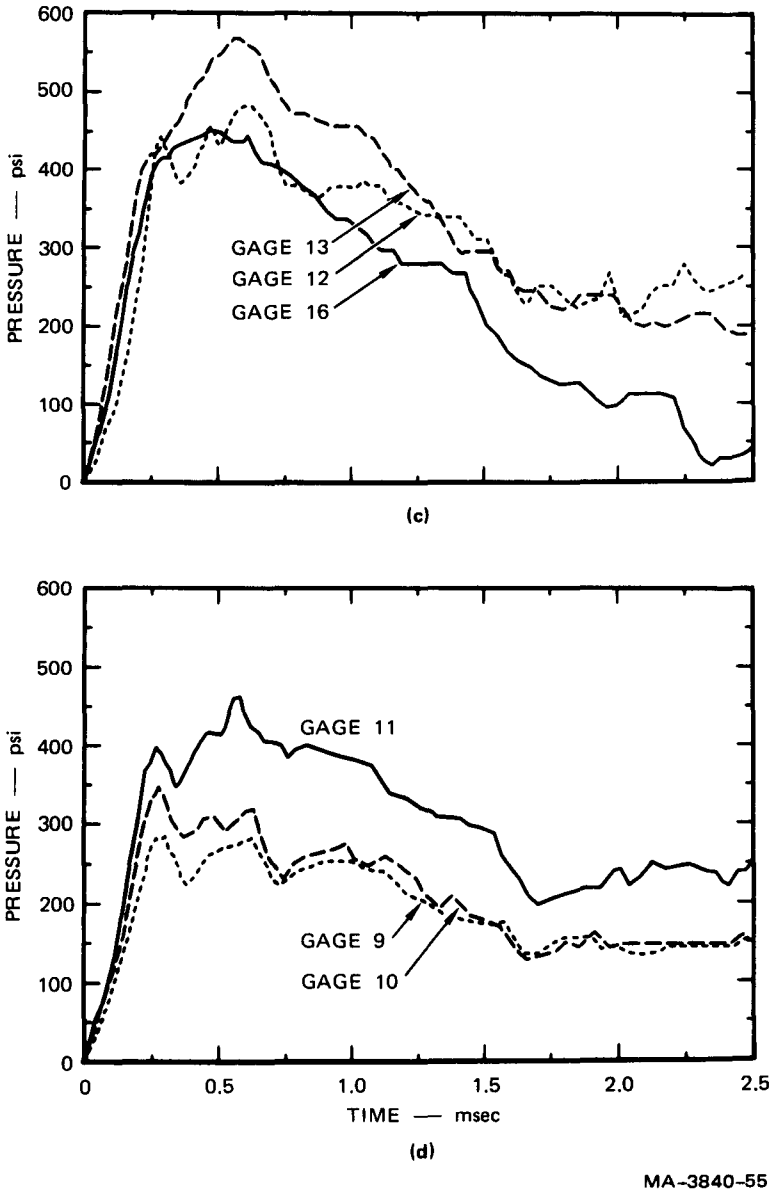

FIGURE E-6 PRESSURE-TIME RECORDS FOR EXPERIMENT L317 (Concluded)

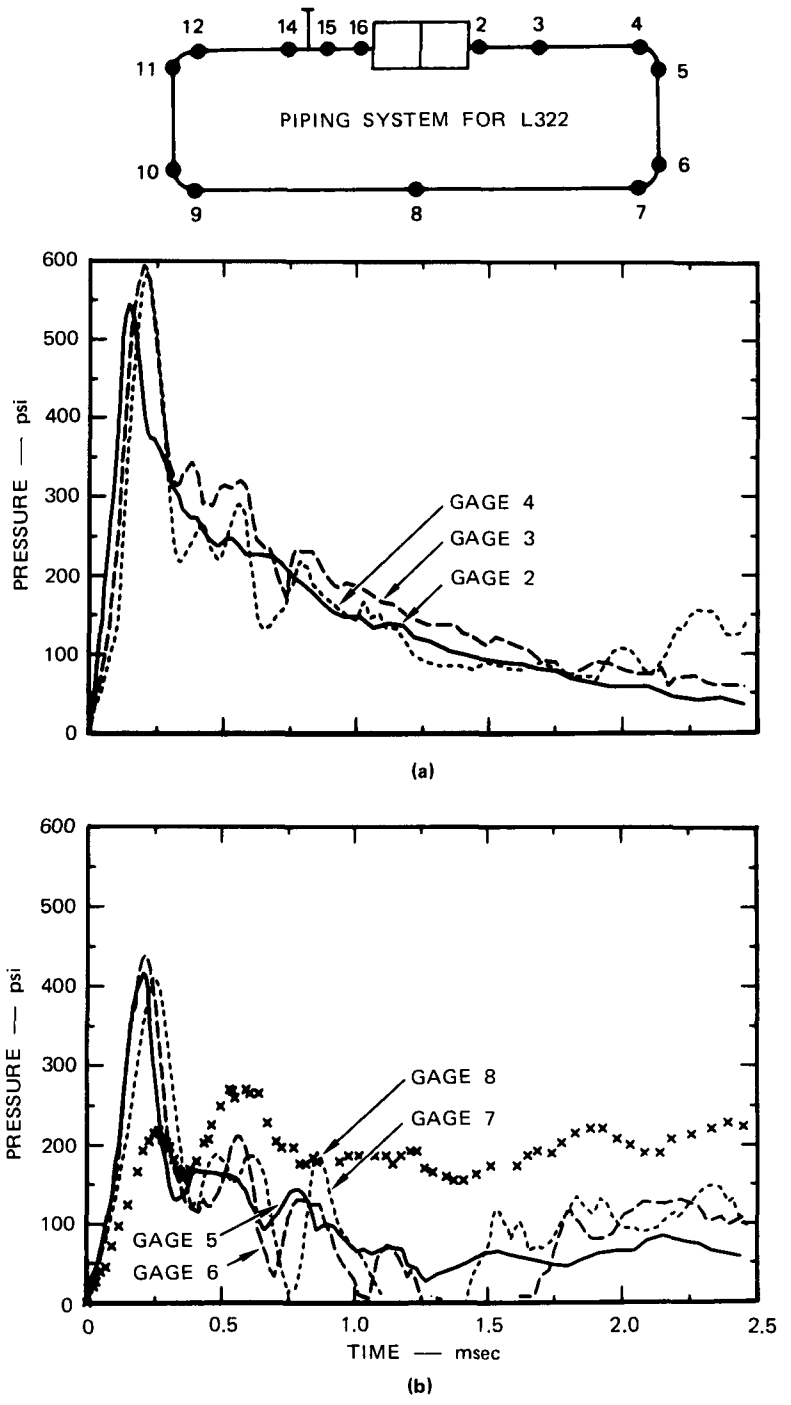

FIGURE E-7 PRESSURE-TIME RECORDS FOR EXPERIMENT L322

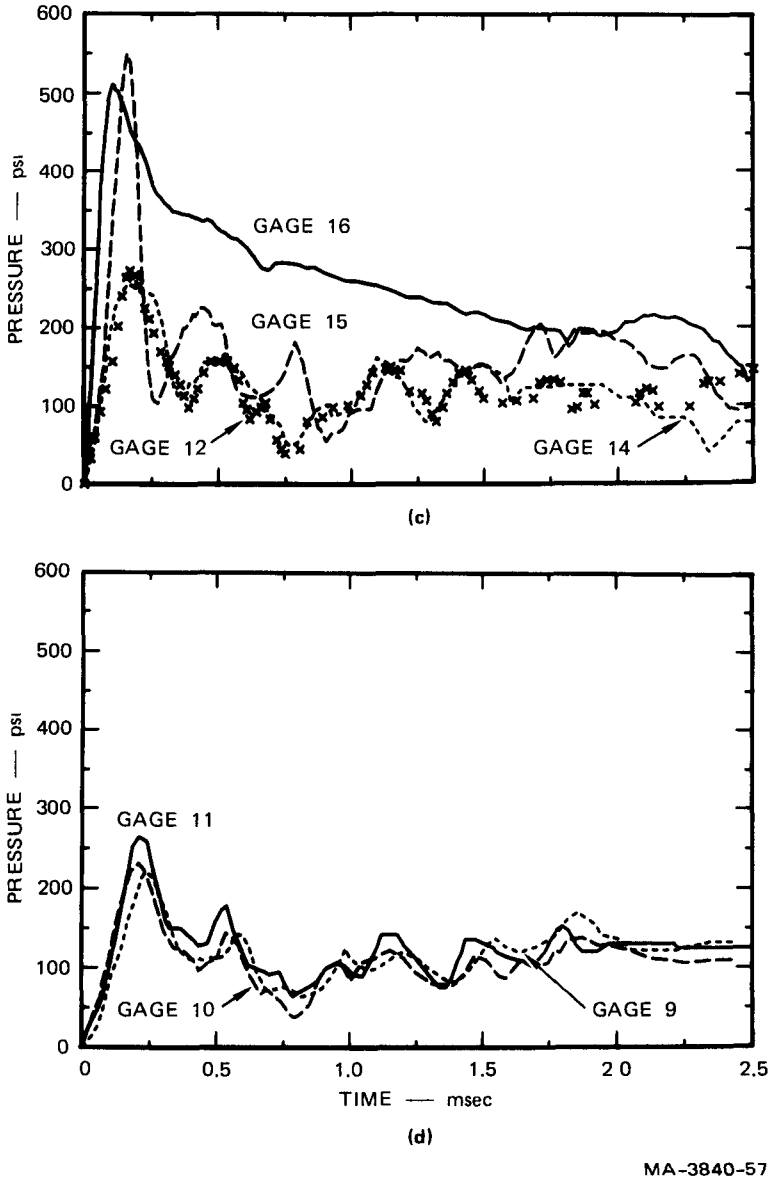

FIGURE E-7 PRESSURE-TIME RECORDS FOR EXPERIMENT L322 (Concluded)

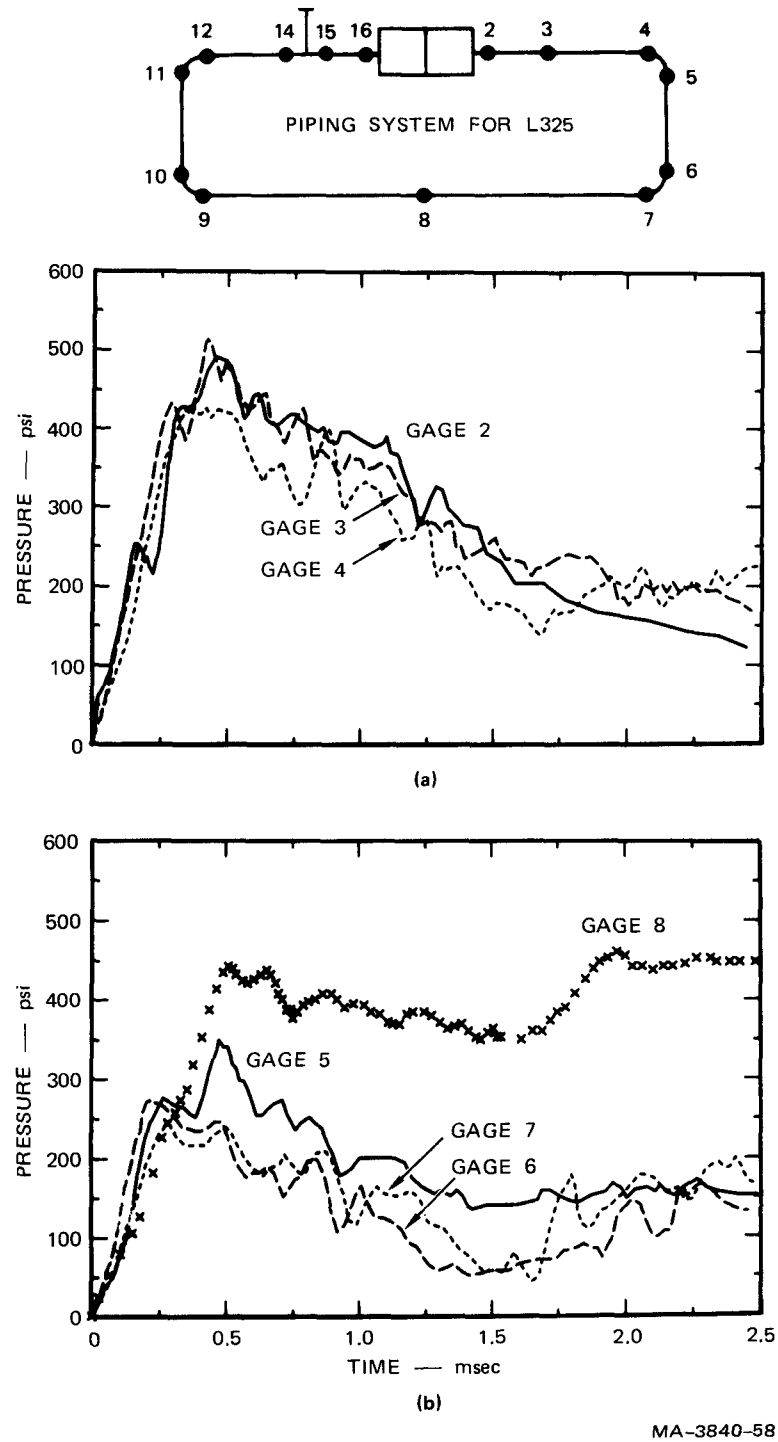

FIGURE E-8 PRESSURE-TIME RECORDS FOR EXPERIMENT L325

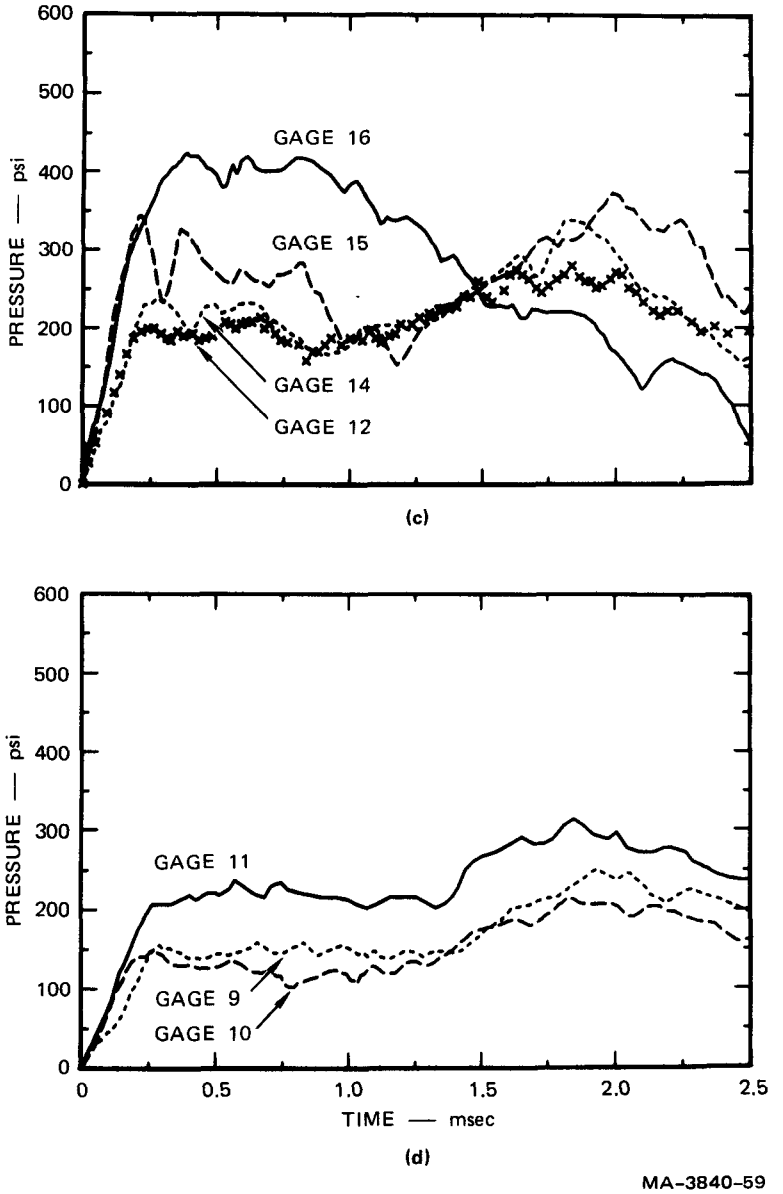

FIGURE E-8 PRESSURE-TIME RECORDS FOR EXPERIMENT L325 (Concluded)

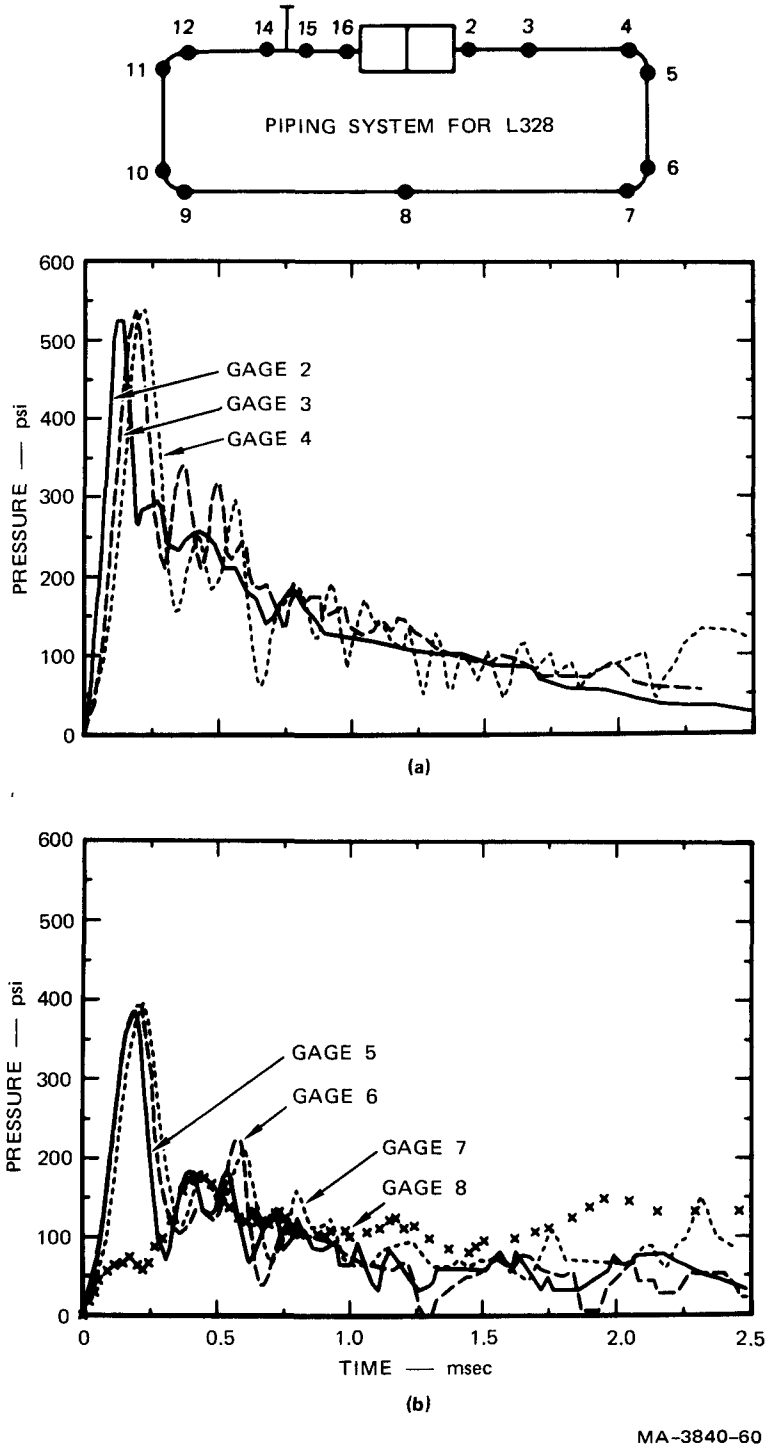

FIGURE E-9 PRESSURE-TIME RECORDS FOR EXPERIMENT L328

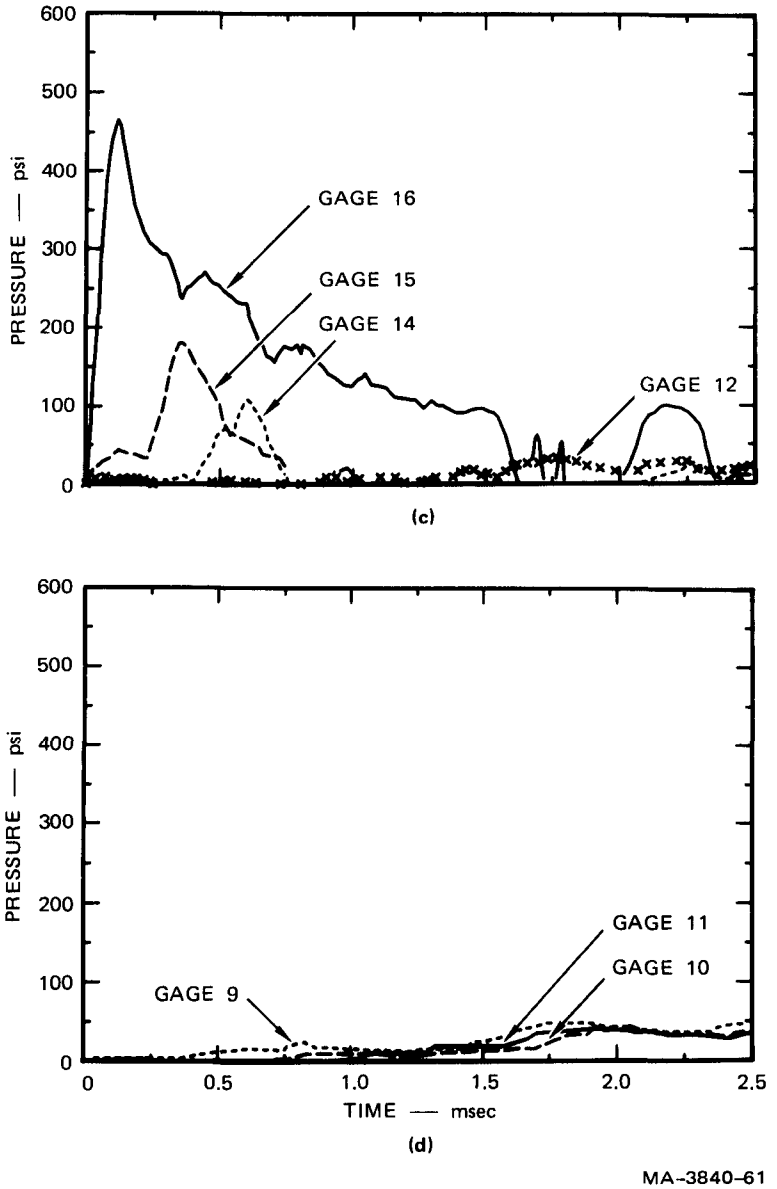

FIGURE E-9 PRESSURE-TIME RECORDS FOR EXPERIMENT L328 (Concluded)

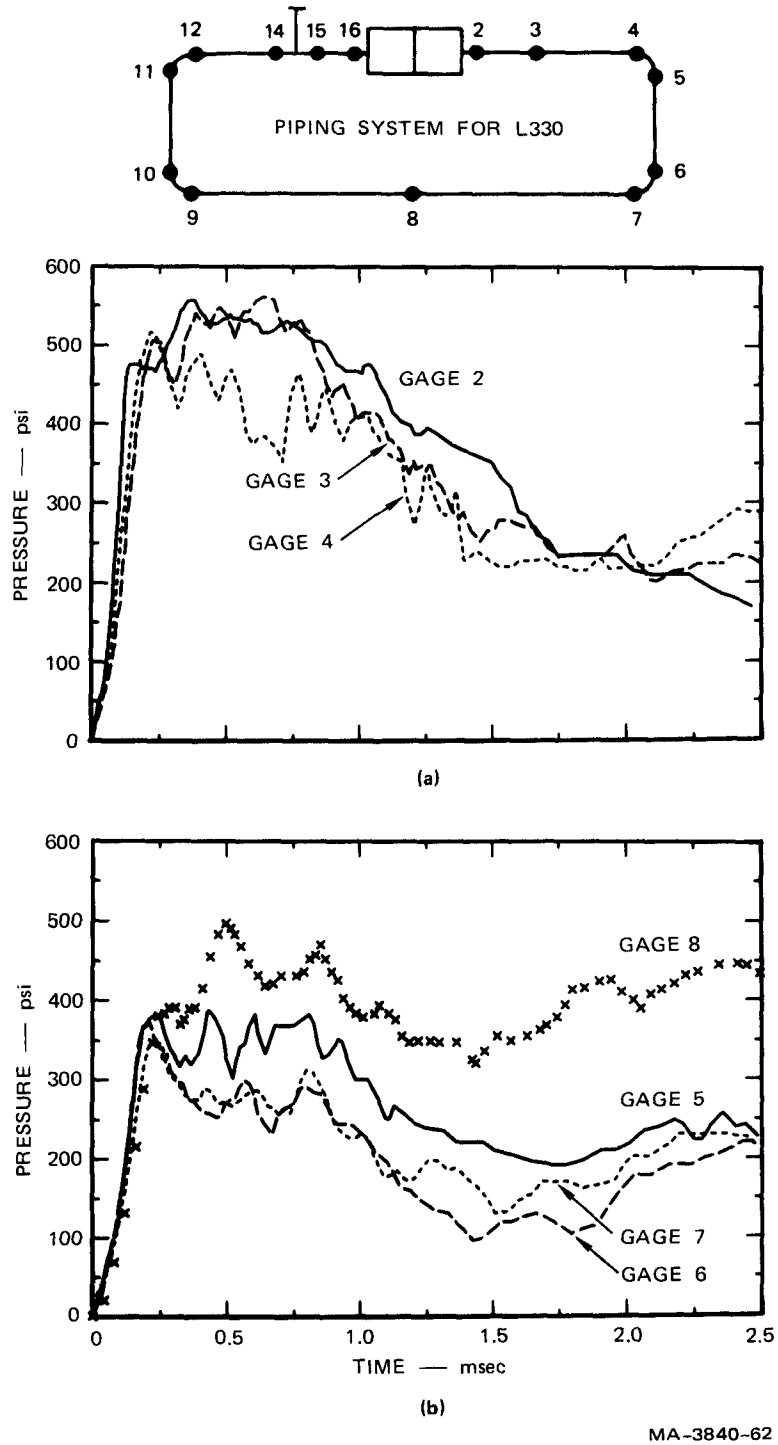

FIGURE E-10 PRESSURE-TIME RECORDS FOR EXPERIMENT L330

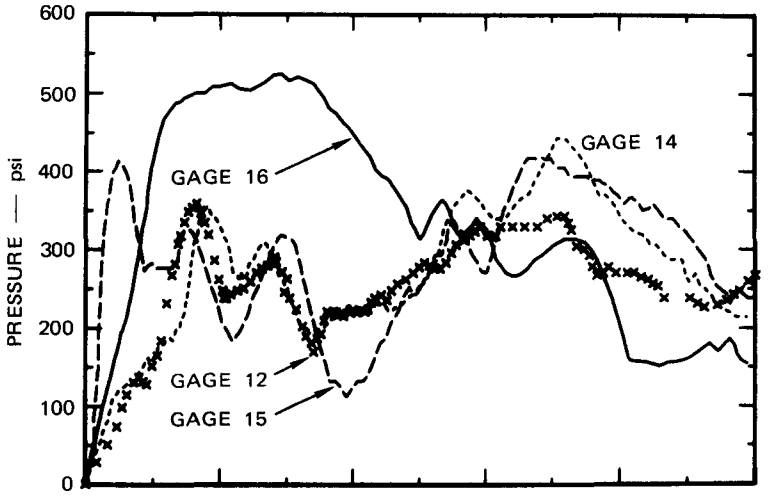

(c)

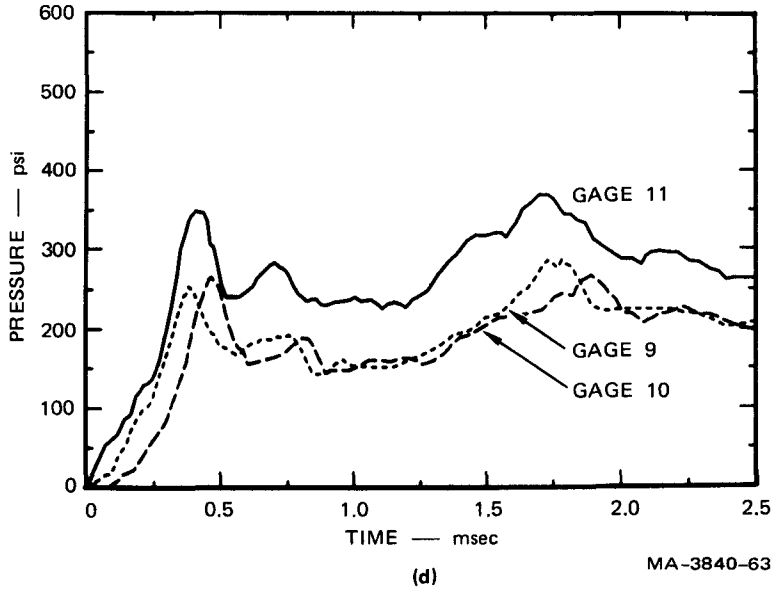

(d)

FIGURE E-10 PRESSURE-TIME RECORDS FOR EXPERIMENT L330 (Concluded)

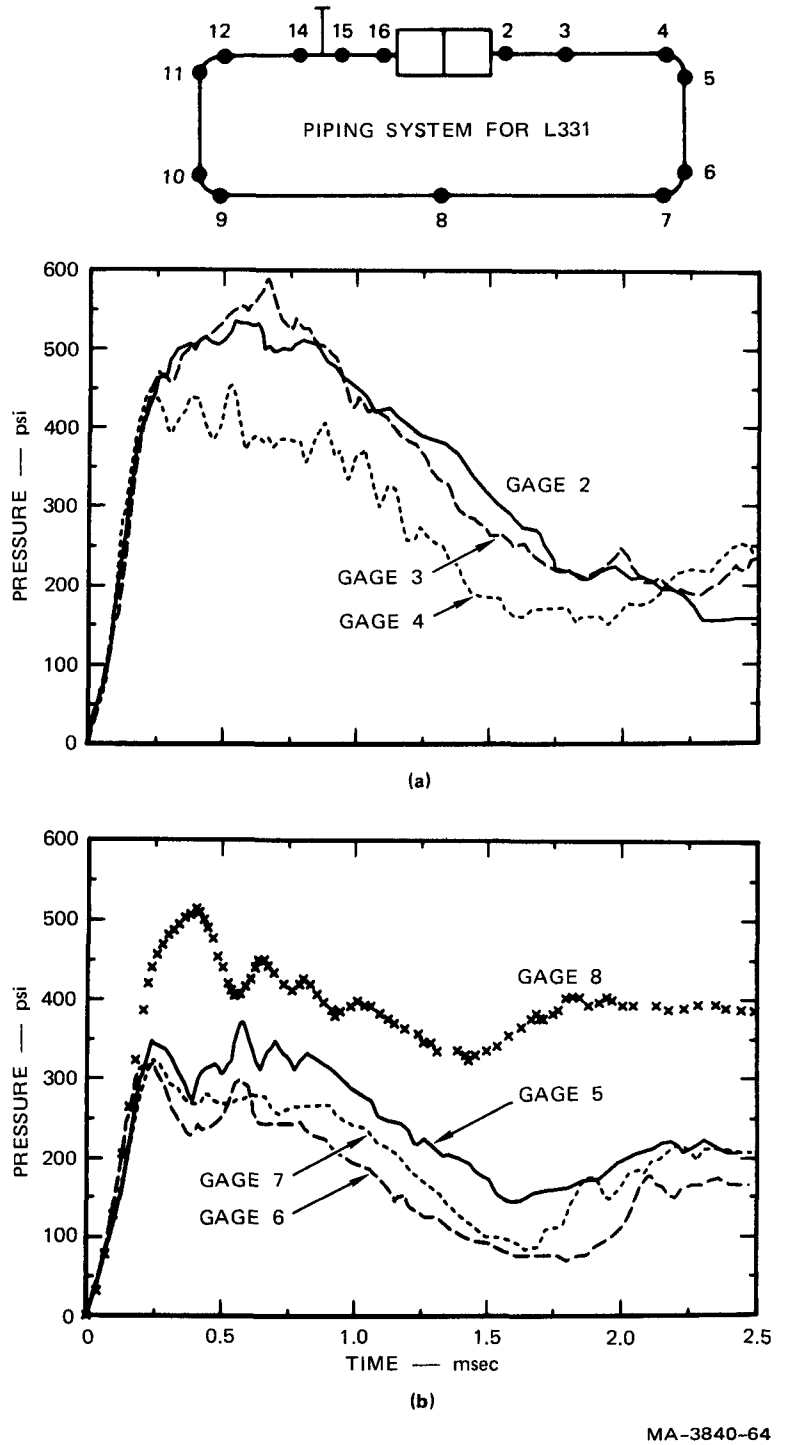

FIGURE E-11 PRESSURE-TIME RECORDS FOR EXPERIMENT L331

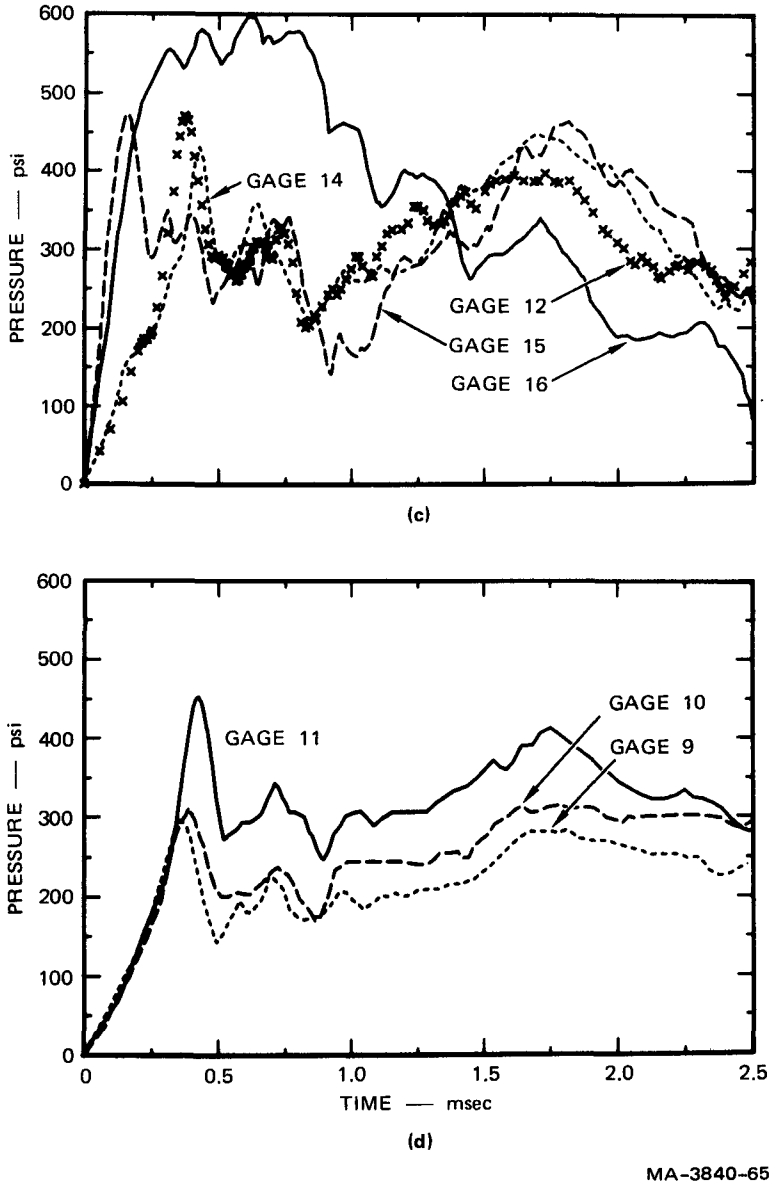

FIGURE E-11 PRESSURE-TIME RECORDS FOR EXPERIMENT L331 (Concluded)

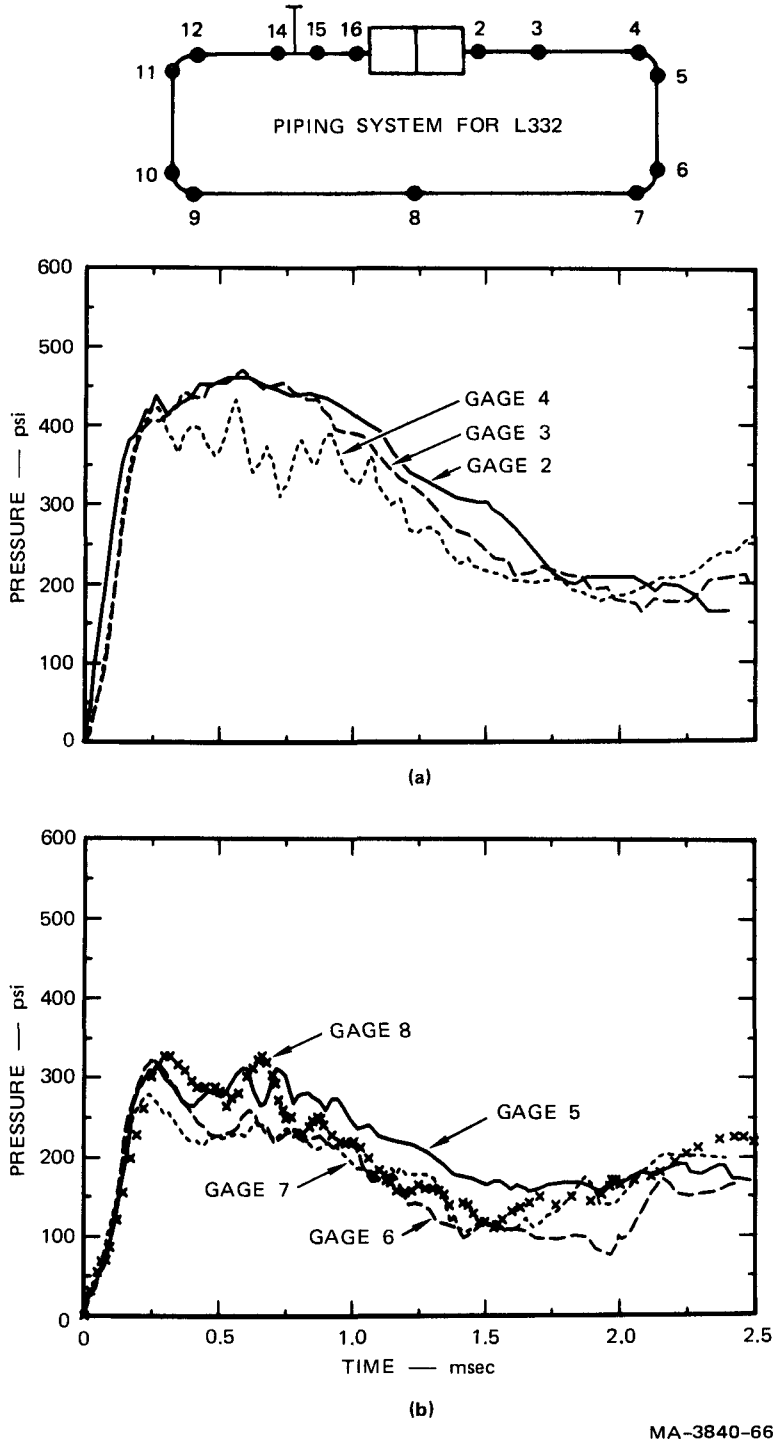

FIGURE E-12 PRESSURE-TIME RECORDS FOR EXPERIMENT L332

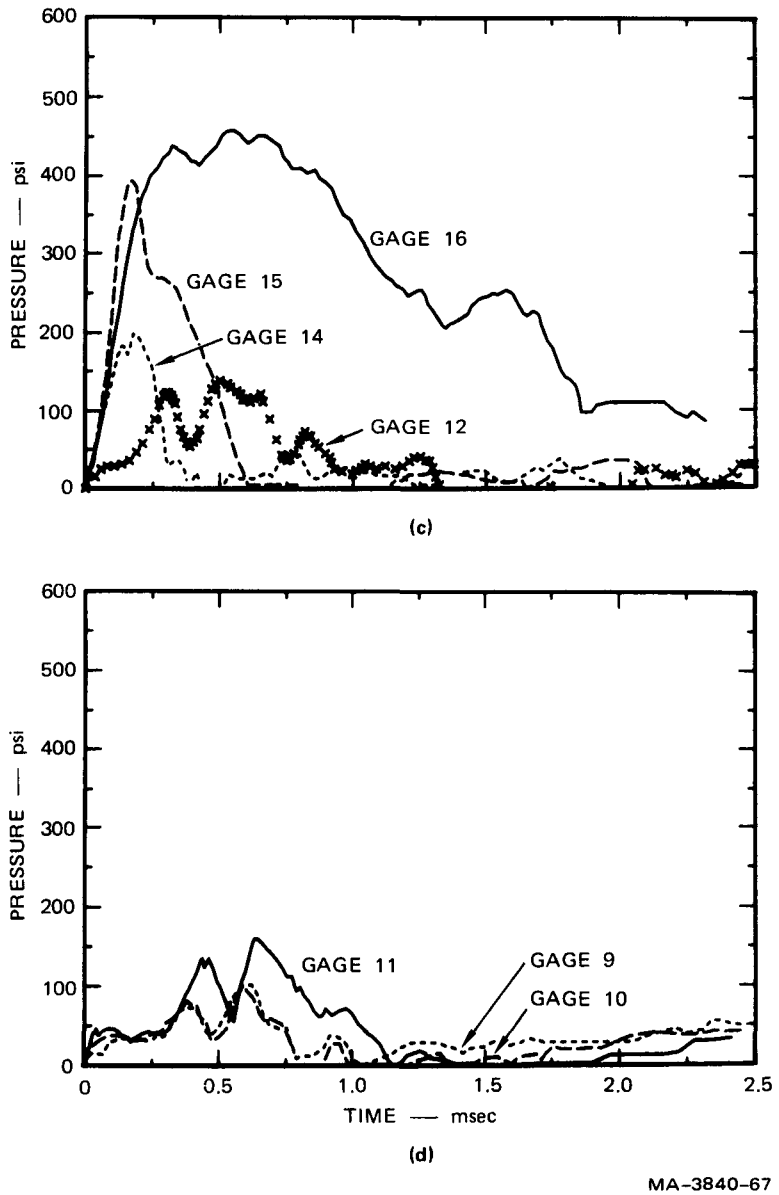

FIGURE E-12 PRESSURE-TIME RECORDS FOR EXPERIMENT L332 (Concluded)

Appendix F

DIGITIZED LISTINGS OF PULSES P I AND P II

The pressure transducer records on magnetic tape were transferred to oscillographs. The oscillograph was expanded optically in a Telereadex machine to obtain listings and plots, and with the aid of crosshairs, the x, y coordinates of points on the signal were automatically transferred to computer cards. The listings and plots of pressure pulses P I and P II at gage 2 (located 0.52 feet from the diaphragm) were taken from experiments L332 and L305 and are given in Tables F-1 and F-2 and Figures F-1 and F-2.

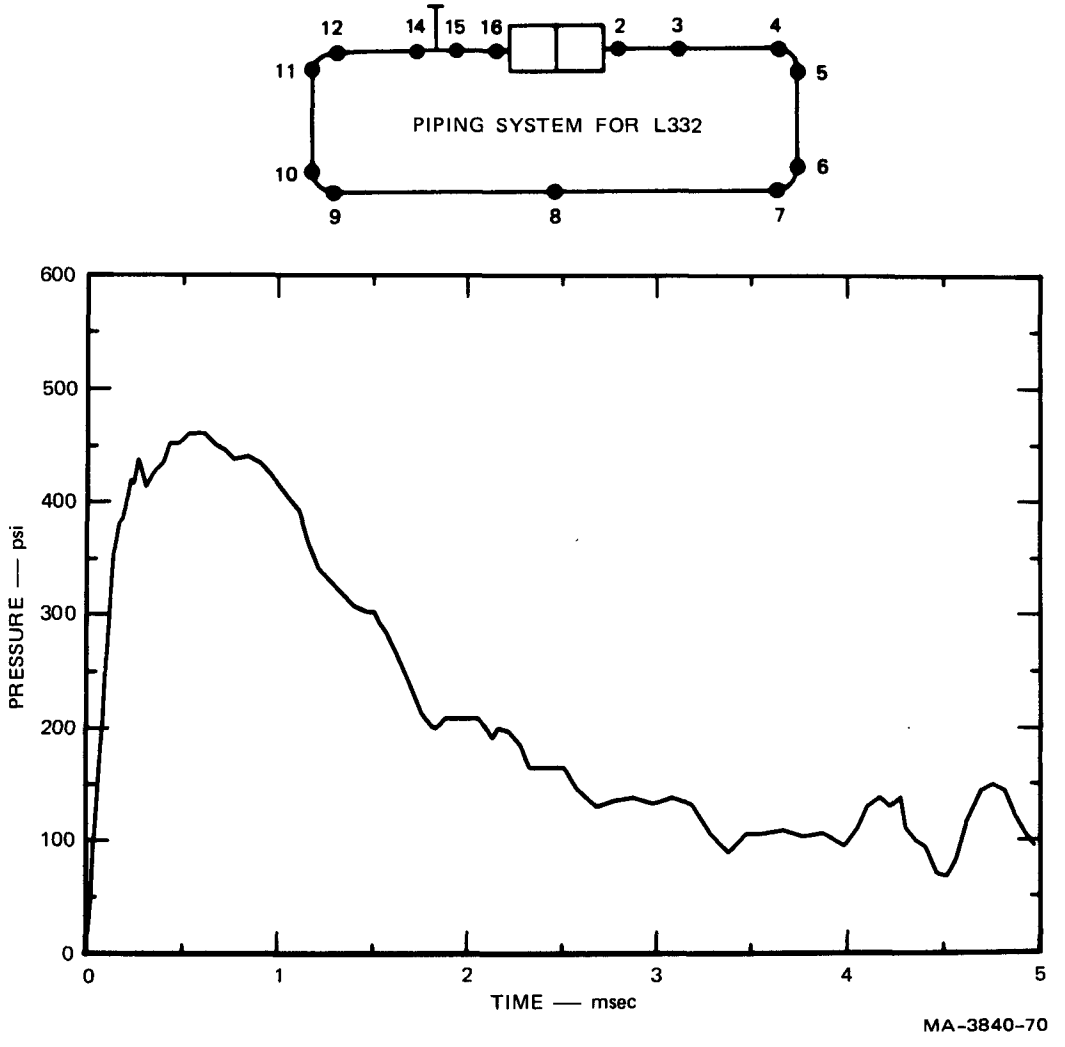

FIGURE F-1 PULSE P I FROM EXPERIMENT L332 GAGE 2

Table F-1

LISTING FOR PULSE P I

03/11/75

L-332 GAGE ? 0.18 MSEC TIME DELAY

XSCALE = 1000.00 MUSEC / 1321 UNITS = .757E-03 MSEC/UNIT
YSCALE = 1000.00 PSI / 341 UNITS = .293E+01 PSI/UNIT

N	X UNITS	Y UNITS	T MSEC	P PSI	P BARS
1	0	0	0.000	0.0	0.0
2	12	8	.009	23.5	1.6
3	29	15	.022	44.0	3.0
4	48	33	.036	96.8	6.7
5	89	60	.067	176.0	12.1
6	121	85	.092	249.3	17.2
7	159	108	.120	316.7	21.8
8	186	121	.141	354.8	24.5
9	216	130	.164	381.2	26.3
10	239	132	.181	387.1	26.7
11	268	136	.203	398.8	27.5
12	298	143	.226	419.4	28.9
13	316	142	.239	416.4	28.7
14	345	149	.261	437.0	30.1
15	368	146	.279	428.2	29.5
16	401	141	.304	413.5	28.5
17	433	144	.328	422.3	29.1
18	469	146	.355	428.2	29.5
19	515	148	.390	434.0	29.9
20	560	154	.424	451.6	31.1
21	630	154	.477	451.6	31.1
22	699	157	.529	460.4	31.8
23	748	157	.566	460.4	31.8
24	805	157	.609	460.4	31.8
25	872	154	.660	451.6	31.1
26	941	152	.712	445.7	30.7
27	1013	149	.767	437.0	30.1
28	1111	150	.841	439.9	30.3
29	1192	148	.902	434.0	29.9
30	1261	145	.955	425.2	29.3
31	1313	142	.994	416.4	28.7
32	1376	138	1.042	404.7	27.9
33	1457	134	1.103	393.0	27.1
34	1525	124	1.154	363.6	25.1
35	1604	116	1.214	340.2	23.5
36	1716	111	1.299	325.5	22.4
37	1838	105	1.391	307.9	21.2
38	1942	103	1.470	302.1	20.8
39	1992	103	1.508	302.1	20.8
40	2017	100	1.527	293.3	20.2
41	2071	97	1.568	284.5	19.6
42	2129	92	1.612	269.8	18.6
43	2208	84	1.671	246.3	17.0

Table F-1 (continued)

44	2317	73	1.750	214.1	14.8
45	2382	69	1.803	202.3	14.0
46	2425	68	1.836	199.4	13.8
47	2482	71	1.879	208.2	14.4
48	2715	71	2.055	208.2	14.4
49	2789	67	2.111	196.5	13.6
50	2820	65	2.135	190.6	13.1
51	2855	68	2.161	199.4	13.8
52	2934	67	2.221	196.5	13.6
53	3014	63	2.282	184.8	12.7
54	3072	56	2.326	164.2	11.3
55	3178	56	2.406	164.2	11.3
56	3323	56	2.516	164.2	11.3
57	3406	50	2.578	146.6	10.1
58	3542	44	2.681	129.0	8.9
59	3675	46	2.782	134.9	9.3
60	3807	47	2.882	137.8	9.5
61	3947	45	2.988	132.0	9.1
62	4077	47	3.086	137.8	9.5
63	4207	45	3.185	132.0	9.1
64	4338	36	3.284	105.6	7.3
65	4462	30	3.378	88.0	6.1
66	4589	36	3.474	105.6	7.3
67	4724	36	3.576	105.6	7.3
68	4854	37	3.674	108.5	7.5
69	4984	35	3.773	102.6	7.1
70	5122	36	3.877	105.6	7.3
71	5266	32	3.986	93.8	6.5
72	5364	38	4.061	111.4	7.7
73	5420	44	4.103	129.0	8.9
74	5513	47	4.173	137.8	9.5
75	5581	44	4.225	129.0	8.9
76	5649	47	4.276	137.8	9.5
77	5683	38	4.302	111.4	7.7
78	5754	34	4.353	99.7	6.9
79	5816	32	4.403	93.8	6.5
80	5890	24	4.459	70.4	4.9
81	5963	23	4.514	67.4	4.7
82	6023	28	4.559	82.1	5.7
83	6096	39	4.615	114.4	7.9
84	6195	49	4.690	143.7	9.9
85	6282	51	4.755	149.6	10.3
86	6363	49	4.817	143.7	9.9
87	6425	42	4.864	123.2	8.5
88	6495	36	4.917	105.6	7.3
89	6558	32	4.964	93.8	6.5
90	6626	32	5.016	93.8	6.5
91	6658	29	5.040	85.0	5.9

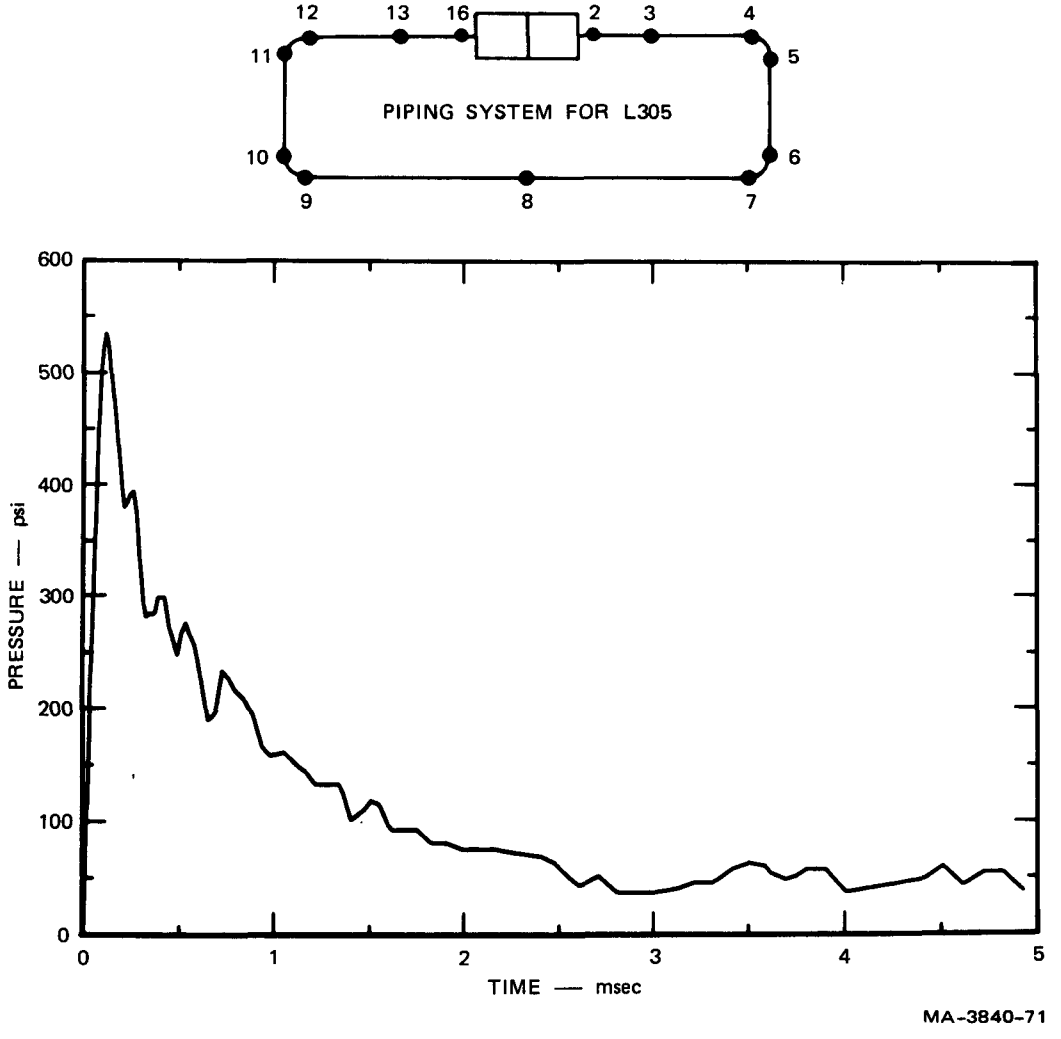

FIGURE F-2 PULSE P II FROM EXPERIMENT L305 GAGE 2

Table F-2

LISTING FOR PULSE P II

03/11/75

L-305 GAGE 2 0.16 MSEC TIME DELAY

XSCALE = 1000.00 MUSEC / 1366 UNITS = .732E-03 MSEC/UNIT
YSCALE = 1000.00 PSI / 348 UNITS = .287E+01 PSI/UNIT

N	X UNITS	Y UNITS	T MSEC	P PSI	P BARS
1	0	0	0.000	0.0	0.0
2	25	38	.018	109.2	7.5
3	51	77	.037	221.3	15.3
4	78	121	.057	347.7	24.0
5	107	157	.078	451.1	31.1
6	121	172	.089	494.3	34.1
7	140	182	.102	523.0	36.1
8	157	186	.115	534.5	36.9
9	170	183	.124	525.9	36.3
10	190	176	.139	505.7	34.9
11	213	166	.156	477.0	32.9
12	241	151	.176	433.9	29.9
13	273	137	.200	393.7	27.2
14	291	132	.213	379.3	26.2
15	313	134	.229	385.1	26.6
16	331	136	.242	390.8	27.0
17	351	137	.257	393.7	27.2
18	375	130	.275	373.6	25.8
19	396	116	.290	333.3	23.0
20	425	102	.311	293.1	20.2
21	444	98	.325	281.6	19.4
22	469	99	.343	284.5	19.6
23	507	99	.371	284.5	19.6
24	532	104	.389	298.9	20.6
25	573	104	.419	298.9	20.6
26	617	94	.452	270.1	18.6
27	664	86	.486	247.1	17.0
28	695	93	.509	267.2	18.4
29	731	96	.535	275.9	19.0
30	759	92	.556	264.4	18.2
31	790	89	.578	255.7	17.6
32	829	80	.607	229.9	15.9
33	865	70	.633	201.1	13.9
34	887	66	.649	189.7	13.1
35	919	67	.673	192.5	13.3
36	946	69	.693	198.3	13.7
37	971	75	.711	215.5	14.9
38	994	81	.728	232.8	16.1
39	1034	79	.757	227.0	15.7
40	1077	75	.788	215.5	14.9
41	1148	72	.840	206.9	14.3
42	1210	67	.886	192.5	13.3
43	1269	58	.929	166.7	11.5

Table F-2 (continued)

44	1336	55	.978	158.0	10.9
45	1432	56	1.048	160.9	11.1
46	1526	52	1.117	149.4	10.3
47	1587	50	1.162	143.7	9.9
48	1660	46	1.215	132.2	9.1
49	1628	46	1.338	132.2	9.1
50	1658	43	1.360	123.6	8.5
51	1912	35	1.400	100.6	6.9
52	2001	38	1.465	109.2	7.5
53	2061	41	1.509	117.8	8.1
54	2115	40	1.548	114.9	7.9
55	2173	34	1.591	97.7	6.7
56	2213	32	1.620	92.0	6.3
57	2286	32	1.673	92.0	6.3
58	2388	32	1.748	92.0	6.3
59	2489	28	1.822	80.5	5.5
60	2544	28	1.862	80.5	5.5
61	2598	28	1.902	80.5	5.5
62	2713	26	1.986	74.7	5.2
63	2849	26	2.086	74.7	5.2
64	2965	26	2.171	74.7	5.2
65	3090	25	2.262	71.8	5.0
66	3294	24	2.411	69.0	4.8
67	3385	22	2.478	63.2	4.4
68	3437	20	2.516	57.5	4.0
69	3565	15	2.610	43.1	3.0
70	3703	18	2.711	51.7	3.6
71	3838	13	2.810	37.4	2.6
72	3979	13	2.913	37.4	2.6
73	4117	13	3.014	37.4	2.6
74	4258	14	3.117	40.2	2.8
75	4395	16	3.217	46.0	3.2
76	4531	16	3.317	46.0	3.2
77	4664	20	3.414	57.5	4.0
78	4796	22	3.511	63.2	4.4
79	4904	21	3.590	60.3	4.2
80	4940	19	3.616	54.6	3.8
81	5039	17	3.689	48.9	3.4
82	5128	18	3.754	51.7	3.6
83	5198	20	3.805	57.5	4.0
84	5337	20	3.907	57.5	4.0
85	5476	13	4.009	37.4	2.6
86	5616	14	4.111	40.2	2.8
87	5754	15	4.212	43.1	3.0
88	5891	16	4.313	46.0	3.2
89	6027	17	4.412	48.9	3.4
90	6162	21	4.511	60.3	4.2
91	6300	15	4.612	43.1	3.0
92	6446	19	4.719	54.6	3.8
93	6587	19	4.822	54.6	3.8
94	6725	13	4.923	37.4	2.6
95	6840	18	5.007	51.7	3.6

Appendix G

EXPERIMENTAL RESULTS FOR PULSE P III

A pulse designated P III was used in the two open rectangular loop experiments, E405 and E406. In these experiments, the vent control plate was removed from the one-direction pulse-source assembly (see Figure B-1) to obtain the shortest possible rise time. The pulse generated is shown in Figure G-1. The resulting rise time was about 0.1 msec, which is similar to that of pulse P II. The peak pressure of pulse P III was 850 psi compared to about 550 psi for pulse P II.

Experiment E406 was analyzed in detail to measure the attenuation of pulse P III in a pipeline. Figure G-2 illustrates the pulse shape behavior as the pulse propagates, and Figure G-3 shows the measured peak pressures and impulses. By use of the same procedure to measure attenuation as that used for pulses P I and P II, Section III-B, the average decrease in peak pressure and impulse were determined as follows:

	Peak Pressure	Impulse
Three elbow average	36%	24%
Two elbow average	41%	21%

These results are almost the same as the results for attenuation of pulse P II shown in Table 4, Section III.

Time-pressure plots for the twelve gages used in experiment E406 are shown in Figure G-4.

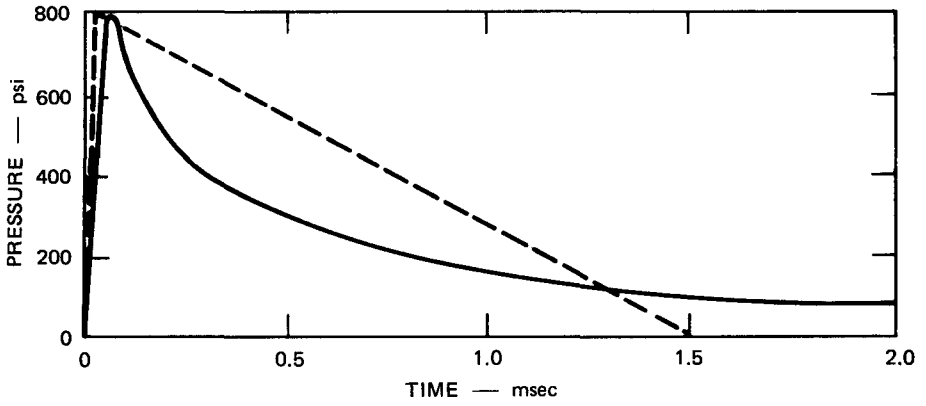

(a) PULSE P III

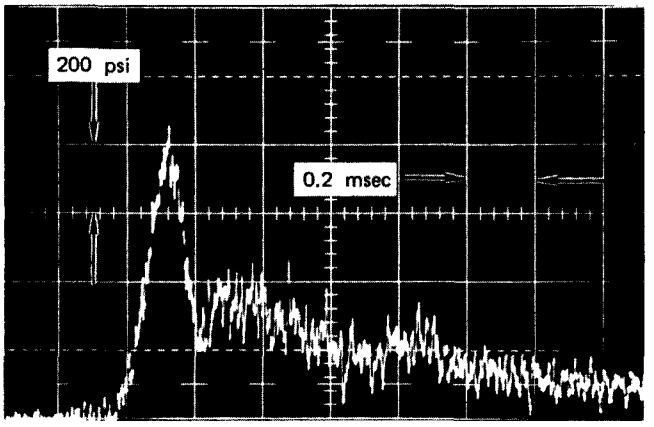

(b) PULSE SHAPE P III AT THE GAGE 3 LOCATION

MP-3840-72

FIGURE G-1 PULSE SHAPE FOR EXPERIMENTS USING PULSE P III

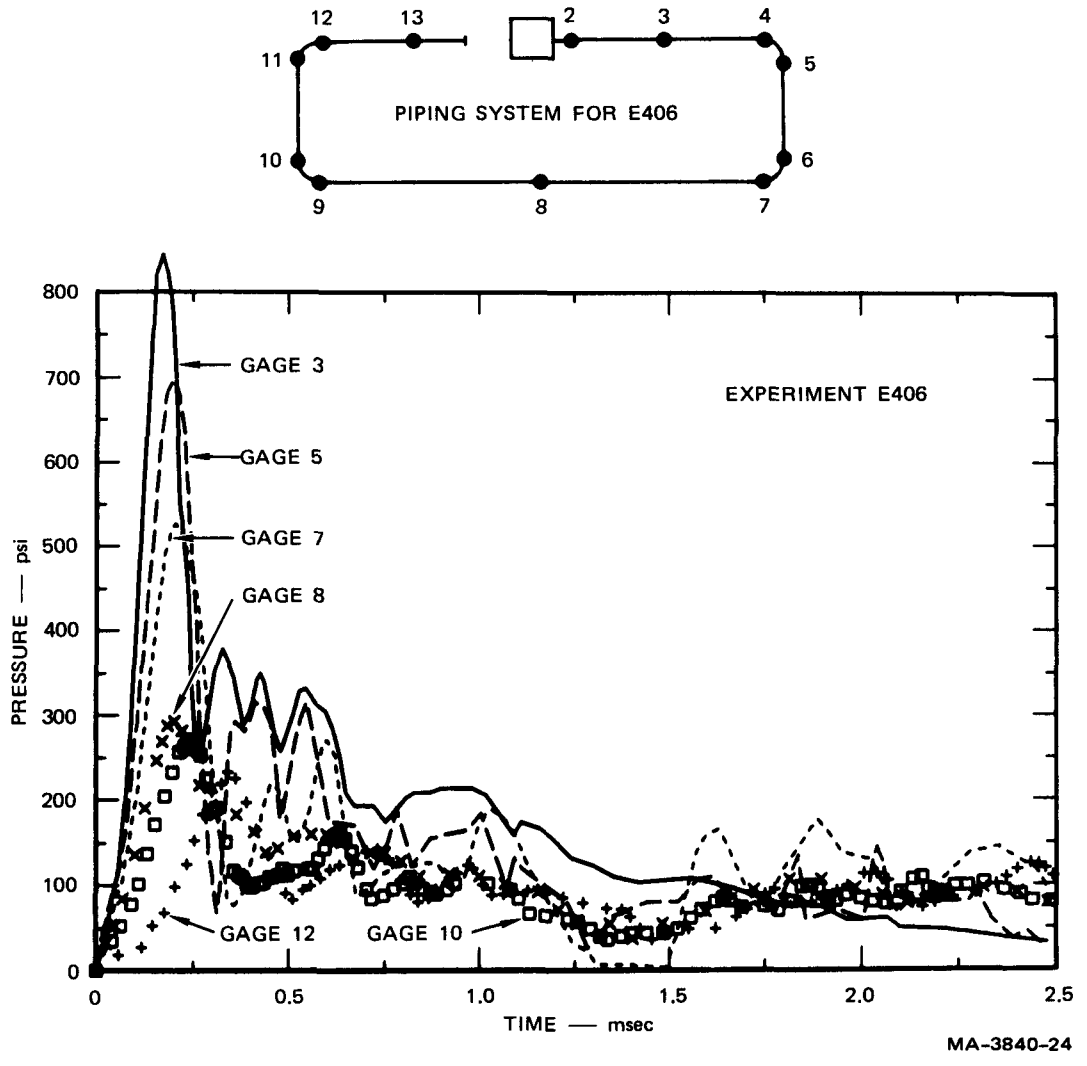

FIGURE G-2 ATTENUATION OF PULSE P III IN AN OPEN LOOP

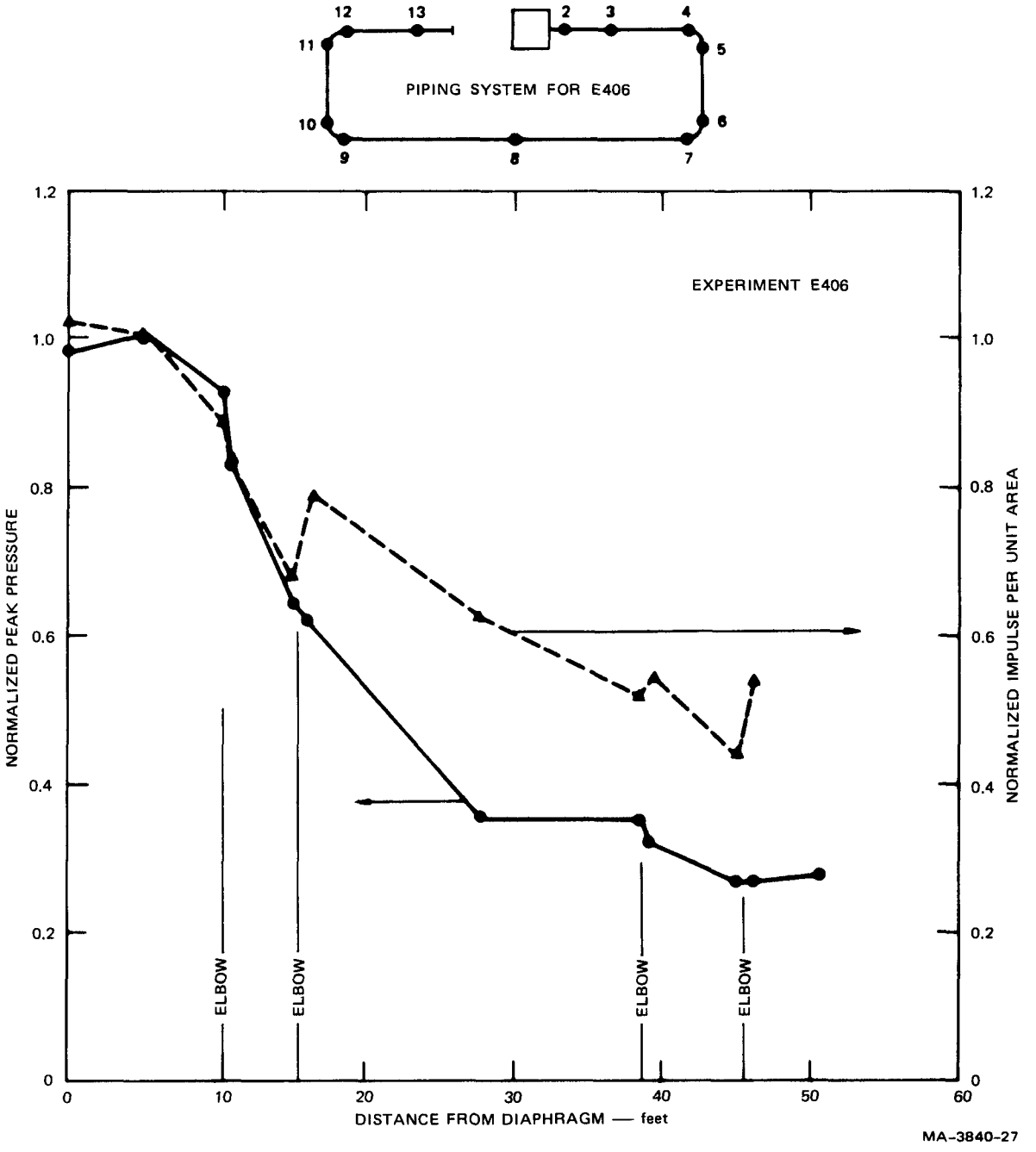

FIGURE G-3 MEASUREMENTS OF THE ATTENUATION OF PULSE P III IN AN OPEN LOOP

Figure G-4

appears on the

following pages

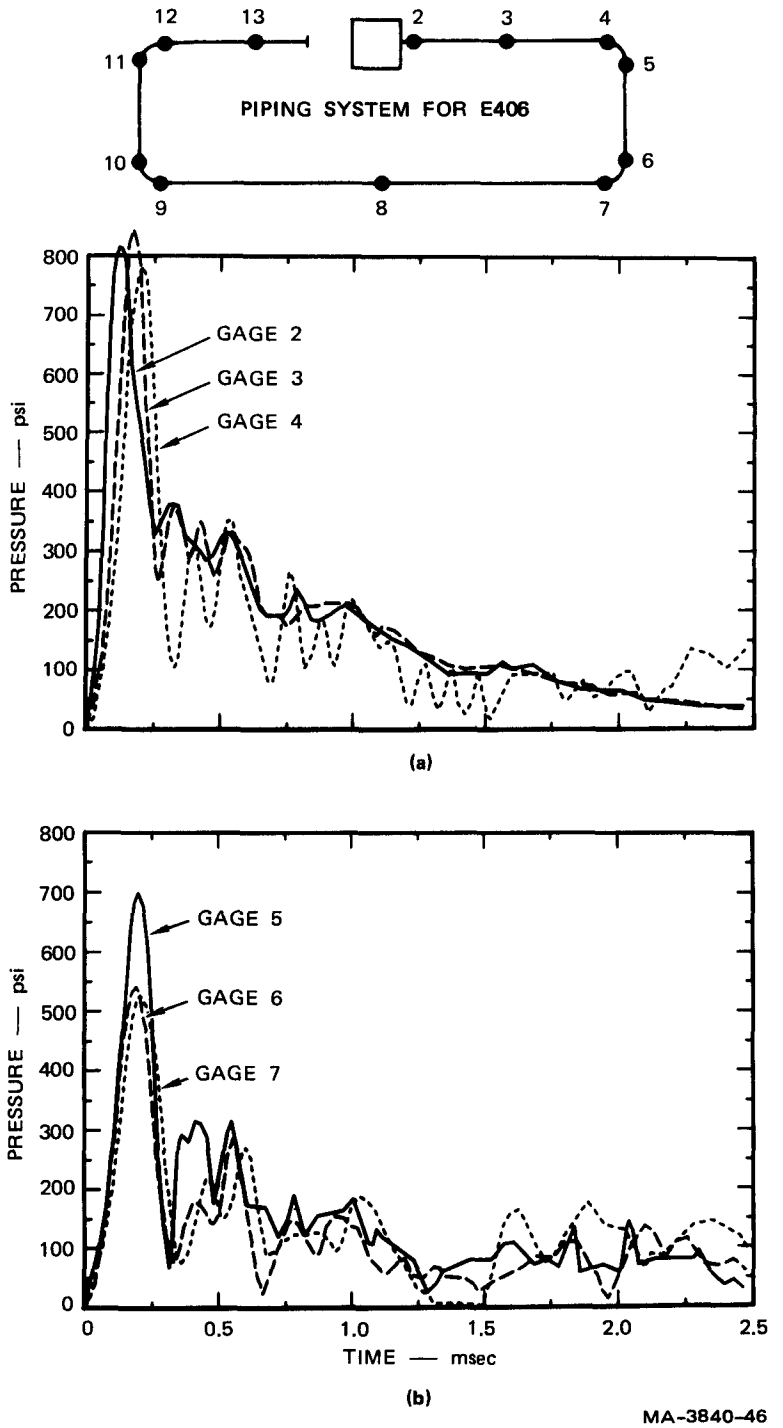

FIGURE G-4 PRESSURE-TIME RECORDS FOR EXPERIMENT E406

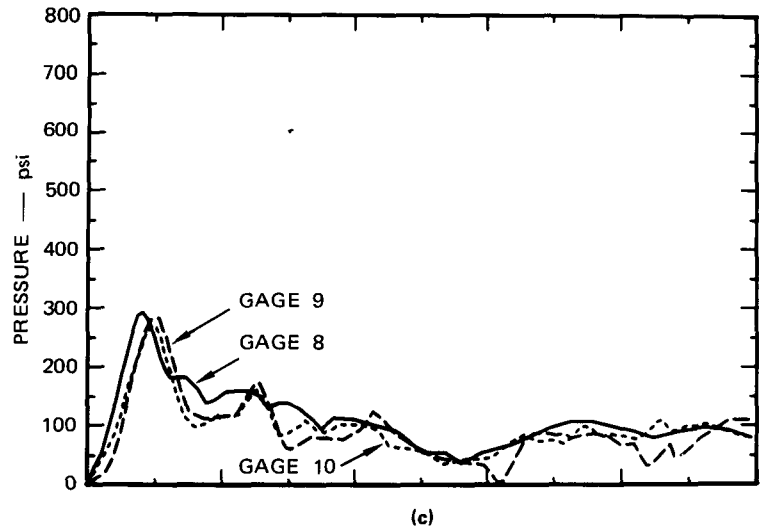

(c)

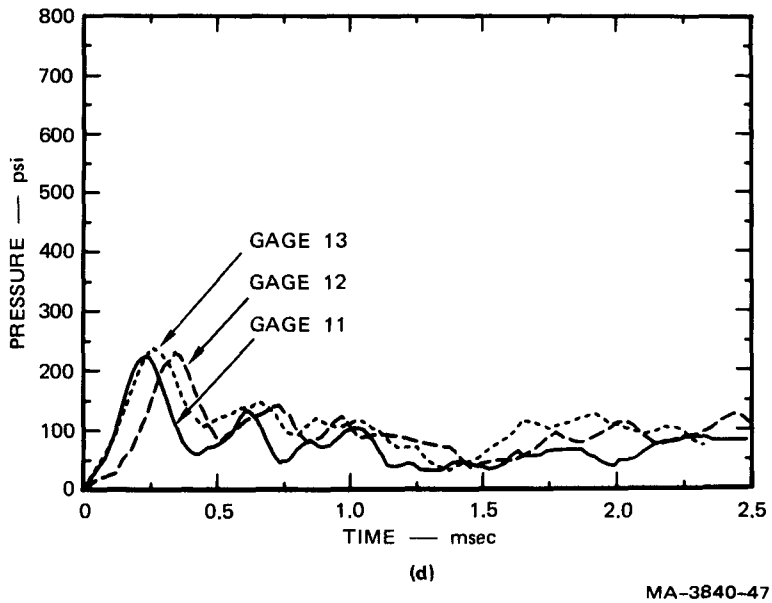

(d)

MA-3840-47

FIGURE G-4 PRESSURE-TIME RECORDS FOR EXPERIMENT E406 (Concluded)